

# Energy Efficiency, Thermal and Visual Comfort – Integrated Building Performance Modelling and Measurement

Anna Maria Atzeri

**bu,press**

bozen  
bolzano  
university  
press





# **Energy Efficiency, Thermal and Visual Comfort – Integrated Building Performance Modelling and Measurement**

Anna Maria Atzeri

**bu,press**

bozen  
bolzano  
university  
press

Cover design: doc.bz / bu,press  
Printer: Digiprint, Bozen-Bolzano  
© 2017 by Bozen-Bolzano University Press  
[www.unibz.it/universitypress](http://www.unibz.it/universitypress)

ISBN 978-88-6046-132-2  
E-ISBN 978-88-6046-133-9



This work—excluding the cover and the quotations—is licensed under the Creative Commons Attribution-ShareAlike 4.0 International License.

# Contents

The unibz junior researcher series .....	VII
Acknowledgements .....	XI
Preface .....	XIII
1. Introduction .....	1
1.1 Motivation .....	1
1.2 Literature analysis.....	5
1.3 Research objectives.....	18
2. Complex Fenestration System (CFS) Global Performance Comparison by Means of Simulation: A Parametric Approach .....	
2.1 Introduction.....	20
2.2 Simulation parameters for parametric analysis .....	22
2.3 Objectives and methods.....	26
2.4 Results and discussion .....	38
2.5 Conclusions .....	59
3. Characterization of a Consistent Set of Representation Metrics for Mapping Buildings' Global Performance: Thermal and Visual Comfort and Energy Efficiency .....	
3.1 Background .....	60
3.2 Representation metrics proposed .....	68
4. Metrics Application in Simulated Environment .....	
4.1 Simulation procedure .....	85
4.2 Reference building and parametrical analysis .....	87
4.3 Control strategies and comfort evaluation grid .....	89
4.4 Results .....	90
4.5 Comments .....	96
4.6 Conclusions .....	103

5.	Practical Aspects: How to Efficiently Model Roller Shading Systems	
5.1	Introduction.....	104
5.2	Simulating roller shades material: State of the art .....	108
5.3	Methodological approach .....	111
5.4	Simulations assumptions: First approach .....	114
5.5	Building model calibration through an optimization based approach.....	118
5.6	Roller shade models validation through on situ measurements .....	126
5.7	Results and discussion .....	134
5.8	Conclusions .....	140
6.	Overall Conclusions and Future Developments .....	141
	References .....	147
	The author.....	159

## The *unibz junior researcher* series

Especially at a time when universities are increasingly expected to produce tangible results, it is clear that one of their main tasks is to promote the work of their young scientists. The decision by the Free University of Bozen-Bolzano to publish the new series *unibz junior researcher*, enabling PhD students to present their research to a wider readership, is designed not so much to promote the work of individual scholars but rather to foster a common university culture. The idea is to publish studies which are exemplary, not just within the standards of the individual discipline, but also because of the wider significance of the issues they deal with and the way they are dealt with.

Due to the ever-increasing pressure in the academic world to publish papers in internationally-renowned journals, there is a danger that a lot of research reaches out to only a narrow field of specialists. But we maintain that it is precisely the role of the university to ensure that knowledge is transmitted to a wider audience, that discussion between different areas of research is stimulated and that a dialogue with a wider readership beyond the university is established. This promotes a public sphere that is better informed and more competent in debating. The studies which are published in the *unibz junior researcher* series will serve future PhD students as reference points for participation in such a culture of research. Engaging in research in isolation from the general public simply ignores the requirements of our times: Universities need to open up and academics need to learn to transmit their knowledge at various levels—all the more so considering the increasing complexity of research topics and the higher demands of research methods. This is the only way to justify public investment in universities, only in this way can universities fulfil their public mandate and contribute to a competent dialogue over impending societal issues.



The first issues of this series convincingly fulfil these criteria. They present PhD research projects judged as excellent by the examining commissions. The Free University of Bozen-Bolzano's excellent research environment has contributed greatly to these results: The authors were able to approach their research topics in a measured way, under the close supervision of members of the respective PhD advisory commission, who were able to offer a range of perspectives on the relevant research methodology. Furthermore, the university's generous bursary scheme gives PhD students the opportunity to spend periods of study and research abroad, and to thereby gain experience of how other universities conduct research on related topics. They could also present their research methodology and preliminary findings at international congresses – a valuable experience in improving communicative competences. Finally, the regional setting of our university gave them access to a rich variety of empirical data which shows that South Tyrol, while being an alpine region, is by no means represents "periphery". Instead, the research projects demonstrate that regional study objects can have international relevance because the condensed dimensions allow processes to be brought into focus more readily and changes to be monitored more precisely. The region of South Tyrol is indeed affected by global change, as witnessed for instance in the environmental field, where its sensitive alpine landscape is particularly susceptible to harmful developments. So it is possible to see South Tyrol as a sort of laboratory where we can register warning signs earlier and experiment with appropriate counter measures. A greater density of transformation processes can equally be seen in the social field. As a traditional border area, South Tyrol has always been at the cross-roads of different cultures. Its historical experience with multilingualism, with different political and legal frameworks and with the cultural interaction of very different reference points for identity, makes for a background against which some of today's major social challenges such as migration or the globalised economy, can be analysed and interpreted.

These chances for new socially-relevant scientific insights find expression in the PhD studies selected for this series. The university authorities hope that these publications will allow the wider public to gain insights into the quality of the work of these young researchers, and to recognize that the fruits of the financial

investment in this university have direct beneficial effects on the local society. I congratulate the authors chosen for this series and wish them every success in their scientific career hoping they will remain intellectually and emotionally linked to their university and to South Tyrol.

Walter Lorenz

Rector (2008–2016)

Free University of Bozen-Bolzano



## Acknowledgements

I would like to thank my supervisor, professor Gasparella, as well as my co-supervisor, assistant professor Cappelletti, for their help in the development of my research and for being always available. Thanks to all my colleagues and all my friends, near and far away, for sharing with me these three years. I am also deeply grateful to my co-supervisor, professor Tzempelikos, for his hospitality at the Lyles School of Civil Engineering in Purdue and to all his research group, especially Iason and Ying-Chieh.

Finally, special thanks go to my family for their constant support and belief in me.



## Preface

This book is the result of a PhD research study based on modelling and experimental studies in the area of buildings' integrated performance. The research has been conducted in Italy, at the Free University of Bolzano/Bozen, and complemented with experiments at the Lyles School of Civil Engineering of Purdue University (Indiana, USA).

The achievement of superior building energy performance is considered one of the main aims of an appropriate design process or of a suitable management strategy during the buildings' operation phase. Nonetheless, the underestimation of different criticalities, mainly related to the quality of the indoor environment, can strongly affect its attainment. Actually, a confined space that is not able to ensure the occupants' well-being not only reduces the satisfaction of the occupants for the indoor environment, but also induces actions and operations that ultimately can compromise energy efficiency. The great importance of also considering the indoor comfort issues when dealing with building energy balance has been pointed out even in the European Directives on the Energy Performance of Building, (EPBD 2002/91/EC, 2002) and (EPBD 2010/31/EC, 2010). Both the Directives underline that the measures to improve the energy performance of buildings should take into account, among other aspects such as climatic and local conditions and cost-effectiveness, the quality of the indoor environment.

The present research deals with the necessity to express all the different aspects of the building's performance looking beyond the mere energy behaviour, in order to reduce the discrepancy between the calculated building's performance and what will be really achieved during the building's operational life. In recent years, many researchers have tried to apply an integrated analysis approach to their studies, regardless of the aim of the research itself, considering both energy consumption and indoor comfort conditions. On the other hand, the lack of a standardized and consistent set of comfort metrics for the indoor

environmental comfort assessment makes it difficult not only to conduct an integrated evaluation, but also to compare the results from different studies. Despite the specific metric chosen for describing the occupants' perception, a metrics' representation able to express the time constancy or space uniformity of comfort and capable to evaluate different comfort aspects simultaneously with the energy behaviour is still missing. In this study, although it is known that different physical elements can influence the occupants' wellbeing, the analysis has focused especially on the visual and thermal comfort aspects. These depend on the inlet solar radiation effects and, consequently, their management assumes a great importance from an energy point of view too. In Chapter 2 the fenestration (glazing + shade) integrated performances have been compared through a parametric analysis in order to define weaknesses or strengths of different methodological approaches. The standard comfort metrics efficacy in describing the solar radiation effects on thermal and visual occupants' perception and energy consumption has been evaluated, with the aim of defining the best simulation approach for the analysis of the global building's performance. Chapter 3 presents an overview of the different thermal and visual comfort metrics available up to now, considering what international regulations and scientific works propose and underlining weaknesses and strengths. Then, the methodological approach to the definition of a consistent set of representation metrics, which can help the designers to analyse and synthesize the global performance of different design characteristics considering at the same time, energy needs and comfort conditions, has been described. In the Chapter 4, the efficacy of the proposed metrics has been verified using an open space office as a reference test case. This open space office can be considered representative of a demanding building typology, because of the size of transparent surfaces, the concurrent relevance of the visual tasks and glare control, the limited possibility, for the occupants, to adapt their position to the transformation of the internal environmental conditions caused by the transient effects of the incoming solar radiation and, finally, the high level of internal gains. After demonstrating the metric's efficacy, different models for representing the roller shades physical behaviour have been compared in the last chapter with a set of measured data, recorded at the Bowen

laboratories at Purdue University (Indiana, USA), combining thermal and lighting simulation. Weaknesses and strengths of the different models have been identified against experimental data, in order to evaluate their influence in assessing comfort and energy aspects, with the aim of understanding to which extent a more sophisticated model can improve the simulation capability in driving the design decisions.

This study can undoubtedly help researchers and professionals to understand how to consider a building as a whole, how to put together inputs coming from energy and comfort issues and how to provide, at the end of the design or research process, a building able to be efficient not only in theory.

A. Gasparella      Free University of Bozen-Bolzano, Italy

A. Tzempelikos      Lyles School of Civil Engineering,  
Purdue University, Indiana, USA

F. Cappelletti      Iuav University of Venice, Italy





# 1. Introduction

## 1.1 Motivation

As the philosopher Hans Jonas stated, we should “Act so that the effects of your action are compatible with the permanence of genuine human life” (Jonas, 1984, p. 11). However, the current way of life of all the industrialized countries, based on the assumption that the earth is an unlimited source of energy, goes in the opposite direction. In the last 20 years, the effects of climate change are becoming more and more evident, pushing several countries to issue energy efficiency policies with the aim of reducing the energy consumption together with the CO<sub>2</sub> emissions.

As underlined in da Silva, Leal, and Andersen (2012) and Eskin and Türkmen (2008), in the European Union the main primary energy consumers are neither transportation nor industry but the building sector, which accounts for 40 % of total primary energy consumption.

Nowadays, the realization of even more high performance buildings, either new or renovated, constitutes one of the most important measures to reduce energy dependency and greenhouse gas emissions.

In recent years, better buildings’ energy performance have been pursued through enhanced insulation and air tightness levels of the opaque envelope, improved glazing and framing systems for windows components, increased use of renewable sources and energy materials. During the same period, the will to maximize solar gains, in order to reduce heating and lighting needs, together with the increasing request for daylighting and external view by the occupants, has determined a more extensive use of large transparent surfaces in building design, especially in the tertiary sector. This trend, due to both energy and architectonic reasons, has increased the ratio between gains and losses, putting the capability of transparent elements to the test to ensure an adequate level of thermal and visual comfort and to contain energy consumption. Even if transparent surfaces facilitate the use of free and renewable energy sources to reduce heating and lighting needs, the inlet solar radiation, if not efficiently controlled, can cause overheating and visual discomfort, thus leading people to react by operating the building in a less efficient way.

Considering these aspects, in this study the analysis of the energy demand for heating, cooling and lighting, and of indoor comfort conditions (thermal and visual), have been carried out considering the effects of the inlet solar radiation through fenestration with the aim of defining a design approach able to ensure thermal and visual comfort while minimizing energy demand for air-conditioning and lighting.

This aim can be reached operationally through technologically advanced fenestrations and efficiently operated solar shading systems. Both can help occupants manage the solar radiation entering rooms. So that it can happen, during the design phase it is necessary to describe realistically the incoming solar radiation effects on the real comfort perception of the occupants and on the building's energy consumption.

Today, thanks to building energy simulation, it is possible to predict the building behavior accounting in a detailed way for the contribution of different components: climate, envelope, internal gains from lighting, equipment, and occupants, heating, cooling, and ventilation systems, schedules of occupants, equipment and lighting. Nevertheless, often the energy used to operate the building during its service life reaches values that are extremely different to what has been calculated; even considering the uncertainties that characterize building design and building energy assessment. Actually, people's interactions in building management, for example adjusting thermostats for comfort, switching on/off lights or opening windows, can have a significant impact on real energy use. The underestimation of the influence of occupant behavior on energy consumption is often related to an incorrect evaluation of the indoor environmental quality (IEQ) during the design phase. In order to achieve better comfort conditions, an occupant who is not satisfied with the internal environment, will probably act in a different way with respect to what he/she is envisaged to do in the design phase, determining in some cases an increase in energy consumption.

The possibility to design the indoor environmental quality realistically can help the designer to reduce the gap between simulated and real occupant behavior and, from this point of view, an efficient building façade design can play a central role.

The importance of considering the occupants' level of satisfaction with the internal environment is also recognized by the European Directives on the Building Energy Performance (EPBD) (EPBD 2002/91/EC, 2002) and (EPBD2010/31/EC, 2010). Unfortunately, even if it is indicated that indoor climate conditions shall be taken into account when putting minimum energy requirements in place "in order to avoid possible negative effects", within the energy efficiency policies issued across the European countries, there are currently no clear requirements describing how this can be achieved. This lack of evident indications often means insufficient attention is paid to ensuring suitable comfort conditions for the occupants by the designers. Through EN 15251:2007 (European Committee for Standardization [CEN], 2007b), the European Committee for Standardization has provided criteria for the calculation of building energy use which are consistent with the provision of an indoor environment that is consistent with the occupants' comfort and wellbeing (Nicol and Wilson, 2010). The same standard affirms that: "uncomfortable occupants are likely to take actions to make themselves comfortable which may have energy implications" (p. 5); "an energy declaration without a declaration related to the indoor environment makes no sense" (p. 5).

Up to now, these concepts are rarely applied during the design phase, and the consequences of this approach can be, at the same time, social, economic and ecological.

Considering that people spend 60–90 % of their life in indoor environments (homes, offices, schools, etc.), their quality can play a very important role in the health of the population, with social consequences and economic implications. For instance, when building occupants feel too warm, they also feel tired, while when they feel too cold, they can be restless and distracted (Kunkel, Kontonasiou, Arcipowska, Mariottini, & Atanasiu, 2015). Daylight also has important effects on the occupants' perception of the confined environment. From a psychological point of view, daylight effectively stimulates the human visual and circadian systems. Concerning a more global concept of well-being, daylight enables occupants to fulfil two basic human requirements: they are able to focus on tasks and to perceive space, as well as experience some environmental stimulation (Kunkel

et al., 2015). Finally, due to the reduction of energy demand, buildings are becoming more airtight while indoor air pollution can be 2–5 times higher than in outside air (Kunkel et al., 2015).

From an economic and ecological point of view, as underlined in Hoes, Hensen, Loomans, de Vries, and Bourgeois (2009), occupants have influence due to their presence and activities in the building and due to their control actions that aim to improve indoor environmental conditions (thermal, air quality, light, noise). This means that the level of occupants' comfort plays a crucial role in determining the amount of energy needed to operate the building (Nielsen, Svendsen, & Jensen, 2011), since unsatisfactory indoor conditions induce occupants to react in order to restore or ensure their comfort (Humphreys & Nicol, 1998). This effect is becoming more and more evident, especially considering the diffusion of low energy buildings, in which the weight of the user's behavior on the building's energy balance is even more important.

Based on the above-mentioned considerations, the need for indoor environmental conditions being treated with the same level of importance as energy efficiency appears clear, enabling energy renovation and comfort enhancement investments to be mutually reinforcing (Kunkel et al., 2015).

The way to achieve really efficient buildings, which are able to consume less energy and maximize comfort conditions, requires an integrated approach to the design process. It can be reached moving from an "energy reduction" building design approach to a "global oriented" approach, able to consider as priorities both the reduction of the energy consumption and the improvement of suitable comfort conditions at the same time.

In this study, a methodology for the calculation and the assessment of the buildings' global performance, considering both the energy needs and the necessity of guaranteeing a high level of indoor environmental quality (IEQ), has been proposed. Special attention has been reserved to the necessity for describing the internal environmental conditions in such a way as to evaluate the uniformity distribution of comfort through the space and its constancy over time, even considering simultaneously different comfort aspects.

## 1.2 Literature analysis

As previously underlined, in this study special attention has been reserved to energy consumption and comfort conditions that can be greatly influenced by the inlet solar radiation. For this reason, the literature analysis has concentrated on the scientific production dedicated to the integrated assessment of different energy and non-energy aspects related to the interaction of opaque and transparent envelope components.

The opaque envelope represents for the building the means through which it communicates with the external environment. It defines the building's shape, allows it to understand what activities are being carried out inside and protects the occupants from heat, cold and bad weather.

Fenestrations, punching the opaque envelope, create a link between the internal and external environment, both from a visual and energy point of view. Obviously, this role of connector can have negative and positive effects. This dichotomy is well represented through the words, used in Latin and in English, to describe the fenestration:

- *finis extra*
- *wind eye*.

Fenestration can be interpreted as a thermal wound, because its thermal transmittance is still lower if compared to a wall and, on the contrary, its transparency can cause overheating problems. At the same time, without the sequence of full and empty elements, without the shades produced by natural light, architecture would not exist. Moreover, if designed in an efficient manner, natural light can have positive effects on the building and occupants' performance from different points of view.

In Chapter 15 of the *2013 ASHRAE Handbook–Fundamentals*, (American Society of Heating Refrigerating and Air Conditioning Engineers [ASHRAE], 2013a, p. 15.1), fenestration is defined as an architectural term that refers to the arrangement, proportion, and design of window, skylight, and door systems in a building. It can serve as a physical and/or visual connection to the outdoors, as well as a means to admit solar radiation for daylighting and heat gain to a space. Actually, fenestration affects building energy use through four basic mechanisms: thermal heat transfer, solar heat gain, air leakage, and daylighting.

Fenestrations with shading devices have a degree of thermal and optical complexity far greater than that of unshaded fenestrations. For this reason they are referred to as complex fenestration systems (CFS).

In the last few years, many researchers have focused their analysis on the fenestration and/or complex fenestration performance, with the aim of assessing the impact of different design parameters (a window's dimension and orientation, thermal and optical properties of glazing and shading systems, control strategies) on energy demand for heating, cooling or lighting, and internal comfort conditions.

Starting from the works' final purpose, the research on fenestration and/or complex fenestration systems can be classified in four main fields, as reported hereunder.

#### 1.2.1 Impact on building energy needs

Eskin and Türkmen (2008) analyzed the effect of different building parameters, among which window areas and glazing systems, on annual heating and cooling energy requirements for office buildings in Turkey, comparing the simulation results to on-site measurements done in Istanbul. Poirazis, Blomsterberg, and Wall (2008) used a comfort set-point strategy for temperature and lighting defining a minimum acceptable level for thermal comfort satisfaction. Tsikaloudaki, Theodosiou, Laskos, and Bikas (2012) evaluated the cooling energy performance of residential windows using a parametric approach, with the aim of highlighting the impact of the window configuration on its energy behavior in terms of geometrical characteristics, thermophysical and optical properties, as well as orientation and shading levels. The relation between the use of shading devices and the availability of natural light was investigated by Kim, Lim, Lim, Schaefer, and Kim (2012), who suggested that optimal shading systems should increase daylight levels while controlling the amount of excessive sunlight. Further, da Silva et al. (2012), analyzed the impact of different shading control models (pattern or strategy) on the calculated overall energy demand for heating, cooling and lighting, as well as the impact on choosing the best-performing transparent facade option for a single-occupant office. Zhu, Chew, Lv, and Wu (2013) compared the influence of window frame type, glass

type and shading type on the heating and cooling energy needs in office buildings.

### 1.2.2 Impact on building energy needs and visual comfort

The selection's optimization of window size and of shade properties with reference to the cooling and lighting energy performance considering different control strategies has been analyzed by Athanassios Tzempelikos and Athienitis (2007). Mahdavi and Dervishi (2011), compared the performance of a predictive simulation-supported lighting and shading control system, with four conventional approaches. They tried to optimize the electrical power for lighting, the mean workstation horizontal illuminance (HI), and the unified glare ratio (UGR) for a reference position in the room, combining all of those inputs in an aggregate utility function (UF). Also Nielsen, Svendsen, and Jensen (2011) analyzed the potential of automated dynamic solar shading in office buildings, quantifying the annual energy demand for heating, cooling and lighting. The temperature set-point was used according to the thermal comfort categories, as prescribed in the technical standards, while the Daylight Factor (DF) and the usable area on the work plane have been utilized for the assessment of the daylight conditions. Ochoa, Aries, van Loenen, and Hensen (2012), proposed energy and visual criteria suitable for multi-optimization analysis techniques. Global energy consumption had to be minimized, with the window's size able to ensure a minimum illuminance value, a Discomfort Glare Index (DGI) of 22, a minimum illuminance uniformity for at least 50 % of the total working hours. Oh, Lee, and Yoon (2012), considered the total energy consumption and DGI to define the optimum automatic control strategy for slat-type blinds. Shen and Tzempelikos (2013) conducted a sensitivity analysis to identify the most influential factors on daylighting and energy performance of perimeter offices with automated shading. Again annual lighting, heating and cooling demand and annual source energy consumption, as well as Useful Daylight Illuminance (UDI), were used as performance indicators. R. Singh, Lazarus, and Kishore (2015) performed a parametrical analysis on different glazing and internal woven roller shades comparing their effects on energy consumption, Daylight Autonomy (DA), UDI and DGI. DA and glare-free annual time have been used



as long term metrics at two reference positions. Fasi and Budaiwi (2015) analyzed the impact of daylight integration and visual comfort on building energy consumption for office buildings in hot climates, using DF and DGI.

### 1.2.3 Impact on building energy needs and thermal comfort

Buratti, Moretti, Belloni, and Cotana (2012), in order to evaluate different glazing types in a classroom, analyzed the heating and cooling annual energy demand and used the average Predicted Mean Vote (PMV) and Predicted Percentage Dissatisfied (PPD) in the occupation period as long-term metrics to describe the thermal discomfort. Wang et al. (2015), developed and validated the energy model of a school built with Passive House standard and evaluated the influence of several factors (indoor set-point temperatures, pre-ventilation, sun shading system, efficiency of the heat recovery facility) on energy consumption and thermal comfort, assessed as internal air temperature frequency. Bessoudo, Tzempelikos, Athienitis, and Zmeureanu (2010), evaluated the impact of shading systems on thermal comfort near facades with large glazing areas using experimental measurements. The hourly evolution of the Mean Radiant Temperature (MRT), corrected for the effect of solar radiation falling on the person, was analyzed for representative days. A. Tzempelikos, Bessoudo, Athienitis, and Zmeureanu (2010), used the same approach to evaluate the effect of different glazing and shading properties on dynamic Thermal Sensation using the two-node thermal comfort model. Hwang and Shu (2011) assessed the effect of building envelope regulations on thermal comfort and cooling consumption. Through a parametric analysis, they evaluated the effect of glazing types, window to wall ratio (WWR) and overhang on the occurrence of discomfort and severity of overheating. Also in this case, the beam and diffused solar radiation falling on the human body was considered in the PMV and PPD calculation. The same was done by Cappelletti, Prada, Romagnoni, and Gasparella (2014), in order to evaluate the influence of different glazing systems on heating and cooling energy needs. An office building was used as the reference case, maintaining fixed comfort conditions. PMV and PPD were used to obtain a long term index in terms of weighted discomfort time, mapping the performance on 9 positions in the room. Kolarik, Toftum, Olesen, and Jensen (2011) used the percentage of working hours during which PPD was larger than 10 % and the

annual primary energy use for cooling and heating in order to evaluate the performance of conventional all-air VAV ventilation system and thermo-active building system (TABS) supplemented with CAV ventilation.

#### 1.2.4 Impact on building energy needs, thermal and visual comfort

David, Donn, Garde, and Lenoir (2011) proposed simple indices to compare thermal and visual efficacy of different solar shading systems, balancing solar protection and natural light. Thermal efficacy is expressed through the fraction of the beam solar irradiation that impacts the glazing with and without the use of solar shadings, while thermal comfort is analyzed as a consequence of the cooling demands. Visual efficacy is assessed by means of DA, UDI and the ratio of the working plane where the illuminance overcomes 8000 lux. In Liu, Wittchen, and Heiselberg (2015), different control strategies for intelligent facades were evaluated looking for the optimization of comfort performance and the minimization of HVAC energy demand for an office building. Long-term thermal comfort was evaluated through the time percentage in the comfort classes suggested by EN 15251:2007 (European Committee for Standardization [CEN], 2007b). Visual comfort is imposed cutting all direct solar radiation. Vanhoutteghem, Skarning, Hviid, and Svendsen (2015) proposed a method to choose different window properties to ensure the requested performance for a Danish nearly Zero Energy Building (nZEB). A long-term index, the period percentage in which the Operative Temperature (OT) overcomes a specific range, and an enhanced DF, which considers the median diffused illuminance available outdoors in specific analysis location, have been used, together with the heating demand, to analyze the influence of size, orientation and glazing properties of facade windows. Mainini, Bonato, Poli, and Speroni (2015) proposed different strategies to improve the transparent part of the envelope in order to obtain low HVAC primary energy consumption and improving comfort conditions. The hourly thermal comfort was evaluated through the PMV and PPD in accordance with ISO 7730 (CEN, 2005c) and expressed as a monthly average. The DGI, calculated for a single point in the room, and the luminance distribution on the glazing surface, were used as visual comfort parameters. In Roetzel, Tsangrassoulis, and Dietrich (2014), the authors compared the impact of building design and occupancy on comfort and energy

performance in offices. Two different occupant behaviors were simulated, analyzing the global energy consumption (heating, lighting, office equipment and cooling), the long-term thermal comfort conditions through the percentage of working time with comfortable temperature according to the ASHRAE Standard 55 – *Thermal Environmental Conditions for Human Occupancy* (2013b) considering 20 % dissatisfied, the DA and the percentage of working time when shading is activated. Yao and Zhu (2012) proposed a thermotropic double-glazed window as a possible technical solution for energy saving (cooling and heating demand) and comfort requests (room base temperature and illumination uniformity). Yao (2014a) carried out field measurements and simulation analysis on a retrofitted residential building in China, considering heating and cooling needs and thermal and visual comfort conditions. Room base temperature, transmitted solar radiation as well as PMV and PPD, in terms of annual profiles, and cumulated percentage distributions, were calculated to assess the thermal comfort, while the DGI was used for the visual comfort evaluation.

Analyzing the described references, some trends appear.

Few studies still use metrics based on standard conditions or typical days, while most of them evaluate the visual and thermal comfort along a reference year, considering the representative climatic conditions, which improves the quality of the information (Carlucci, Causone, De Rosa, and Pagliano, 2015).

This leads to the need for synthesizing the metrics over the considered period (long-term metrics).

Attempts have been made in this direction considering average values, frequency distributions or cumulative occurrence (global discomfort time, fraction of time in comfort, comfort classes) (Carlucci and Pagliano, 2012).

Moreover, those metrics are typically related to a specific position. With the exception of thermal comfort, which is assumed as an indicator of the average conditions in the space, there is the need to account for the variability over the space. This has been addressed in some cases assuming some representative positions, in some other considering average values, and in a few cases mapping the values on the surface.

Most of the papers that underline the importance of evaluating the building's performance taking into account both the energy consumption and the indoor comfort conditions, suggest including visual and thermal aspects. Analyzing the building's performance only through its energy consumption can lead to wrong conclusions, especially considering the weight of occupant behavior different to what has been envisaged during the design phase.

The lack of a standardized and consistent set of comfort metrics hinders not only conducting an integrated evaluation, but also comparing the results from different studies. The availability of proper and consistent synthetic indicators, able to express the comfort time constancy or space uniformity and to evaluate different comfort aspects simultaneously with the energy behavior, therefore seems opportune.

Through the following tables, the literature analysis has been summarized, in order to provide a quick comparison between the four main fields. The energy aspects have been subdivided according to the consumption analyzed and the index used to represent them. Visual and thermal comfort indexes have been distinguished according to their typology. The intended use of the reference test case has been reported, as well as the methodology and the type of analysis used.

The following list introduces the acronyms used in the literature analysis tables:

- Energy consumption: H = heating, C = cooling, L = lighting, V = ventilation, E = electricity;
- Index for energy consumption: S = site energy, P = primary energy;
- Visual and thermal comfort indices typology: L = local, Z = zonal, St = short term, Lt = long term;
- Intended use: O = office; R = residential, S = school;
- Methodology: S = simulation, SM = simulation and measurements;
- Analysis: PA = parametrical analysis, O = optimization, SA = sensitivity analysis, MV = model validation, StA = statistical analysis.

Table 1 – Energy needs

Reference	Energy		Visual Comfort	Thermal Comfort	Intended Use	Methodology	Software	Analysis
da Silva et al. (2012)	H - C - L	S			O	S	Energy Plus	SA
Eskin and Türkmen (2008)	H - C	S			O	SM	Energy Plus	PA - MV
Poirazis et al. (2008)	H - C - L - E	S			O	S	IDA ICE 3.0	SA
Tsikaloudaki et al. (2012)	C	qc			R	S	Energy Plus	PA - StA
Kim et al. (2012)	H - C	S			R	S	IES	PA
Zhu et al. (2013)	H - C - L - E							
	S				O	S	Tianzheng Building Energy Consumption Software	PA

Table 2 – Energy needs and visual comfort

Reference	Energy		Visual comfort		Thermal Comfort	Intended Use	Methodology	Software	Analysis
Tzempelikos and Athienitis (2007)	H-C-L	S	L/Lt	DAR		O	S	In-house thermal + lighting code	PA
Mahdavi and Dervishi (2011)	L	S	L/St	WP ill		O	S	Radiance	PA
Nielsen et al. (2011b)	H-C-L	P	L/St	DF		O	S	iDBuild	PA
Ochoa et al. (2012)	H-C-L-V	P	L/St	DGI		O	S	Energy Plus	O
Oh et al. (2012)	H-C-L	S	L/St	DGI		O	S	Energy Plus	PA



Reference	Energy		Visual Comfort	Thermal Comfort		Intended Use	Methodology	Software		Analysis
Buratti et al. (2012)	H - C	P		L/Lt	PMV	S	SM	TRNSYS	Energy Plus	PA
Wang et al. (2015)	H - C - V	P		L/St	Int Tair frequency	S	SM	TRNSYS		MV PA
Bessoudo et al. (2010)	H	P		L/St	OT <sub>IRR</sub> - RTA	O	SM	In-house thermal code		MV PA
A. Tzempelikos et al. (2010)	H	P		L/St	RTA - MRT <sub>IRR</sub>	O	SM	In-house thermal code		MV PA
Cappelletti et al. (2014)	H - C	P		L/Lt	PMV <sub>IRR</sub> - PPD <sub>IRR</sub>	O	S	TRNSYS		PA
Kolarik et al. (2011)	H - C	P		L/Lt	PPD	O	S	IDA/ICE		PA



Table 4 – Energy needs, thermal and visual comfort

Reference	Energy		Visual comfort		Thermal Comfort		Intended Use	Methodology	Software	Analysis
Vanhoutteghem et al. (2015)	H	S	L/St	DF enhanced	L/Lt	OT	O	S	Energy Plus - Daysim	PA
David et al. (2011)	C-L	S	L/Lt	UDI <sub>mod</sub>	L/Lt	Solar shading coefficient	O	S	Energy Plus	PA
Liu et al. (2015)	H-C-L-V	P	L/Lt	Direct solar radiation	L/Lt	EN 15251:2007	O	SM	In-house thermal + lighting code	PA
Mainini et al. (2015)	C-L	P	L/St	DGI	L/Lt	PMV- PPD	O	S	Energy Plus -Radiance	PA
			Lum unif							

Reference			Energy			Visual comfort			Thermal Comfort	Intended Use	Methodology	Software	Analysis
Yao (2014a)	H -C	S	H -C-L - E	S	L/ILt	L/ILt	% time	DA	L/Lt	ASHRAE 55	O	S	Energy Plus
	L/ILt	DGI	H -C	S	L/Lt	Ill unif	L/Lt	T <sub>room</sub>	R	S	Energy Plus	PA	PA
	L/Lt	L/Lt	PMV - PPD	R	SM	Energy Plus	PA	PA	PA	PA	PA	PA	PA
	Transmitted solar radiation	T <sub>room</sub>											
Roetzel et al. (2014)	H -C-L - E	S	L/ILt	L/ILt	DA	L/Lt	ASHRAE 55	O	S	Energy Plus	PA	PA	PA

### 1.3 Research objectives

The main aim of this research is the definition of a methodology for the calculation and the assessment of buildings' global performance, considering both the energy needs and the necessity of guaranteeing a high level of indoor environmental quality (IEQ).

Generally the IEQ of a confined space is described through its thermal, visual and acoustic comfort conditions and its air quality. As previously underlined, in recent years modern architecture has been characterized by a more and more intensive use of large transparent surfaces, which means a more and more intensive solar radiation entering confined space. Considering this fact, the thermal and visual aspects, which represent the comfort sensations more influenced by solar radiation, have been chosen as the main aspects to investigate for the indoor environmental quality evaluation.

In this study the analysis has focused on the evaluation of the integrated performance of the fenestration systems, shaded or unshaded, putting their capacity of influencing the building's performance to the test considering both energy consumption and comfort conditions.

Summarizing, three working steps have been identified:

#### 1.3.1 Comparison of fenestrations and complex fenestration integrated performance by means of simulation

The fenestration integrated performances have been compared through a parametric analysis in order to define weaknesses or strengths of different methodological approaches. The main aims of this step were:

- the evaluation of the standard comfort metrics efficacy in describing the solar radiation effects on thermal and visual occupants' perception and energy consumption;
- the definition of the best simulation approach for the analysis of the global building's performance identifying the most suitable building simulation software

### 1.3.2 The characterization of consistent set of representation metrics for mapping building's global performance:

#### Thermal and visual comfort and energy efficiency

As underlined in Chapter 1.2, the literature analysis highlighted the lack of a standardized and consistent set of representation metrics able to express the time constancy or space uniformity of comfort and to evaluate different comfort aspects simultaneously with the energy behavior. This step proposes a possible set of representation metrics, which can help the designers to analyze and synthesize the global performance of different design characteristics considering together, and at the same time, different comfort aspects. Then these representation metrics have been tested on a simulated environment in order to prove their capability to reproduce and qualify the performance of the envelope components when comparing building configurations characterized by high solar and daylighting gains and different window and shading configurations. An integrated way of representing comfort and energy performance has been proposed, in order to enable a quick comparison between different design configurations.

### 1.3.3 Comparison of different simulation models for the evaluation of roller shading systems

Regardless of the metrics chosen to represent the complex fenestration (glazing plus shade) influence on comfort conditions, first of all a model able to realistically simulate this component's performance is needed. Solar transmission, considering both the visible and thermal part, through glazing systems no longer represents a problem. The widely used building simulation codes are able to manage this task in a very effective way. On the contrary, the large number of studies which deal with the assessment of solar shading systems representation models, demonstrates the lack of a standardized approach. In the last chapter of this study, different approaches for the characterization of the roller shade materials behavior embedded in the common simulation codes have been evaluated, with the aim of understanding which one is able to provide more realistic results. In order to reach this goal, a set of measured data, recorded at the Bowen laboratories of the Purdue University (Indiana, USA), called LAB1 and LAB2, has been used to verify and validate the different roller shade models.

## 2. Complex Fenestration System (CFS) Global Performance Comparison by Means of Simulation: A Parametric Approach

### 2.1 Introduction

As underlined in the Introduction, only by analyzing the overall performance of a complex fenestration system (CFS), which means considering its influence both on energy needs and comfort conditions, is it possible to predict the global energy consumption, related not only to the building's envelope and equipment but also to the occupants' actions.

Like all systems in nature, buildings can also be considered a dynamic system. In order to evaluate and predict the behavior of a system which continuously changes over time, it is necessary to build a model of the reality able to describe which variations happen on the system as time passes.

By means of dynamic simulation software, a numerical model of the energy processes which characterize the building can be built, and thanks to this model, reality can be represented with the aim of understanding and predicting how the building system works.

According to EN 15251:2007 (European Committee for Standardization [CEN], 2007b), three different calculation methods can be applied in order to predict the building's energy behavior:

1. a monthly calculation, which gives correct results on an annual basis, but the results for individual months close to the beginning and the end of the heating and cooling season can have large relative errors;
2. an hourly calculation method, which tries to join the precision of some dynamic methods with the simplicity of the monthly one. This method produces hourly results, but the results for individual hours are not validated and individual hourly values can have large relative errors;
3. a dynamic method, more accurate and based on the use of very complex models and software which need the input of several building's parameters.

All the three methods listed can be considered reliable under specific limits and purposes. However, when it is necessary to analyze environmental conditions characterized by high variability, a dynamic analysis becomes opportune. This happens, for example, when lighting and cooling consumptions are considered.

Moreover, dynamic simulation software is able to account, in a detailed way, for the contribution of all the different components. It can provide information about the building's global performance, including not only energy consumption but also comfort aspects, and verifying as they change according to the design decisions.

Considering that the inlet solar radiation is characterized by a high variability, not only over the year but also during the same hour in a day, the dynamic approach has been chosen in order to analyze the strengths and weaknesses of the complex fenestration systems in a realistic way. Actually, in order to assess the buildings' global performance correctly, the detailed analysis of the inlet solar radiation (visible and thermal), and its indoor distribution, represents a crucial aspect.

Building simulation techniques can help to reach this target, as they allow us to predict the building's behavior right from the early design steps, and to account, in a detailed way, for the contribution of all the different components (opaque envelope, glazing and shading systems, HVAC systems, control strategies, etc.). Even if with some complexity, they can provide information about the global performance, including thermal energy, lighting and daylighting, thermal and visual comfort aspects.

Nowadays, various simulation tools are available to designers both commercially and free-of-charge. The decision as to which tool to use is closely correlated with the aim and the objectives of the analysis. Moreover, often it could be necessary to couple different simulation softwares or programming codes, in order to maximize and optimize the results that can be obtained singularly from each one of them.

Before describing the objectives of each step of the simulation procedure and the methodology used for reaching them, it is necessary to remember that the main aim of the analysis was the definition of a methodology for the assessment of the building's global performance; a methodology which has to be able to assess, simultaneously, energy consumption and comfort conditions.

## 2.2 Simulation parameters for parametric analysis

A parametric analysis can help researchers and designers to understand better how and how much buildings' performance can be affected by variations of specific, passive or active, components.

Since in this study the analysis focused on the fenestration systems, only those elements whose modification can have an effect on them have been considered as variables. This is the reason why the factorial plan used to perform the parametric analysis has combined the following three design characteristics:

- windows, varying their sizes, orientation and position;
- glazing, modifying their solar and optical characteristics;
- shading systems, changing their typology, solar and optical properties and location compared to the window.

Other building characteristics, such as the intended use, the geometric dimension, the opaque elements' stratigraphy and the systems (heating, cooling and lighting) typology have remained fixed, considering that these building characteristics have less impact on the incoming solar radiation availability and distribution.

Moreover, in order to compare different design configurations' performance under equivalent comfort conditions, precise settings for heating, cooling and lighting systems management and shading device control have been used.

In the following, only the buildings' characteristics which have not been changed across the different steps of the parametrical analysis, either because they are not considered as variables or because the specific methodological approach used did not require a modification, will be described.

### 2.2.1 Reference test case: Intended use and geometrical characteristics

An open space office has been chosen as a reference test case. It can be considered as representative of a specific demanding building typology, because of the size of transparent surfaces, the concurrent relevance of the visual tasks and glare control, the limited possibility, for the occupants, to adapt their position to the transformation of the internal environmental conditions caused by the transient effects of the incoming solar radiation and, finally, the high level of internal gains.

The floor surface is equal to 100 m<sup>2</sup>, with 3 m of internal height. Regarding the envelope, only the walls and roof are exposed to the external environment. The floor has been considered as an adiabatic surface, supposing that the environmental conditions of the adjacent spaces were the same as the reference model. All the simulations were performed using the same climatic location: Rome, Italy (Lat. N 42° 54' 39''; HDD18: 1420 K d - CDD18: 827 K d).

### 2.2.2 Characteristics of components: Opaque envelope

The stratigraphy of all the opaque elements, both the vertical walls and roof slab, is identical, with an internal clay block layer of 20 cm thick and an external insulation layer. In a first phase, the thickness of the insulation layer was set equal to 0.05 m and then to 0.10 m, in order to obtain a thermal transmittance equal to 0.45 W m<sup>-2</sup> K<sup>-1</sup>. Both the solar and visible absorptance coefficients were set to 0.6 for the floor (internal side) and 0.3 for the vertical walls and the roof (both sides). The wall emissivity is 0.9, both for the internal and the external side.

### 2.2.3 Characteristics of components: Transparent envelope

The windows were distributed on a single façade or on opposite façades, and the room oriented towards 2 different orientations, varying the glazed area (2 sizes) and the glazing systems (4 types). The following table describes the values assumed in the simulations:



Table 5 – Transparent envelope characteristics

Glazing	DH: Double Glazings with high SHGC
	$U_{gl} = 1.140 \text{ W m}^{-2} \text{ K}^{-1}$ ; SHGC = 0.608; $\tau_d = 0.439$
	DL: Double glazing with low SHGC
	$U_{gl} = 1.099 \text{ W m}^{-2} \text{ K}^{-1}$ ; SHGC = 0.352; $\tau_d = 0.205$
	TH: Triple Glazings with high SHGC
	$U_{gl} = 0.613 \text{ W m}^{-2} \text{ K}^{-1}$ ; SHGC = 0.575; $\tau_d = 0.391$
Window Size	TL: Triple Glazings with low SHGC
	$U_{gl} = 0.602 \text{ W m}^{-2} \text{ K}^{-1}$ ; SHGC = 0.343; $\tau_d = 0.191$
Window Size	S1: width = 9; height = 1.5 m; area = 13.5 m <sup>2</sup> (WWR 45 %)
	S2: width = 9; height = 2.5 m; area = 22.5 m <sup>2</sup> (WWR 75 %)
Window distribution	East (E); East + West (E+W); South (S); South + North (S+N)

#### 2.2.4 Heating, cooling and lighting systems

The building's performance related to the HVAC system was studied without modelling a full system in detail. It was simulated as an ideal unit that mixes air at the zone exhaust condition with the specified amount of outdoor air, and then adds or removes heat and moisture at 100 % efficiency in order to produce a supply air stream at the specified conditions.

Regarding the HVAC system, the inlet air temperature during working hours is controlled to maintain the Operative Temperature (OT) within the comfort range 20 °C–24 °C in the heating season and 23 °C–26 °C in the cooling one, as suggested for the II class comfort level according to EN 15251:2007 (CEN, 2007b). The relation between the air temperature,  $T_a$ , the mean radiant temperature,  $T_{mr}$  and the operative temperature,  $T_o$ , is in agreement with the technical standard EN ISO 13790:2008 (CEN, 2008).

$$T_a = 1.52 \cdot T_{mr} + 2.52 \cdot T_o \quad (1)$$

Equation 1 – Relation between air, mean radiant and operative temperature

During the non-occupation period, the system is operated only if the operative temperature is lower than 15 °C, and a maximum value, which depends on the

hour of the day. This is 38 °C from 18:00 to 24:00 and it then gradually reduces to 28 °C at 8:00.

The heating and cooling systems controlled by means of  $T_{op}$  allow us to use the energy demand as an indicator of the envelope's passive energy and comfort performance. Moreover, the energy performance of different cases can be compared under equivalent comfort conditions.

Regarding the lighting system, given the specific intended use of the simulated environment, a Light Power Density (LPD) equal to 12 W m<sup>-2</sup> was considered, as suggested in Chapter 18 of the *2013 ASHRAE Handbook–Fundamentals* (American Society of Heating Refrigerating and Air Conditioning Engineers [ASHRAE], 2013a). The luminaires were equipped with T-8 fluorescent lamps installed on the ceiling. The lighting's schedule considers the system always to be switched off during the weekend and the non-occupation hours. Considering that connection elements, such as stairs or aisles were not considered, a hypothetical consumption related with an emergency system was neglected. The electric power requested by the lighting system increases or decreases continuously and linearly, depending on the level of illumination provided by natural light in order to maintain a precise illuminance target above the work plane. The illuminance target was fixed equal to 500 lux as prescribed by EN 12464-1 (CEN, 2011a) for office use.

The energy consumption for heating, cooling and lighting was expressed as the primary energy use in order to allow the comparison through a single global indicator. Conventional values of 0.8 as the seasonal thermal energy production efficiency, 3 as the seasonal Energy Efficiency Ratio for cooling and 2.174 primary energy content per unit of electrical energy were assumed.

### 2.2.5 Internal gains

The office occupation period is from 8:00 am to 6:00 pm, Monday to Friday. According to the standard UNI 10339:1995 (Ente italiano di normazione [UNI], 1995) the occupancy index for an open office can be fixed as 0.12 people m<sup>-2</sup> which corresponds to 12 occupants. The occupants' activity is defined as sedentary, with a metabolic flux equal to 70 W m<sup>-2</sup> or 1.2 met. The heat flow is divided into the sensible portion of 75 W (58 % as radiant exchange) and latent heat of 55 W. The unit thermal resistance of clothing is 1 clo (such as with typical work

clothing with long pants, shirt, tie and jacket) during the winter season, and 0.5 clo (such as with lightweight summer pants and light long-sleeved shirt) during the summer season. The conventional winter season is from October 1 to March 31, while the summer season from April 1 to September 30. The internal loads related to electrical equipment are quantified considering 12 computers, 12 monitors, a laser printer and a copier, with constant average power during the occupation period, and are equal to  $13.7 \text{ W m}^{-2}$ .

### 2.2.6 Analysis grid

The variability of the internal comfort conditions has been evaluated by means of an analysis grid consisting of 9 points.

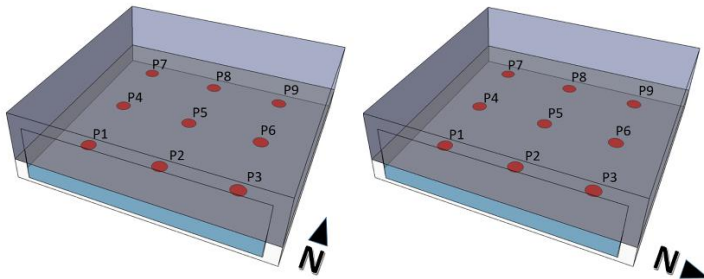


Figure 1 – Plan of the office module with the analysis grid representation

## 2.3 Objectives and methods

Along the different steps which have characterized the parametric analysis, a share objective can be recognized: the evaluation of different complex fenestration systems effects on visual and thermal comfort and on the total building energy needs for heating, cooling and lighting.

### 2.3.1 Step 1: CFS global performance assessment with the application of standard comfort metrics

#### a. Thermal comfort

The evaluation of the long-term comfort conditions (on a seasonal basis) was conducted by computing the hourly value of the standard Predicted Mean Vote

(PMV) index in 9 different positions in the office and considering some statistical indicators of distribution (the median, minimum, maximum and the inter-quartile range).

According to EN ISO 7730:2005 (CEN, 2005c), PMV is an index that predicts the mean value of the votes of a large group of people on the 7-point thermal sensation scale, based on the heat balance of the human body. Thermal balance is obtained when the internal heat production in the body is equal to the loss of heat to the environment. In a moderate environment, the human thermoregulatory system will automatically attempt to modify skin temperature and sweat secretion to maintain heat balance. The evaluation of the confined space through the index deviation compared to a reference value, allows us to avoid the analytical analysis of the quantities which act on the microclimate due to the index ability of expressing the consequences on the human body.

#### b. Visual comfort

Visual discomfort conditions have been assessed through the calculation of the total hours in a year during which a certain value of the Discomfort Glare Index (DGI) has been overcome. Even if DGI is a short term and local index, calculating the percentage of likely discomfort hours with respect to the total number of occupied hours allows for the distribution of the discomfort sensation along a reference period, and to obtain a long-term evaluation.

According to Carlucci et al. (2015), DGI derives from the CGI and aims to predict glare from large sources, such as a window, described by its luminance  $L_{win}$ .

$$DGI = 10 \log \left[ 0.478 \sum_{i=1}^n \left( \frac{L_{s,i}^{1.6} \cdot \omega_{s,i}^{0.8}}{L_b + 0.07 \omega^{0.5} \cdot L_{win} \cdot P_i^{1.6}} \right) \right] \quad (2)$$

Equation 2 – DGI equation according to Chauvel, Collins, Dogniaux, and Longmore (1982)

Where:  $L_s$  is the luminance of the glare source (i.e. the maximum luminance as observed from the user's viewpoint);  $L_b$  is the background luminance (i.e. the average luminance in the field of view with the glare source removed);  $\omega$  is the solid angle subtending each source from the point of view of the observer,

modified with respect to field of view and Guth position index of each luminaire (i). DGI values are associated with several levels of discomfort glare. As specified in EN 15251:2007 (CEN, 2007b), considering the specific intended use of the simulated environment, the Unified Glare Rating (UGR) should lie in the range 16-19, which corresponds to a DGI range 20–22. For this study a value equal to 22 was chosen.

c. Daylight availability

In this step, the daylight availability related to the different design configurations was not considered.

d. Simulation environment

Both the energy performance and the internal comfort conditions have been calculated by means of Energy Plus 7.1.

e. Shading device: Typology, properties and simulation approach

In this step, three different moveable shading systems have been considered: one roller shades and two venetian blinds with different reflectivity values. All the systems were considered to be located externally compared to the window position. The data related with the solar and visible properties of the shading devices were taken from the Energy Plus DataSet. The following tables summarize the shading characteristics:

Table 6 – Roller shade solar and visible properties

	$\tau_s$	$Q_s$	$\tau_v$	$Q_v$
RS	0.4	0.5	0.4	0.5

Table 7 – Venetian blind solar and visible properties

	Front side beam $Q_s$	Back side beam $Q_s$	Front side diffuse $Q_s$	Back side diffuse $Q_s$
BH	0.8	0.8	0.8	0.8
BL	0.2	0.2	0.2	0.2

As described in the *EnergyPlus Input Output Reference* ( Lawrence Berkeley National Laboratory, n. d.) the WindowMaterial:Shade object assumes that the transmission, absorption and reflection of material such as drapery or translucent roller shades are not dependent of incidence angle. In other words, they are considered to be perfect diffusers (all transmitted and reflected radiation is hemispherically-diffused). Moreover, reflectance and emissivity properties are assumed to be the same on both sides of the shade.

On the contrary, WindowMaterial:Blind has solar and visible transmission and reflection properties that strongly depend on the slat angle and the angle of incidence of solar radiation.

#### f. Visual comfort control settings

The shading devices are closed in relation to the amount of incident radiation on the outdoor surface of the windows using as a trigger value  $150 \text{ W m}^{-2}$ . This set-point value was chosen considering that people do not usually shut the shades when solar radiation is below  $50\text{--}60 \text{ W m}^{-2}$  while normally they need to close them above  $250\text{--}300 \text{ W m}^{-2}$  (Inoue, Kawase, Ibamoto, Takakusa, and Matsuo, 1988; Newsham, 1994; C. Reinhart and Voss, 2003). Venetian blind tilt is controlled in order to reject beam solar radiation, using as a threshold a DGI value of 22 calculated in position P5.

Considering that daylight glare from a window depends on occupant view direction and that it is highest when the occupant looks directly at the glare source, the view direction is eastward when windows are south oriented, and northern when windows are east oriented.

### 2.3.2 Step 2: CFS global performance assessment considering solar radiation effects on thermal comfort

#### a. Thermal comfort

Besides the standard PMV, the PMV corrected ( $\text{PMV}_{\text{irr}}$ ) considering the mean radiant temperature which includes the effect of solar radiation that directly reaches the occupant (La Gennusa, Nucara, Pietrafesa, & Rizzo, 2007; La Gennusa, Nucara, Rizzo, & Scaccianoce, 2005), has been calculated for the positions P5 (the set-point control position) and P2. The latter is considered a particularly critical point due its proximity to the windows.

The long-term comfort conditions evaluation, on a seasonal basis, was conducted considering some statistical indicators of distribution (the median, minimum, maximum and the interquartile range) calculated for both the standard and the irradiated PMV.

For this aim, a new mean radiant temperature ( $MRT_{irr}$ ) was determined adding to the standard MRT the contributions of diffused and beam solar radiation entering the windows and reaching the occupant:

$$MRT_{irr}^4 = \sum_{i=1}^N F_{s \rightarrow i} I_{d,j}^{in} + \frac{\alpha_{irr,b}}{\varepsilon \sigma} f_p I_{bn}^{in} \quad (3)$$

Equation 3 – Enhanced MRT equation according to (La Gennusa et al., 2005) and (La Gennusa et al., 2007)

**b. Visual comfort**

As in the previous step, the visual comfort was assessed by means of the total hours in a year during which a certain DGI was overcome.

**c. Daylight availability**

As in the previous step the daylight availability related to the different design configurations was not considered.

**d. Simulation environment**

The energy performance and the visual comfort conditions were calculated by means of Energy Plus 8.1, while the MRT corrected according to the contributions of diffused and beam solar radiation, and then the  $PMV_{irr}$ , were calculated through a spreadsheet using the following list of Energy Plus output variables as input data:

- Solar Azimuth Angle;
- Solar Azimuth Angle;
- Solar Altitude Angle;
- Beam Solar Incident Angle Cosine Value: for each external window's surface;
- Window Transmitted Beam Solar Radiation: for each external window's surface. For a bare window, this transmitted radiation consists of beam

radiation passing through the glass (assumed transparent) and diffuse radiation from the beam component reflected from the outside window reveal, if present. For a window with a shade, this transmitted radiation is totally diffused (shades are assumed to be perfect diffusers).

- Window Transmitted Diffuse Solar Radiation Rate: for each external window's surface. For a bare window, this transmitted radiation consists of diffused radiation passing through the glass. For a window with a shade, this transmitted radiation is totally diffused (shades are assumed to be perfect diffusers).
- Zone Mean Air Temperature;
- Zone Air Relative Humidity;
- Standard Mean Radiant Temperature: for each point of the analysis grid.

e. Shading device: Typology, properties and simulation approach

Considering that roller shades represent one of the most common shading devices used in buildings, in particular in the tertiary sector, in this step three different types of roller shades, located both internally and externally, were considered in the analysis. Kirimtat, Koyunbaba, Chatzikonstantinou, and Sariyildiz (2016), analyzing the studies about simulation modelling on shading devices on building from 1996 to 2015, pointed out that roller shades constitute the third type of shading devices most commonly studied in literature. Not only can they be easily installed and maintained, but they also often represent the only design choice when existing buildings are considered.

The following table summarizes the solar and visible characteristics used in the simulation.

Table 8 – Roller shade solar and visible properties

	$\tau_s$	$Q_s$	$\tau_v$	$Q_v$
SH_1	0.16	0.58	0.15	0.9
SH_2	0.10	0.37	0.10	0.57
SH_3	0.05	0.13	0.05	0.1



The properties used for the SH\_1 and SH\_3 shades (Figure 2) refer to two commercial fabrics produced by Helioscreen (Helioscreen, 2017, p. 35, 36), while the SH\_2 shade values have been obtained from analytical relations.



Figure 2 – Commercial shades material solar and optical characteristics

#### f. Visual comfort settings

The visual comfort control setting was not changed.

### 2.3.3 Step 3: CFS global performance assessment evaluating long-term performance: Thermal and visual comfort and daylight availability

#### a. Thermal comfort

For the long-term thermal comfort analysis, the Predicted Mean Vote and the Discomfort Time weighted by the Predicted Percent of Dissatisfied, including the effect of the diffused and beam solar radiation, were used. PPD-weighted discomfort time (WDTPPD) is the number of hours during which the PMV (either standard or irradiated) overcomes the comfort category range chosen, i.e.  $\pm 0.5$  (category B) (CEN, 2007b), weighted by a factor calculated as follows:

$$wf = \frac{PPD}{PPD_{lim}} \quad (4)$$

Equation 4 – Weighted PPD factor

Where:  $PPD_{lim}$  is the acceptable limit for the considered comfort category, i.e. 10 % for the category B (CEN, 2007b), PPD is the hourly Predicted Percentage of Dissatisfied (standard or corrected for irradiation effect). The weighting

factor becomes 1 when 10 % of the occupants are dissatisfied. During each season the  $WDT_{PPD}$  should be calculated separately for cool ( $PMV < -0.5$ ) and warm ( $PMV > 0.5$ ) sensations respectively.

Considering the definition of the  $WDT_{PPD}$ , the ratio between this quantity and the corresponding (not weighted) Discomfort Time, DT, represents the average weighting factor that is the average percentage of dissatisfied people during all the DT. In particular, with a  $PPD_{lim}$  of 10 %, a WDT equal to the DT means that, during the discomfort time, 10 % of people (on average) are dissatisfied. With a WDT twice as much of DT, the average percentage of dissatisfied would be 20 % and so on.

#### b. Visual comfort

As in the previous step, the visual comfort was assessed by means of the total hours in a year during which a certain value of the DGI was overcome.

#### c. Daylight availability

For each configuration the climate-based Daylighting Metrics called spatial Daylight Autonomy (sDA) was calculated to summarize annual daylighting performance throughout the space (Illuminating Engineering Society [IES], 2012). sDA provides a measure of daylight illuminance sufficiency for a given area, reporting the percentage of floor area that exceeds a specified illuminance level (e.g. 300 lux) for a specified number of annual hours (e.g. 50 % of the hours from 8am-6pm). In this study an illuminance threshold of 500 lux was chosen, according to EN 12464-1:2011(CEN, 2011a).

#### d. Simulation environment

Energy Plus 8.1 was used in order to calculate the energy and visual performance and the needed data for assessing long-term discomfort indexes corrected by direct and diffuse solar radiation, computed through a code developed in MatLab. Considering the limits which characterize Energy Plus regarding the evaluation of indoor illuminance (Ramos and Ghisi, 2010), the annual illuminance profiles needed for the sDA assessment were calculated by means of DIVA, which uses Radiance and DAYSIM calculation algorithms. Then they were post processed through a code developed in Matlab in order to calculate the sDA values according to the shades schedules obtained from the energy simulation.

e. Shading device: Typology, properties and simulation approach

The TRANS Radiance material was used in order to simulate the roller shades. This material allows us to define beam/diffused ratio but still does not consider angular differences. However, Apian-Bennewitz, (2013) suggested that this function is the most suitable one for Radiance (for modeling roller shades) when BSDF information or other angular solar optical properties are not available. A TRANS material is defined through its RGB reflectance; its transmissivity, which is the fraction of penetrating light that travels all the way through the material; its transmitted specular component, which is the fraction of transmitted light that is not diffusely scattered. Regarding SH1 and SH3, the light's rate transmitted directly and in a diffused way through the shades were obtained from the manufacturer's technical data sheets, while the SH2 values were calculated by means of analytical relations.

In the following, an example of the material description code.

```
# Translucent material for shade SH1 from HELIOSCREEN 101217
whitepearl
# light total transmittance: 14.9 %
# diffused part : 12 %
# direct part : 2.9 %
mod trans SH1
0
0
7 0.9 0.9 0.9 0 0 0.2 0.19
```

f. Visual comfort control settings

The visual comfort control setting was not changed.

g. Simulated environment simulation approach: Optical properties

The choice of using different software for calculating the indoor annual illuminance profiles determined the necessity to introduce a set of new materials to describe the optical properties of the simulated environment.

All the opaque components (wall, ceiling and floor) were simulated by means of PLASTIC Radiance material. The material PLASTIC is defined through its RGB reflectance, its fraction of specularity, and its roughness value. As was reported in paragraph 2.2.2, in the Energy Plus environment the opaque elements were

simulated using a visible absorptance equal to 0.3 for wall and ceiling and equal to 0.6 for the floor. Those values correspond respectively to a reflectance equal to 0.7 for wall and ceiling and to 0.4 for floor; plaster and tiles very light colored. All the opaque materials have a specularity and a roughness equal to 0.

In the following, an example of the material description code.

```
# material name: InteriorFloor_30
# material type: opaque
# comment: This is a purely diffuse reflector with a standard Floor
reflectivity of 30 %
void plastic InterioFloorl_30
0
0
5 0.3 0.3 0.3 0 0
```

The GLASS Radiance material was used in order to simulate the glazing systems. The GLASS material is defined through its transmissivity at normal incidence, where the transmissivity is the amount of light not absorbed in one traversal of the material. Instead, the value usually measured is the transmittance, the total light transmitted through the pane including multiple reflections. The equation which allows us to compute transmissivity (tn) from transmittance (Tn) is the following:

$$tn = \sqrt{\frac{((0.8402528435 + 0.0072522239) \cdot Tn \cdot Tn) - 0.9166530661}{\frac{0.0036261119}{Tn}}} \quad (5)$$

Equation 5 – Transmittance to transmissivity equation

In the following, an example of the material description code is presented.

```
# Glazing_DH:  $\tau_{\text{au\_vis}} = 0.81$ ; SHGC= 0.60 ;  $U_w = 1.14 \text{ W m}^{-2} \text{ K}^{-1}$   
# visual transmittance: 81.2%  
# visual transmissivity: 88.4 %  
void glass Glazing_DH_81  
0  
0  
3 0.88 0.88 0.88
```

#### 2.3.4 Step 4: CFS global performance assessment comparing zonal and local evaluation

Performance metrics: general information

The performance of the simulated environment was evaluated by means of two different types of indicators. The first type, called “Extensive – Long-term quantitative performance metrics”, describes the percentage of annual working hours during which each point, belonging to a specified grid, is above a specified level. Through this indicator a spatial description of the simulated environment can be obtained.

The second type, called “Synthetic – Spatial long-term quantitative performance”, describes the percentage of floor area in which the respect of a specified limit value, for a certain percentage of working hours, is maintained.

Regarding the comfort performances, thermal and visual comfort, the extensive metrics used express a condition of discomfort, while the synthetics express a positive performance.

##### a. Thermal comfort

The PPD index, standard and corrected considering the effect of direct and diffused solar radiation, was used as a base quantity in order to build the thermal comfort metrics. The extensive metric was called Thermal Discomfort Time ( $\text{TDT}_{\text{PPD}}$ ), and it represents the percentage of annual working hours during which the PPD, at a given point in the space, overcomes the limit value, 10 %, threshold values for B category, according to EN 15251:2007 (CEN 2007b). Otherwise, since the objective of the study is also the evaluation of the office’s

performance in its entirety, a comprehensive indicator, Spatial Thermal Comfort ( $sTC_{10,90\%}$ ), was calculated. It represents the percentage of floor area in which the PPD is less than 10 % for 90 % of the annual working hours considering both the standard and the irradiated index.

**b. Visual comfort**

The Daylight Glare Probability (DGP), (Wienold & Christoffersen, 2005; Wienold and Christoffersen, 2006), calculated in 9 positions over the space, was used as a base quantity to build the visual comfort metrics. In order to avoid glare issues related to the look's direction towards the lighting source (the sun), it was considered that the occupants' view direction was parallel to the window plane, Northward for East windows. The extensive performance was evaluated by means of a metric called Visual Discomfort Time ( $VDT_{DGP}$ ), which expresses the percentage of annual working hours during which the DGP at a given point in the space overcomes 0.35, which is considered the lower limit of acceptable glare values (Wienold & Christoffersen, 2005; Wienold & Christoffersen, 2006). Finally, a comprehensive metric was calculated to account for the glare's spatial variability, called spatial Visual Comfort ( $sVC_{0.35,100\%}$ ), and it was defined as the percentage of floor area in which there is never glare discomfort.

**c. Daylight availability**

As an extensive metric, the percentage of working hours when the daylight illuminance is above 500 lux (Daylight Autonomy - DA) was used.

As a synthetic metric, in order to summarize annual daylighting performance throughout the space, the spatial Daylight Autonomy (sDA) was calculated.

**d. Simulation environment**

The simulation environment was not changed.

**e. Shading device: typology, properties and simulation approach**

The shading device typology, properties and simulation approach were not changed.

**f. Visual comfort control settings**

The visual comfort control settings were not changed.

#### g. Energy performance

The synthetic metric related to the energy performance was built considering the ratio between the energy performance of a specific case with shade and the reference case without shade ( $EP_{sh/wo}$ ).

## 2.4 Results and discussion

In the following, the results coming from the different analysis steps will be described and compared with the aim of emphasising the aspects with which each approach is concerned.

### 2.4.1 Step 1: CFS global performance assessment applying standard comfort metrics

In the first step, the PMV trend related to the winter and summer season was represented by means of some statistical indicators of distribution. The upper line represents the maximum value assumed by the PMV in the specific configuration, the lower line the minimum, the point in the middle the median and the rectangular box the range between the first quartile and the third quartile calculated during the occupied hours.

The PMV distribution during the winter season (c), irrespective of the windows' dimension, remains within the range  $\pm 0.5$  for 75 % of PMV values. Nevertheless, the PMV has a greater dispersion during the winter season and the application of the external shading devices seems useful in order to reduce the variability of the comfort index.

According to the season, heating and cooling needs were plotted in the same graph, in order to provide an easier comparison between the two consumption. Actually, the use of sun protection systems generally increases the heating needs, while decreasing the cooling needs thanks to their capacity of controlling solar gains. The problem is understood if globally they are able to reduce the total consumption.

During winter, both heating and cooling needs are present (Figure 3, Figure 4). Considering the small windows (Figure 3), for almost all the cases the increase in heating needs overcomes the decrease in cooling needs, while for large windows (Figure 4), the reduction of cooling needs due to shades overcomes the increment of heating needs.

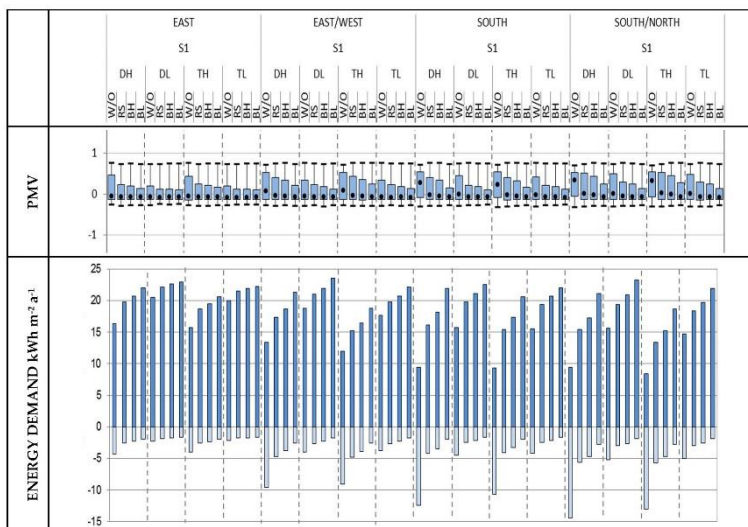


Figure 3 – Winter PMV distribution position P5 and energy needs for heating and cooling for small windows

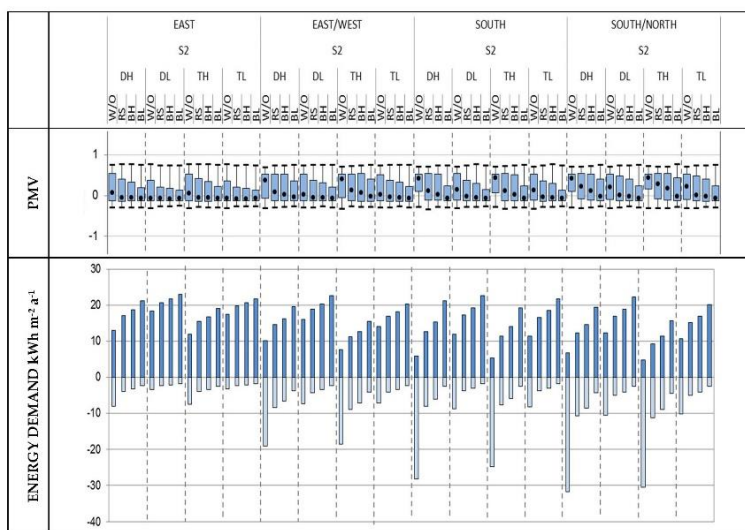


Figure 4 – Winter PMV distribution position P5 and energy needs for heating and cooling for large windows



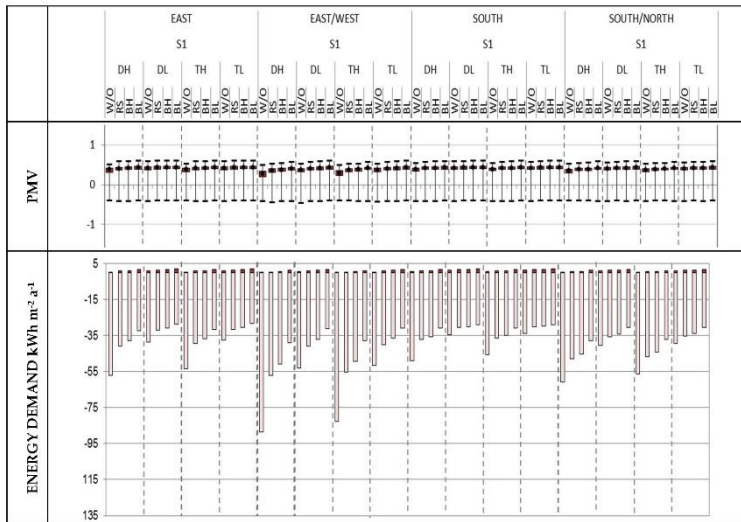


Figure 5 – Summer PMV distribution position P5 and energy needs for heating and cooling for small windows

During the summer, the PMV dispersion is significantly reduced, notwithstanding the presence of solar shades. Heating energy needs are almost null both for small and large windows (Figure 5, Figure 6) and shading devices seem to be fundamental for the reduction of cooling needs. For each shading device, size and kind of glazing, for the E and E/W orientations the cooling energy needs are larger. Regarding the windows' size, the larger the windows, the larger the cooling needs, but the increase is not the same in percentage for all the shading conditions: the increment is at a maximum for glazing without shades (from 107 % to 23 %) and it is at a minimum for the venetian blinds with low reflectivity (from 55 % to 3 %). Roller shades and blinds with high reflectivity have a similar behavior even if the blinds give the lower energy needs (Figure 5).

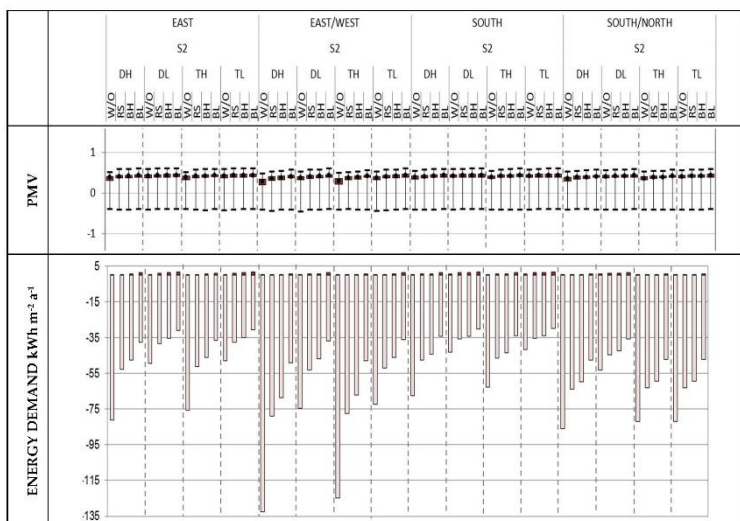


Figure 6 – Summer PMV distribution position P5 and energy needs for heating and cooling for large windows

Regarding the glare discomfort associated with configurations without sun-screen, for the South or South/North orientation the hours of glare discomfort are approximately in the range of 760–600. This means that the occupants will find themselves under conditions of visual stress for about 30 % of their working time because annually the hours of occupation are 2500. The use of blinds with slats at high or low reflectivity reduces to zero (or near to zero) the hours of discomfort with both window sizes.

The roller shades do not allow us to reach the same results, with even an increasing time of glare discomfort when considering windows size S2 and E or E/W orientation. In general the sun protection systems, if adjusted depending on the amount of radiation incident and on the glare index, lead to an increase in artificial lighting needs. However, the control system set for the artificial lighting is usually able to reduce the consumption of electricity from 30 % to 60 % compared to a system switched on and off manually (Galasiu, Atif, and MacDonald, 2004).

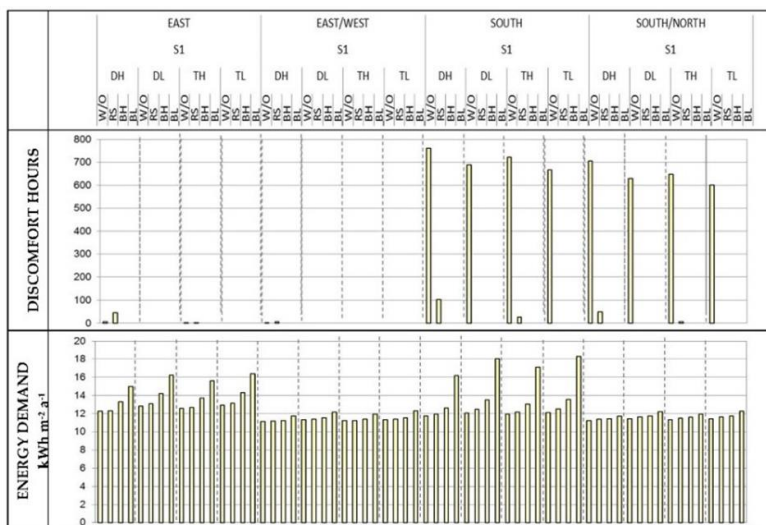


Figure 7 – Hours of visual discomfort position P2 and lighting energy needs for small windows

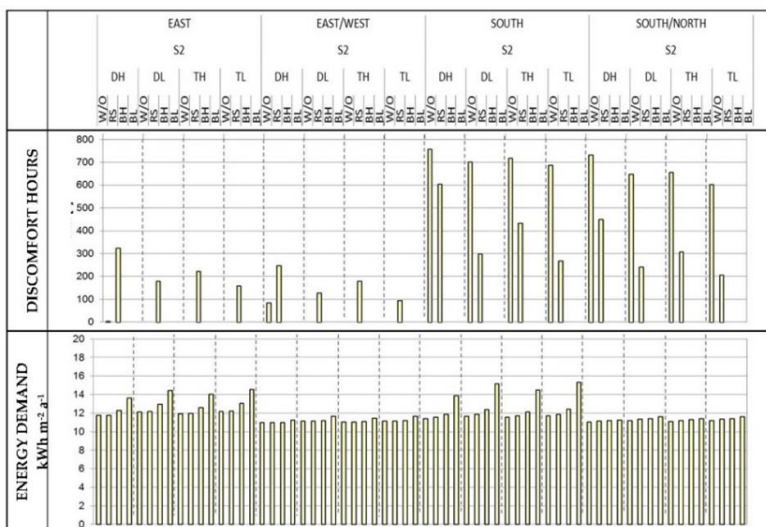


Figure 8 – Hours of visual discomfort position P2 and lighting energy needs for large windows

The comparison of primary energy demand for heating, cooling and lighting allow to evaluate the CFS global energy performance. As previously underlined, the use of shading devices determines a heating and lighting consumption increase. At the same time, in most of the cases, their use leads to a reduction in the total needs, thanks to the shades' capacity of decreasing the cooling primary energy needs.

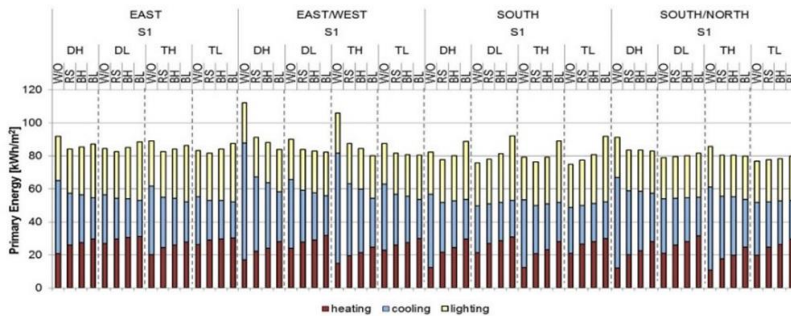


Figure 9 – Total primary energy need for small windows

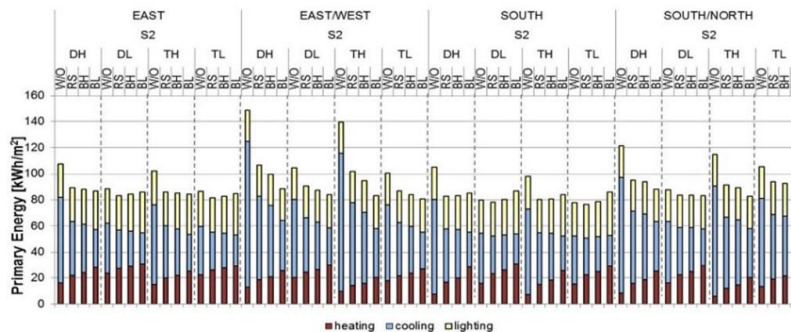


Figure 10 – Total primary energy need for large windows

## 2.4.2 Step 2: CFS global performance assessment considering solar radiation effects on thermal comfort

In the previous paragraph the PMV standard, as an index for assessing the thermal comfort perception, underlined a simulated environment able to respect the comfort range irrespective of the design configuration. Essentially the shading devices appear useful, in particular during the winter season, only to reduce the index dispersion.

On the contrary, the PMV irradiated underlines some critical situations in which, especially during the winter season and with bare windows (Figure 11, Figure 12), both the maximum and the range between the first quartile and the third quartile exceed the comfort range. Comparing external and internal roller shades performance, as expected, the second allow us to reach even higher maximum PMV values due to the fact that they are not able to block solar gains before entering the room. During the summer season (Figure 13, Figure 14) the  $PMV_{irr}$  dispersion decreases, while the maximum values move from the S or S/N orientation to the E-E/W, due to the sun's higher position in the sky vault. In general all the shades with lower transmittance allow us to maintain the PMV within an acceptable range.

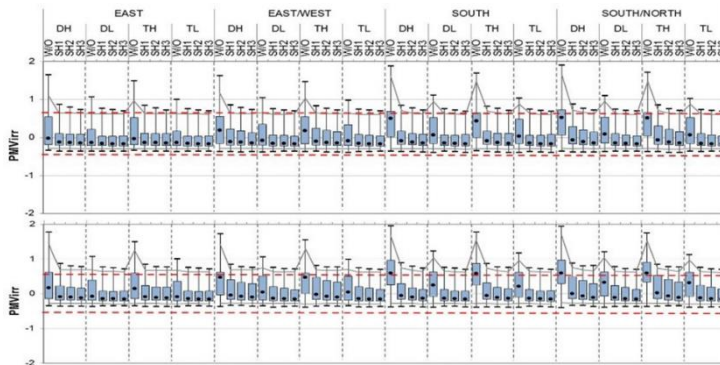


Figure 11 – Winter  $PMV_{irr}$  with small and large windows and external roller shades point P2

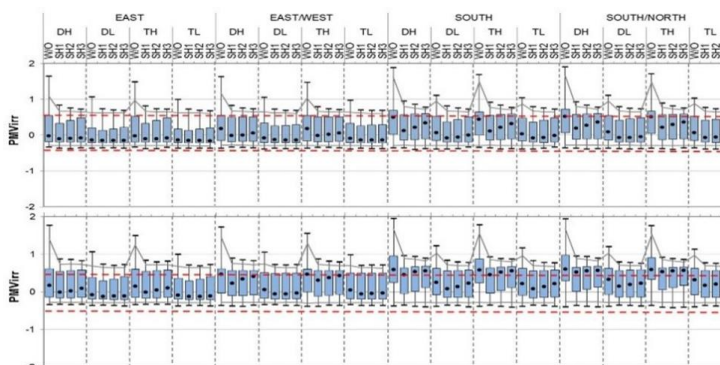


Figure 12 – Winter  $PMV_{irr}$  with small and large windows and internal roller shades point P2

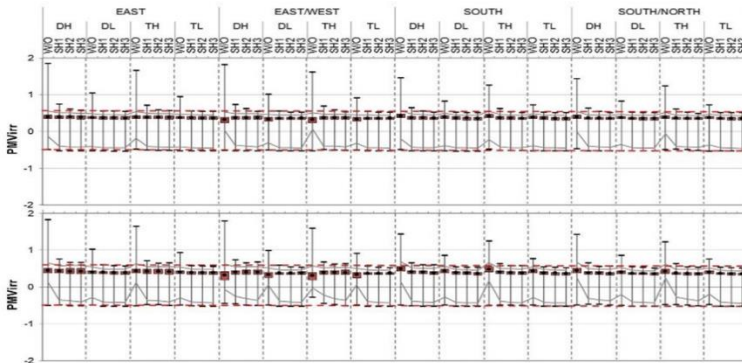


Figure 13 – Summer PMVirr with small and large windows and external roller shades point P2

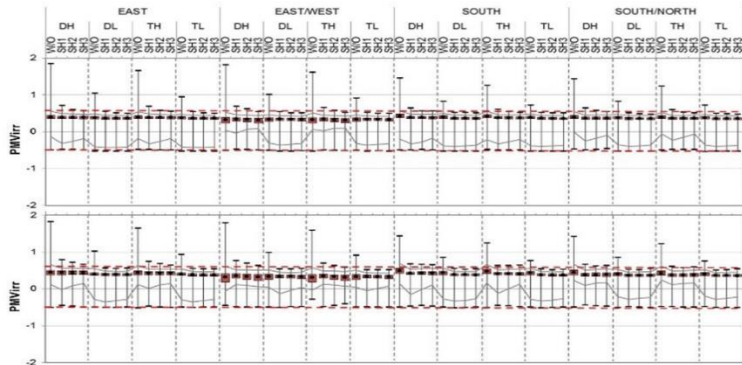


Figure 14 – Summer PMVirr with small and large windows and internal roller shades point P2

Regarding the visual discomfort, the trend underlined in the previous paragraph has been confirmed irrespective of the shades' position. The use of roller shades makes the hours of discomfort insignificant, no matter if they are internal or external. The glare evaluation for configurations without shading devices for the S or S+N orientations indicates, as in step 1, more than 700 discomfort hours per year, whatever the kind of glazing. This means that the occupants in position 2 will fall under conditions of visual stress for about 30 % of their working time.

As pointed out in the previous step, generally speaking the shading devices increase the primary energy needs for heating and lighting and reduce the cooling needs. Instead, looking at the shade position some different trends can be drawn. Shading systems increase lighting needs both for the external and



internal position. However, while for the external position cooling needs are reduced and heating consumption is slightly increased, internal shades give a significant increase in heating needs that is not compensated by a corresponding reduction in the cooling. Therefore, external systems always perform better than internal ones.

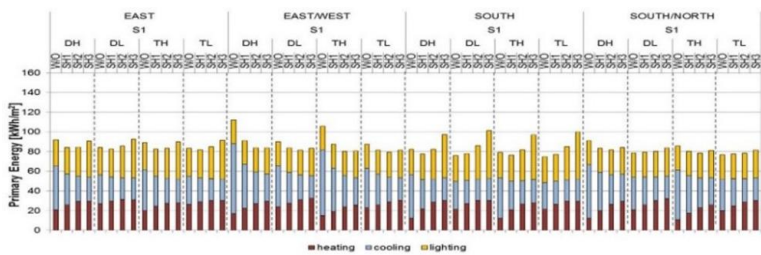


Figure 15 – Primary energy needs for small windows

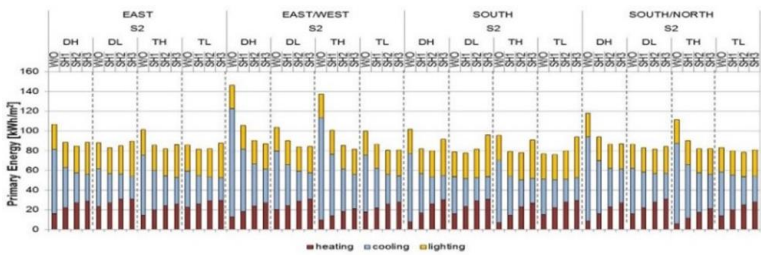


Figure 16 – Primary energy needs for large windows

### 2.4.3 Step 3: CFS global performance assessment evaluating long-term performance: Thermal and visual comfort and daylight availability

Even if the  $PMV_{irr}$  is able to underline the solar radiation effect on thermal comfort perception, pointing out critical situations otherwise ignored, the statistical representation through the box plot cannot communicate for how long the simulated environment remains in conditions of discomfort. On the contrary, showing the weighted number of hours of discomfort related to each position, it is possible to underline how much a specific situation has to be considered negative. Also in this case, the comparison of the results achievable using the standard or corrected PMV index demonstrates the necessity to consider the solar radiation influence in order to assess a correct evaluation of the thermal environmental quality. Each rectangle (Figure 17, Figure 18) represents the office plan configuration and it is divided into 9 colored cells which contain the number of discomfort hours related to the specific position inside the room. Colors are scaled according to the entity of the discomfort time. The graphical representation shows the shades' capacity of reducing the number of discomfort hours. This is particularly important for the critical configuration of windows oriented towards the south and for a glazing system with high SHGC: in this case internal shades (Figure 18) halve the highest discomfort time near the windows, while external shades (Figure 17) can reduce the time by about 80 %. Taking the case without shading as a reference we can comment on some trends. The maximum advantage in reducing discomfort is given by external shades rather than internal shades. With internal shades the positions exposed to solar radiation have a discomfort time period which is twice the one with external shades. In general, the discomfort time is reduced with internal shades, even though with DL glazing it slightly increases at points far from the windows. Comparing the three types of shades, when positioned externally, their efficiency depends on the solar transmission coefficient: thus shade SH2 is better than SH1 and SH3 is better than SH2. For internal shades, there is not a specific trend and the three shades have similar efficacy.



	Standard			Irradiated			Standard			Irradiated			Standard			Irradiated		
	DH_E_S2			DH_EW_S2			DH_S_S2			DH_SN_S2			DH_SN_S2			DH_SN_S2		
WO	154	236	212	223	432	924	143	182	122	970	628	916	87	140	113	113	213	164
	242	178	346	309	367	965	252	125	220	1048	453	818	130	101	101	368	292	394
	156	232	215	208	355	543	149	170	127	649	322	278	170	374	171	1922	2522	2041
SH_1	173	203	194	193	222	265	206	248	193	354	321	323	161	219	206	179	230	217
	205	182	220	216	208	289	285	181	265	388	274	320	218	189	189	234	215	213
	172	200	192	191	220	245	196	221	185	324	270	222	220	253	221	298	358	322
SH_2	167	192	186	182	208	239	211	242	191	301	284	284	158	192	185	164	196	190
	193	169	208	203	198	262	264	185	256	340	247	289	190	167	167	198	183	183
	166	191	184	179	207	223	207	215	184	282	252	212	190	209	190	228	269	239
SH_3	165	190	184	179	206	227	206	229	195	264	256	253	153	184	178	159	187	180
	193	167	209	204	197	252	243	188	241	292	229	260	181	166	166	186	175	173
	162	189	182	177	205	222	204	213	193	253	236	206	180	198	180	201	231	213

Figure 17 – Winter WDT-PPD<sub>st</sub> and WDT-PPD<sub>irr</sub> distribution for large windows with external shades

	Standard			Irradiated			Standard			Irradiated			Standard			Irradiated		
	DH_E_S2			DH_EW_S2			DH_S_S2			DH_SN_S2			DH_SN_S2			DH_SN_S2		
WO	154	236	212	223	432	924	143	182	122	970	628	916	87	140	113	113	213	164
	242	178	346	309	367	965	252	125	220	###	453	818	130	101	101	368	292	394
	156	232	215	208	355	543	149	170	127	649	322	278	170	374	171	1922	2522	2041
SH_1	191	266	326	237	305	443	253	231	225	554	419	448	114	172	149	127	197	167
	263	216	373	279	286	504	409	165	332	652	324	466	194	160	160	253	243	252
	187	265	322	230	299	407	245	192	220	507	296	286	540	670	542	780	970	821
SH_2	195	274	365	236	308	484	327	211	255	548	368	429	92	140	118	101	151	127
	265	226	435	285	289	538	452	150	361	668	271	460	161	136	136	189	192	206
	188	269	360	233	304	451	322	181	253	507	259	297	671	842	674	846	1051	875
SH_3	183	269	402	234	303	497	366	196	284	559	337	415	86	127	114	92	137	120
	261	210	475	277	282	567	488	135	396	691	253	465	135	108	108	171	146	155
	181	263	394	230	298	482	363	164	280	536	234	329	782	980	783	887	###	908

Figure 18 – Winter WDT-PPD<sub>st</sub> and WDT-PPD<sub>irr</sub> distribution for large windows with internal shades

During the summer the weighted discomfort time is lower than in winter (Figure 19, Figure 20). The presence of shades increases the discomfort time at points not reached by solar irradiation, while they are very useful to mitigate the warm discomfort at the west and south positions. Both internal and external shadings assure good indoor thermal comfort. In general the WDT-PPD<sub>irr</sub> is slightly higher for external shades: this is a consequence of the type of control used for the heating and cooling set-point. Giving a set-point for the operative temperature, the air temperature controlled by the system depends on the MRT value at each time step, thus leading to situations in which even though the

indoor MRT is lower with external shades, the air temperature is higher and the sensation is warmer than with internal shadings. The efficacy of the three shades is similar when located on the external side of the windows, while on the internal side SH2 and SH3 are slightly preferable than SH1.

	Standard	Irradiated	Standard	Irradiated	Standard	Irradiated	Standard	Irradiated
	DH_E_S2		DH_EW_S2		DH_S_S2		DH_SN_S2	
WO	9	5 5	6	2 453	17	6 5	722	81 346
	5	6 2	2	2 699	12	6 1	906	80 346
	9	5 5	6	2 382	17	6 5	680	75 240
SH_1	46	31 32	37	17 72	27	20 25	36	5 38
	27	40 17	21	24 299	18	26 15	162	16 45
	47	31 33	37	18 62	27	25 25	28	11 36
SH_2	48	34 34	40	18 47	31	23 30	14	6 22
	32	43 20	24	27 268	20	31 17	122	16 26
	48	34 35	40	18 41	31	25 30	14	13 24
SH_3	45	34 37	41	25 40	31	21 31	18	9 14
	31	40 21	24	32 40	16	31 15	155	17 11
	45	34 38	41	25 253	31	25 31	19	16 23

Figure 19 – Summer WDT-PPD<sub>st</sub> and WDT-PPD<sub>irr</sub> distribution for large windows with external shades

	Standard	Irradiated	Standard	Irradiated	Standard	Irradiated	Standard	Irradiated
	DH_E_S2		DH_EW_S2		DH_S_S2		DH_SN_S2	
WO	9	5 5	6	2 453	17	6 5	722	81 346
	5	6 2	2	2 699	12	6 1	906	80 346
	9	5 5	6	2 382	17	6 5	680	75 240
SH_1	15	9 9	12	5 60	6	2 3	41	1 43
	11	11 7	9	7 264	3	5 2	151	2 63
	15	9 9	12	5 47	6	3 3	35	2 25
SH_2	12	7 5	10	3 34	2	2 2	7	2 16
	4	5 17	4	4 225	3	2 4	82	2 48
	12	4 5	10	3 26	2	2 2	7	2 9
SH_3	5	4 4	5	4 14	2	2 2	2	1 4
	4	5 21	4	4 183	4	2 9	35	2 33
	5	4 4	5	4 12	2	2 2	2	2 4

Figure 20 – Summer WDT-PPD<sub>st</sub> and WDT-PPD<sub>irr</sub> distribution for large windows with internal shades

A detailed analysis of the influence of shading devices on position P2 (Figure 21, Figure 22, Figure 23, Figure 24) was carried out because point P2 is the one mostly influenced by the solar radiation through the window. In winter at point P2 the discomfort sensation is due to the warm feeling. The presence of external

shades neutralizes the dependence of the comfort sensation on the windows' orientation; while with internal shades a South exposure gives the highest discomfort. As previously said, external shading ensures better conditions compared to internal devices. If external shades are considered, the WDT-PPD, even if it is irradiated or not, shows a similar trend. On the contrary, with internal shading, the contribution of solar radiation on thermal discomfort is important just when shades are coupled with high SHGC glazings and, in particular, for South and South-North orientations. Looking at the summer season, the discomfort time is very low, both with internal and with external devices. Considering the WDT<sub>PPD<sub>st</sub></sub>, the sensation would be of coolness and more than 10 % of people would seem to be dissatisfied. If we take into account the solar radiation, as occurs in areal situation, it can be seen that the use of shading always means that no more than 10 % of people are dissatisfied. During the summer season the discomfort time is very low, whatever the shades' position. Considering the WDT standard, apparently there are no discomfort hours related with a warm sensation, while the solar shades improve the cool sensation, but if the WDT is corrected analyzed the trend is completely divergent.

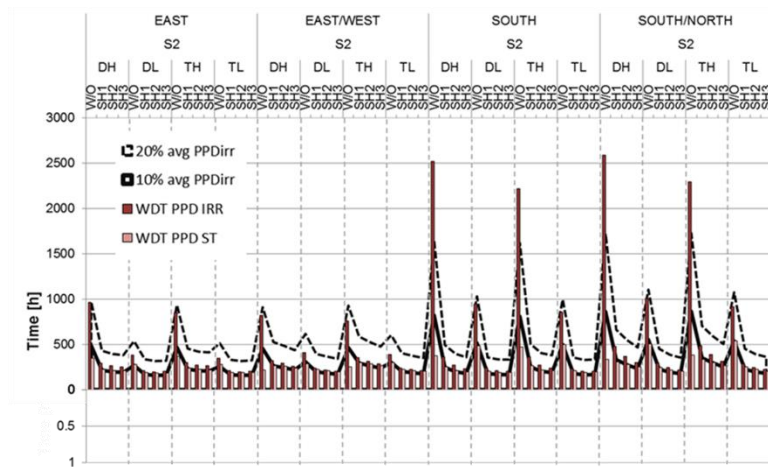


Figure 21 – WDTPPD standard and irradiated winter season point P2 with external roller shades

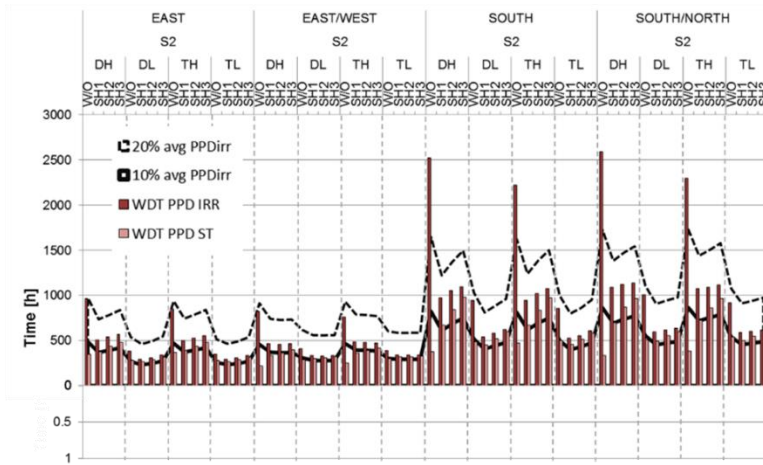


Figure 22 – WDTPPD standard and irradiated winter season point P2 with internal roller shades

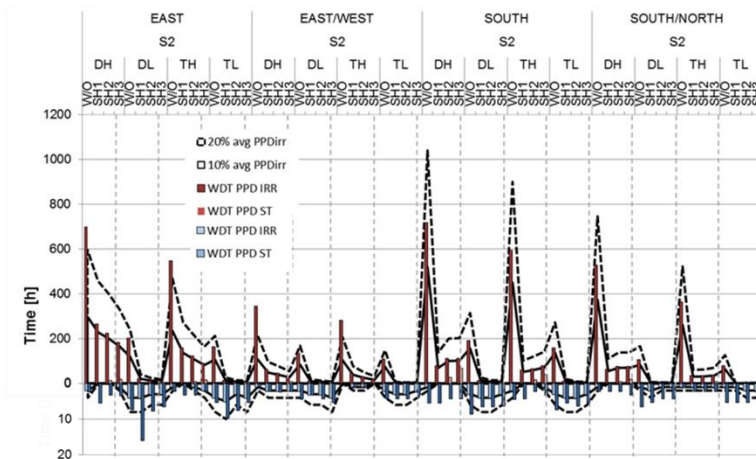


Figure 23 – WDTPPD standard and irradiated summer season point P2 with external roller shades

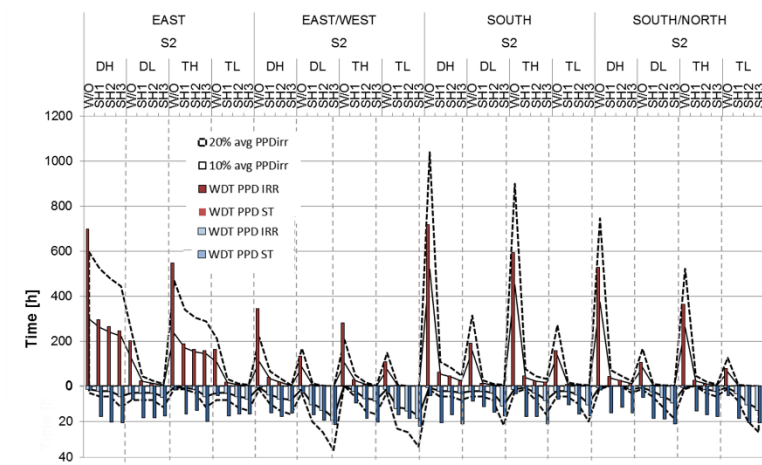


Figure 24 – WDTPPD standard and irradiated summer season point P2 with internal roller shades

As already underlined in the previous steps, point P2 in the unshaded configurations for the S or S+N orientations shows more than 700 discomfort hours per year, independent of the glazing type, while the use of the three roller shades analyzed eliminates glare hours. However if Daylight Glare Probability is used instead of DGI and the shades are simulated accounting for direct-direct transmission through fabric, even if constant, glare is bound to occur even with closed shades, since vertical illuminance will be significantly close to the windows (Figure 25, Figure 26, Figure 27).

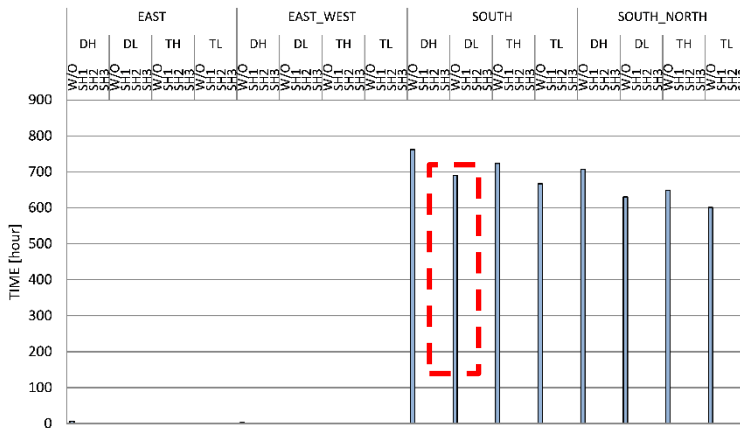


Figure 25 – Hours of visual discomfort with DGI>22 for large windows external shades point P2

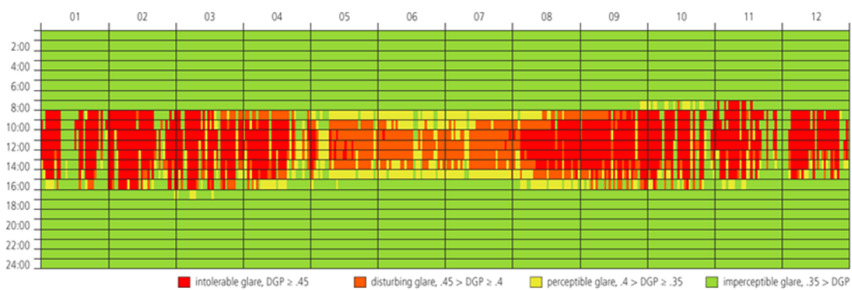


Figure 26 – DGP profile for large southern windows, no shades, glazing DH, point P2

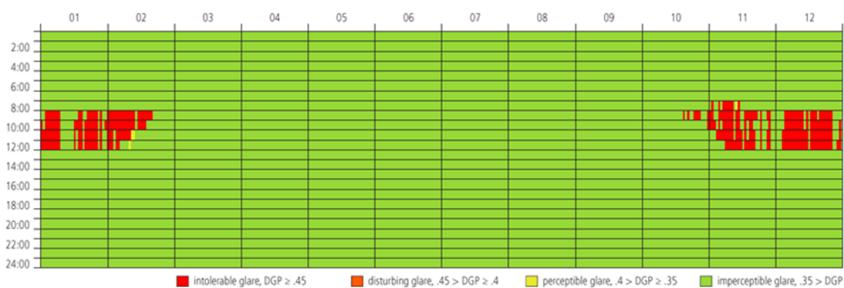


Figure 27 – DGP profile for large southern windows, shade SH\_1 external, glazing DH, point P2

Table 9 shows the sDA values for the bare windows and for the CFS with SH1 and SH3 roller shades. The configuration without shades allows us to reach the sDA threshold value only with the double glazed façade, regardless of the glazing system chosen. Considering the space dimension, it is clear that a single glazed façade is able to reach the threshold value only with the larger windows oriented towards South, and with a high SHGC glazing system. The roller shades SH1 and SH3, because of the control schedule chosen, always prevent acceptable daylight autonomy.

Table 9 – sDA large and small windows with shades SH1 and SH3 and for bare windows

Configuration	sDA <sub>500,50%</sub>								
	WO			SH1			SH3		
	DH	DL/TL	TH	DH	DL/TL	TH	DH	DL/TL	TH
S_S1	53%	47%	49%	28%	21%	27%	11%	7%	10%
S_S2	57%	51%	56%	30%	22%	27%	11%	10%	11%
SN_S1	100%	100%	100%	37%	22%	23%	11%	9%	10%
SN_S2	100%	100%	100%	40%	25%	33%	11%	10%	11%
E_S1	40%	33%	37%	11%	10%	11%	0%	0%	0%
E_S2	43%	33%	40%	11%	11%	11%	0%	0%	0%
EW_S1	100%	100%	100%	30%	22%	22%	5%	0%	0%
EW_S2	100%	100%	100%	31%	22%	26%	4%	0%	2%

Also the primary energy needs maintain the same trend. The use of shading systems (internal and external) will increase lighting needs compared to no shading. However, while for the external position cooling needs are reduced and heating needs are slightly increased, internal shades may result in an increase in cooling needs that cannot be compensated by a corresponding reduction of heating requirements, depending on reflectivity and solar transmission. Therefore, external systems perform better than internal ones from an energy point of view.

#### 2.4.4 Step 4: CFS global performance assessment comparing zonal and local evaluation

Regarding the index representation, the previous step underlined the importance and the necessity of describing the long-term performance using both local and zonal indices. However, the first deliver a detailed visualization of the index magnitude over the whole space, while the latter provide a single value representing the whole environment under analysis (Carlucci et al., 2015). For this

reason in this step two different ways of representing metrics were used to assess the global building performance: “Extensive – Long-term quantitative performance metrics” and “Synthetic – Spatial long-term quantitative performance”. The  $sTC_{10,90\%}$  metric calculated with the standard index (Table 10) highlights a thermal environment able to stay within the chosen limit, except for the internal shades. When we consider the contribution of the solar radiation (Table 11), with the small windows coupled with the external shades, we are always able to ensure the right thermal comfort conditions, but the unshaded configurations and the internal shades can respect the threshold only using the low SHGC glazing. With the larger windows, the comfort conditions requested can be reached only through the TL glazing coupled with the external shades. The  $TDT_{PPD}$  index (Figure 28 – Thermal discomfort time) highlights the distribution of the thermal discomfort sensation through the space. In this case, if we analyze the results correlated with the standard index, the thermal environment keeps homogenous, regardless of the shade’s presence. The irradiated  $TDT_{PPD}$ , instead, shows how and how much the thermal discomfort arises as we consider the positions closest to the transparent surfaces. Moreover, whereas the shade SH3, located externally, can reduce the thermal discomfort time up to 60 % compared to unshaded configuration, the same shade located internally is not able to reduce the  $TDT_{PPD}$  more than 35 %.

Table 10 – Spatial thermal comfort standard

Configuration	$sTC_{10,90\%}$ - STANDARD																							
	WO				SH1 <sub>ext</sub>				SH2 <sub>ext</sub>				SH3 <sub>ext</sub>				SH1 <sub>int</sub>				SH2 <sub>int</sub>			
	DH	DL	TH	TL	DH	DL	TH	TL	DH	DL	TH	TL	DH	DL	TH	TL	DH	DL	TH	TL	DH	DL	TH	TL
E_S1	100	100	100	100	100	100	100	100	100	100	100	100	100	100	100	100	100	100	100	100	89	100	89	100
E_S2	100	100	100	100	100	100	100	100	100	100	100	100	100	100	100	100	67	100	33	100	44	100	33	89

Table 11 – Spatial thermal comfort irradiated

Configuration	$sTC_{10,90\%}$ - IRRADIATED																							
	WO				SH1 <sub>ext</sub>				SH2 <sub>ext</sub>				SH3 <sub>ext</sub>				SH1 <sub>int</sub>				SH2 <sub>int</sub>			
	DH	DL	TH	TL	DH	DL	TH	TL	DH	DL	TH	TL	DH	DL	TH	TL	DH	DL	TH	TL	DH	DL	TH	TL
E_S1	56	100	67	100	100	100	100	100	100	100	100	100	100	100	100	100	89	100	89	100	67	100	67	100
E_S2	67	89	78	100	78	89	67	100	89	89	89	100	89	89	89	100	33	78	22	78	22	67	22	78



TDT <sub>WFO</sub> - EXTERNAL SHADE									
	Standard			Irradiated			Standard		
	DH_E_S2			DL_E_S2			TH_E_S2		
WO	8	8	8	10	16	26	8	8	8
	8	8	8	13	14	37	8	8	8
	8	8	8	10	14	22	8	8	8
SH_1	8	8	8	8	8	11	8	8	8
	8	8	8	8	8	18	8	8	8
	8	8	8	8	8	10	8	8	8
SH_2	8	8	8	8	7	9	8	8	8
	8	8	8	7	8	16	8	8	8
	8	8	8	8	7	9	8	8	8
SH_3	8	8	8	8	7	9	8	8	8
	8	8	8	7	8	15	8	8	8
	8	8	8	8	7	9	8	8	8

Figure 28 – Thermal discomfort time

For visual comfort and daylighting performance, we obtain very similar results regardless of the shade's position. The use of the roller shading system leads, globally, to a decrease of the sDA<sub>500,50%</sub> (Table 12) for both window sizes and the DA<sub>500</sub> (Figure 29 – Daylight autonomy) decreases faster distancing from the transparent surfaces. The view's direction used for the simulation makes sure that even the unshaded combinations remain close to the limit chosen for the sVC<sub>0.35,100%</sub> (Table 13), but only thanks to the shades can we ensure the visual comfort for all the positions analyzed. If we analyze the visual discomfort locally (Figure 30), with the bare windows the points closest to the biggest windows can stay under discomfort conditions up to 29 % of the annual working hours.

Table 12 – Spatial daylight autonomy

Configuration	sDA <sub>500,50%</sub>																							
	WO				SH1 <sub>ext</sub>				SH2 <sub>ext</sub>				SH3 <sub>ext</sub>				SH1 <sub>int</sub>				SH2 <sub>int</sub>			
	DH	DL	TH	TL	DH	DL	TH	TL	DH	DL	TH	TL	DH	DL	TH	TL	DH	DL	TH	TL	DH	DL	TH	TL
E_S1	56	44	56	44	37	33	38	33	33	31	32	32	11	22	20	22	37	33	36	33	32	31	32	32
E_S2	73	56	67	56	44	40	42	38	33	33	33	33	11	22	11	21	41	38	41	38	33	33	32	33

Daylight Autonomy 500 lux - EXTERNAL SHADE												
	Standard			Irradiated			Standard			Irradiated		
	DH_E_S2			DL_E_S2			TH_E_S2			TL_E_S2		
WO	25	59	88	42	69	88	15	41	85	29	54	86
	28	61	88	44	72	89	16	43	86	29	57	86
	22	59	88	43	70	88	13	36	85	25	54	86
SH_1	0	27	77	7	37	77	0	12	82	0	30	81
	0	30	78	9	40	79	0	16	83	1	34	82
	0	25	76	8	37	78	0	7	81	0	29	80
SH_2	0	15	71	0	27	68	0	11	69	0	20	73
	0	19	71	1	30	68	0	14	69	1	23	73
	0	14	70	1	26	68	0	8	64	0	19	71
SH_3	0	13	48	0	18	42	0	11	57	0	19	54
	0	16	47	1	20	42	0	14	58	0	22	54
	0	14	46	1	19	41	0	8	56	0	19	52

Figure 29 – Daylight autonomy

Table 13 – Spatial visual comfort

Configuration	sVC <sub>0.35,100%</sub>																											
	WO				SH1 <sub>ext</sub>				SH2 <sub>ext</sub>				SH3 <sub>ext</sub>				SH1 <sub>int</sub>				SH2 <sub>int</sub>				SH2 <sub>int</sub>			
	DH	DL	TH	TL	DH	DL	TH	TL	DH	DL	TH	TL	DH	DL	TH	TL	DH	DL	TH	TL	DH	DL	TH	TL	DH	DL	TH	TL
E_S1	93	96	93	96	100	100	100	100	100	100	100	100	100	100	100	100	100	100	100	100	100	100	100	100	100	100	100	100
E_S2	89	94	91	93	100	100	100	100	100	100	100	100	100	100	100	100	100	100	100	100	100	100	100	100	100	100	100	100

Visual Discomfort Time <sub>PCR</sub> - EXTERNAL SHADE												
	Standard			Irradiated			Standard			Irradiated		
	DH_E_S2			DL_E_S2			TH_E_S2			TL_E_S2		
WO	1	4	20	1	5	27	0	2	14	0	3	19
	0	3	19	1	5	29	0	0	9	0	1	18
	0	1	16	0	5	27	0	0	7	0	0	15
SH_1	0	0	0	1	0	0	0	0	0	0	0	0
	0	0	0	0	0	0	0	0	0	0	0	0
	0	0	0	0	0	0	0	0	0	0	0	0
SH_2	0	0	0	0	0	0	0	0	0	0	0	0
	0	0	0	1	0	0	0	0	0	0	0	0
	0	0	0	1	0	0	0	0	0	0	0	0
SH_3	0	0	0	0	0	0	0	0	0	0	0	0
	0	0	0	0	0	0	0	0	0	0	0	0
	0	0	0	0	0	0	0	0	0	0	0	0

Figure 30 – Visual discomfort time

With the smallest windows, the use of the roller shading systems lead to an increase in the primary energy needs, except for the configurations with the glazing DH, TH or TL coupled with the shade SH1 located externally. With the

biggest windows, and the shades located externally, we obtain for all the configurations analyzed a reduction of the overall primary energy consumption except for the glazing DH coupled with the shade SH3. Essentially, considering that the use of the roller shading systems cause, in all the cases analyzed, an increase in the primary energy consumptions related with the lighting and heating systems, we can obtain a reduction of the overall primary energy needs only when the cooling needs reduction is able to overcome the other two increases.

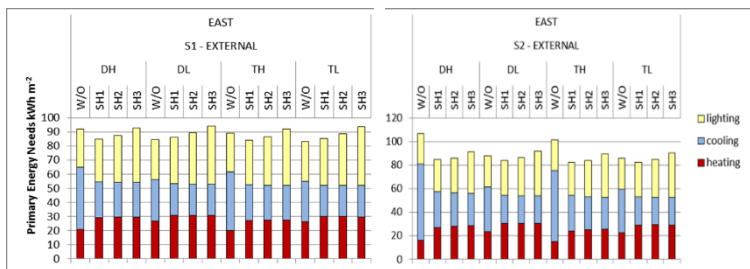


Figure 31 – Primary energy needs for heating, cooling and lighting

Table 14 – Ratio between PE and PE0

Configuration	PE/PE <sub>0</sub>																							
	WO				SH1 <sub>ext</sub>				SH2 <sub>ext</sub>				SH3 <sub>ext</sub>				SH1 <sub>int</sub>				SH2 <sub>int</sub>			
	DH	DL	TH	TL	DH	DL	TH	TL	DH	DL	TH	TL	DH	DL	TH	TL	DH	DL	TH	TL	DH	DL	TH	TL
E_S1	100	100	100	100	92	102	94	103	95	106	97	107	93	112	103	112	98	105	101	106	104	109	106	110
E_S2	100	100	100	100	80	95	81	96	81	98	83	97	85	104	88	105	91	101	94	102	98	105	100	106

In order to allow for a direct comparison between the long term performances of each configurations, a single graph (Figure 32) has been used to assess the variation of the synthetic metrics.

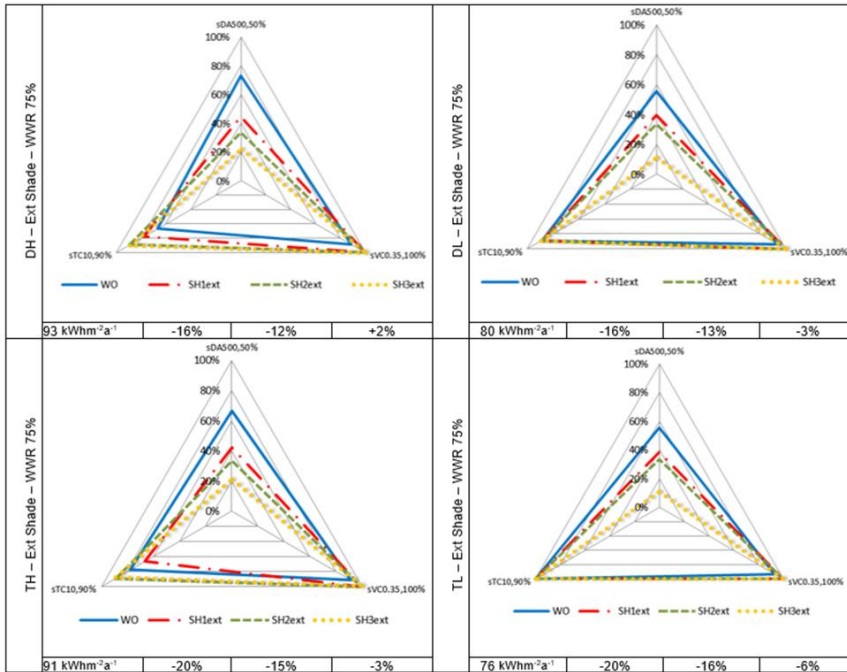


Figure 32 – Integrated performance plot

## 2.5 Conclusions

Through the parametric analysis of different Complex Fenestrations System (CFS) by means of dynamic simulation software, the energy consumption and internal environmental quality related to each design configuration were compared with an integrated approach. Considering that the main aim of this research is the definition of a methodology for the calculation and the assessment of the buildings global performance, taking into account both the energy needs and the necessity of guaranteeing a high level of indoor environmental quality (IEQ), some aspects can be underlined:

The necessity of considering at the same time energy consumption and comfort conditions, in order to prevent the possibility that a poor environmental quality determines an increase in the energy consumption due to the occupants' actions during the service building life.

The importance of assessing the direct and diffuse solar radiation effects on occupants' well-being during the evaluation of thermal and visual comfort. It has been demonstrated that a thermal comfort index which does not account for solar radiation can underestimate critical situations that can determine overheating discomfort conditions. At the same time, neglecting the contribution of the direct-direct component of the visible radiation when assessing visual comfort can make certain design configurations seem visually comfortable even if in reality are not so.

Finally, as already underlined in the Introduction, there is still a lack of a standardized and consistent set of representation metrics able to express the time constancy or space uniformity of comfort and to evaluate different comfort aspects simultaneously with the energy behavior.

### 3. Characterization of a Consistent Set of Representation Metrics for Mapping Buildings' Global Performance: Thermal and Visual Comfort and Energy Efficiency

#### 3.1 Background

##### 3.1.1 Metrics for thermal comfort

###### a. State of the art

Thermal comfort is defined in EN ISO 7730:2005 (CEN 2005c) as “that condition of mind which expresses satisfaction with the thermal environment” (p. 10). Similar definitions can be found also in EN 15251:2007 (CEN, 2007b) and in the 9<sup>th</sup> Chapter of the *2013 ASHRAE Handbook–Fundamentals* (ASHRAE, 2013a), even if the latter standard underlines the subjective character of such a concept by adding to the previous definition the sentence “[...] and is assessed by subjective evaluation” (Attia & Carlucci, 2015).

If we consider that occupants can modify indoor environments basically altering the building envelope or inner partitions (opening doors, windows, or vents; closing curtains, lowering blinds, etc.) or scheduling or adjusting the set point of some controller device, and that these actions are determined by the

necessity to establish a comfortable environment, the thermal comfort condition can be better defined as a state in which there are no driving impulses to correct the environment by behavior (Hensen, 1991).

The definition of what can be considered as a comfortable environment is particularly hard. It is known that the thermal perception of a certain environment, no matter whether it is open or confined, changes from person to person. Thermal sensations can be different among people even in the same environment, which makes it impossible to create a thermal climate where everybody is satisfied (Kunkel et al., 2015). In any case, as specified in EN ISO 7730:2005 (CEN, 2005c), even if there will always be a percentage of dissatisfied occupants, it is possible to specify environments predicted to be acceptable by a certain percentage of the occupants.

The human body interacts with the environment to maintain the thermal balance between metabolic thermal power and thermal loss mechanisms. From a physiological point of view this happens through an increased blood flow and sweating, when heat sensors send impulses to the hypothalamus of a high skin temperature; or through a reduced blood flow and shivering when the skin temperature is too low. These mechanisms are the human body's automatic response to the inputs coming from the environment in which it is inserted, which influences the human thermal balance by air temperature, mean radiant temperature, relative air velocity and relative humidity, according to EN ISO 7730:2005 (CEN, 2005c) and EN 15251:2007 (CEN, 2007b). Humans can adapt themselves also in a conscious way to these stimuli; for instance through their clothing or activity, choosing a different location or, as underlined before, acting on the building's envelope or on its systems. Obviously, the occupants cannot have the same level of freedom in every environment.

As reported in Djongyang (2010), two different approaches currently exist for the assessment of the indoor thermal comfort: the rational or heat-balance approach, which uses data from climate chamber studies, and the adaptive approach, which uses data from field studies of people in building.

Fanger's comfort model (Fanger, 1972) and the two node model of Gagge's et al. (Gagge, Fobelets, and Berglund, 1985) belong to the rational or heat balance approach. Djongyang (2010) underlined that the PMV-PPD model, derived from the Fanger's comfort model, widely used and accepted for design and

field assessment of thermal comfort also in standards in force, is useful only for predicting steady-state comfort responses while a two-node model can be used to predict physiological responses or responses to transient situations.

The adaptive approach, however, has the purpose of analyzing the real acceptability of the thermal environment, which strongly depends on the context, the behavior of occupants and their expectations (Djongyang, 2010). The adaptive approach is now included in some standards and guides for comfort, in particular for buildings which are not heated or cooled (ASHRAE, 2013a; CEN, 2007b).

Essentially, as underlined in Attia and Carlucci (2015), all standards on thermal comfort basically agree with suggesting the adoption of Fanger's model for mechanically heated and/or cooled buildings, while Chapter 18 of the 2013 *ASHRAE Handbook–Fundamentals* (ASHRAE, 2013a) offers the possibility to use the American adaptive model in “naturally ventilated building” whether the “mean monthly outdoor air temperature” falls into a given temperature domain ( $10 \div 33.5^{\circ}\text{C}$ ) and the European standard EN 15251:2007 (CEN, 2007b) allows for the use of the European adaptive model in “buildings without mechanical cooling” if the “exponentially weighted running mean of the daily outdoor air temperature” falls into a given temperature domain ( $10 \div 30^{\circ}\text{C}$ ).

**b. Critical aspects: how considering the solar radiation effects**

As underlined in the previous paragraph, the Fanger's approach links the thermal sensation to six primary factors. Four of them, air temperature, mean radiant temperature, air velocity, humidity are defined as environmental parameters; two of them, metabolic rate and clothing, as personal parameters. The air temperature and the mean radiant temperature are used to calculate the operative temperature, which represents the “real temperature” perceived by the occupants. For this reason the standard EN ISO 7730:2005 (CEN, 2005c) has been used as a design criterion to design comfortable environments. The problem is, as underlined in Halawa, van Hoof, and Soebarto (2014), that the graphs contained in the international standards for evaluating the acceptable ranges of operative temperature can be misleading because they are constructed using the simplified assumption that mean radiant temperature and air temperature are equal.

The same author underlines that also the adaptive model, which relates the indoor comfort (operative) temperature to the outdoor temperature and assumes that occupants adapt to the outdoor conditions in a practical way, does not clearly express the effect of radiation in its equations.

In short, the existing comfort standards, which are generally interpreted as the main guidance for building design, do not clearly factor in the effect of mean radiant temperature (Halawa et al., 2014). Arens et al. (2015) and A. Tzempelikos et al. (2010) also came to the same conclusion, underlining that both the approaches, the rational and the adaptive, do not mention shortwave and longwave radiation, and the discomfort condition related with the solar radiation hitting the occupants, and that they are not able to evaluate the incoming solar radiation influence on the transient thermal conditions and on the mean radiant temperature.

Arens E, Gonzalez R (1986) emphasized that when “envelope-dominated” buildings are considered as buildings where climate conditions directly interact with the indoor environment, for instance in the form of sunshine through windows, natural ventilation, and thermal transfer through walls and roof, a close coupling exists between outdoor climate and occupant comfort requirements. For this reason they revised the bioclimatic chart, developed by Olgyay in the 1950s, using the J.B. Pierce two-node thermophysical model and the Thermal Standard 55-81 (ASHRAE, 1981), to determine the equal comfort levels under an extended range of environmental conditions. Starting from the definition of effective radiant field (EFR), able to measure the additional long-wave radiation energy received by the body when surrounding surface temperatures are different from the air temperature, they enhanced this metric inserting the effect of the total (direct plus diffuse) radiation falling on a horizontal surface (ITH).

In Arens et al. (2015) a solar calculator (SolarCal), based on the method previously cited was described. It can be used to quickly estimate the solar radiation in undetermined environments or in environments with simple geometries. The calculation results have been compared with a human subject test of solar effects and comfort (Hodder and Parsons, 2006). As underlined by the same authors, the SolarCal model is intentionally simplified, but it is able to



underline how and how much the direct warming effect of solar radiation on occupants may cause discomfort.

Starting from the Thailand regulations about the energy use in buildings, Chaiyapinunt, Phueakphongsuriya, Mongkornsaksit, and Khomporn (2005) introduced a methodology to rate the thermal performance, in terms of heat transmission and thermal comfort, of glass windows and glass windows with films under local design conditions. The PPD was used as a thermal comfort index, but in order to take into account the effect of solar radiation striking on the person in the enclosure, two mean radiant temperatures were used. One of them does not account for solar radiation, which means that mean radiant temperature is mainly dominated by glass surface temperature. The second mean radiant temperature accounts for the effect from surface temperature and solar radiation. The global PMV, which considers the solar radiation effect and is used for obtaining PPD, was calculated by using the relation suggested by Huizenga et al. (2006) and Sullivan (1986) as:

$$PMV = PMV_{no\ solar} + \frac{dPMV}{dq} q \quad (6)$$

Where  $q$  represents the solar radiation passing through a glass window. The authors underlined that the PPD due to solar radiation is greater than the PPD due to surface temperature for most of glasses considered, except the ones with the reflective glass as the outer pane.

The same approach was used in M. C. Singh, Garg, and Jha (2008) to evaluate the impact of fifteen different glazing systems, ranging from 3 mm single-glazed clear glass to double glazed with low-e and solar control coating, on human thermal comfort.

Even if the research is focused on thermal comfort sensation inside vehicles, the conclusions which were presented by Hodder and Parsons (2006) demonstrated the strong connection between solar radiation and thermal comfort. They exposed 8 subjects to three different experimental conditions: four levels of simulated solar radiation (0, 200, 400 and 600 Wm<sup>-2</sup>); solar radiation with four different spectral contents, each with a total intensity of 400 Wm<sup>-2</sup> or 1000 W m<sup>-2</sup> on the subject. The Mean Radiant Temperature (MRT) was measured with two

globe thermometers: one located close to the subject and exposed to the simulated solar radiation, the other exposed to the same environmental conditions but shaded. They found an increase in thermal sensation of one scale unit for an increased exposure of around  $200 \text{ Wm}^{-2}$  of radiation to the body, while the effect of spectral content of the radiation on thermal sensation has no practical significance.

Further, La Gennusa et al. (2007) proposed an analytical method to correct the classical definition of the Predicted Mean Vote (PMV) to take into account the effect of direct and diffused solar radiation entering through the glazed areas and directly reaching people. Using the following equation:

$$T_{r,irr} = \sqrt[4]{\sum_{i=1}^N F_{S \rightarrow i} T_i^4 + \frac{C_{dn}}{\epsilon \sigma} \left( \alpha_{irr,d} \sum_{j=1}^M F_{S \rightarrow j} I_{dj}^{in} + C_S^{in} \alpha_{irr,b} f_p I_{bn}^{in} \right)} \quad (7)$$

in order to determine the local mean radiant temperature ( $T_{r,irr}$ ) of a given enclosure when complex radiant fields take place, mainly due to the presence of solar radiation on the human body. Moreover, the method proposed for computing view factors between people and surrounding surfaces, allows for the calculating of the thermal balance for each point of the bottom of the room, obtaining in this way a useful map of the thermal comfort conditions inside the room itself.

The analytical method introduced in La Gennusa et al. (2007) was used also in Mak (2008), Bessoudo et al. (2010), A. Tzempelikos et al. (2010), Hwang and Shu (2011), Cappelletti et al. (2014) and Marino, Nucara, and Pietrafesa (2015). In the first study, measurements were also carried out to test the goodness of fit for applications in Hong Kong climate and to verify if furniture inside a room would possibly violate the basic assumptions of the model. Bessoudo et al. (2010) compared the experimental measurements collected in a perimeter zone of an office building in Montreal with a transient building thermal model, able to calculate indoor environmental indices under the presence of solar radiation. In order to verify thermal comfort conditions, the authors took into account especially the local discomfort due to radiant asymmetry. In A. Tzempelikos et al. (2010) the validated thermal model, combined with a transient two-node

thermal comfort model, was used to investigate the impact of varying exterior climatic conditions, glazing properties and shading properties on indoor thermal comfort and heating demand in such spaces under the presence of transmitted solar radiation. In Hwang and Shu (2011) the effect of building envelope regulations on thermal comfort and on cooling consumption were assessed. Through a parametric analysis, they evaluated the effect of glazing types, WWR and overhang on the occurrence of discomfort and severity of overheating. The aim of the analysis carried out in Cappelletti et al. (2014) was evaluating heating and cooling energy needs related with different glazing systems maintaining fixed comfort conditions in an office building. PMV and PPD were used to obtain a long term index in terms of weighted discomfort time, mapping the performance on 9 positions in the room. In Marino et al. (2015) the PPD values, calculated considering the MRT influenced by solar radiation, were exploited to realize the classification of the thermal comfort quality of the environment by means of a quality index named Environment Quality Index (EQI).

Thellier, Monchoux, Bonnis-Sassi, and Lartigue (2008) proposed a more complex model to evaluate the solar radiation effect on human thermal comfort, considering the occupant as composed of six groups of surfaces (head, trunk, arms, hands, legs and feet) whose geometry can vary with his/her location and posture. The irradiated areas are calculated with a ray tracing method in order to take shadow into account.

As the literature review has underlined, in the last few years many researchers have tried to define a methodology which allows us to overcome the limits which characterize the thermal comfort model suggested by the regulations. Beyond the considerations closely related to the scientific aspects of this problem, we believe that a “good” methodology should be able to support architects and engineers during the design, providing them, since the very beginning, with all the essential information useful to project an environment characterized by high global efficiency. The detailed analysis of the solar radiation (visible and thermal) through the window components and its distribution in the internal environment is one of the crucial aspects to assess the global performance of the building correctly. Edward Arens et al. (2015) highlighted the lack of design tools for predicting the effect of solar radiation falling

directly on occupants in buildings, probably caused by the complexity of the task: identifying an occupant's position, determining the position of solar beam radiation on interior room surfaces, determining the shading and reflection from interior furnishings and the effect of solar altitude and azimuth on the occupant's non-cylindrical body shape. The multi-segment thermal physiology and comfort models, used especially in the automotive design, offer a very detailed representation of the thermal exchanges but they are excessively time-consuming to be applied during the building's design process. At the same time, we believe that also an excessive simplification of the problem could lead to underestimate potentially critical aspects. For these reasons in this study, between the different methodologies analyzed, the method proposed by La Gennusa et al. (2007) has been chosen for the analysis of the solar radiation effects on occupants thermal comfort.

### 3.1.2 Metrics for visual comfort: State of the art

According to EN 12665:2001 (CEN, 2011b) visual comfort can be described as "a subjective condition of visual well-being induced by the visual environment". Regardless of whether the source of light is natural or artificial, the main parameters which determine the luminous environment in indoor work spaces are: luminance distribution, illuminance, directionality of light or lighting in the interior space, variability of light (levels and color of light), color rendering and color appearance of the light, glare and flicker (CEN, 2011a). The standard EN 15251:2007 (CEN, 2007b), specifies that, especially considering non-residential buildings, in order to enable people to perform visual tasks efficiently and accurately, adequate light (without side effects like glare and blinding) shall be provided. Moreover, for health, comfort and energy reasons, in most cases the use of daylight (maybe with some additional lighting) is preferred over the use of artificial light. The regulation rates the lighting quality of a building by means of measurement of illuminance, which can be provided by natural or artificial light. In specific cases also more qualitative aspects (UGR, Ra values and luminaire illuminance) can be evaluated.

Even if the last two decades have been characterized by a huge increase in studies aimed at identifying metrics able to evaluate visual comfort conditions, the indexes proposed are concentrated mostly on glare and amount of light,

while there is still a lack of a single metric able to summarize all the effects which can influence the luminous environment: amount of light, uniformity of light, quality of light in rendering colors, prediction of the risk of glare for occupants (Carlucci et al., 2015).

As suggested by Carlucci et al. (2015), visual comfort metrics can be distinguished according to: the specific aspect they aim to analyze, the light source (natural or artificial), the space discretization of the calculation output (local or zonal indexes), the time discretization (short term or long term indexes), the acceptability criterion (one-tailed or two-tailed). They analyzed on the whole 34 indexes related with visual comfort; 50 % devoted to assessing or predicting firstly glare, 26 % the amount of light, 21 % the light quality and 3 % the light uniformity.

Synthetically it is possible to say that: existent metrics evaluate just one of the coexisting factors which influence visual comfort at a time; regarding illuminance indices there is no agreement on thresholds; the different metrics which deal with glare evaluate in a different way the factors which cause the phenomena and an international agreement about color rendering is still missing (Carlucci et al., 2015).

## 3.2 Representation metrics proposed

### 3.2.1 Introduction

As previously underlined, one of the main aims of this study is to define a methodology that can build a consistent set of representation metrics which can help designers to analyze and synthesize the global performance of different design characteristics considering together, and at the same time, different comfort conditions. As underlined in Atzeri, Cappelletti, Gasparella, and Tzempelikos (2011), if the performance of a specific building element is analyzed only considering a specific comfort aspect, thermal rather than visual, and not its influence on all the comfort conditions, it can cause an underestimation of possible problems.

As it has been underlined analyzing the references reported in Chapter 1, as far as the use of thermal and visual comfort metrics in the scientific literature is concerned, some trends can be underlined:

- Few works still use metrics based on standard conditions or typical days, while most of them evaluate the visual and thermal comfort along a reference year, considering the representative climatic conditions, which is good to enhance the quality of the information (Carlucci et al., 2015);
- This lead to the need for synthesizing the metrics over the considered period (long-term metrics). Attempts made in this direction consider average values, frequency distributions or cumulative occurrence (global discomfort time, fraction of time in comfort, comfort classes); moreover, those metrics are typically referred to a specific position. With the exception for thermal comfort, which is assumed as a good indicator of the average conditions in the space, especially when based on the air temperature, there is the need to account for the variability over the space. That has been addressed in some cases assuming some representative positions, in some others considering average values, and in a few cases mapping the values on the surface.
- Most of the papers which underline the importance of evaluating the building's performance, taking into account both the energy consumption and the internal comfort conditions, suggest to include visual and thermal aspects.
- On the other hand, the lack of a standardized and consistent set of comfort metrics makes it difficult not only to conduct an integrated evaluation, but also to compare the results from different studies.
- The availability of proper and consistent synthetic indicators to express the time constancy or space uniformity of comfort and to evaluate the simultaneousness of different comfort aspects together with the energy behavior seems then opportune.

Starting from the above considerations, a methodological approach to the definition of a consistent set of representation metrics, which try to overcome the underlined limitations, and which can help the designers to analyze and synthesize the global performance of different design characteristics considering together, and at the same time, different comfort aspects has been proposed.

In order to reach this goal two families of metric have been proposed based on the concepts of time comfort availability and space comfort usability. When the comfort performance has been represented with respect to a position or to an instant, the metrics represent the fraction of time and space in comfort condition,

respectively. Instead, when a representation with respect to the overall building surface or reference period is necessary, spatial availability and time or temporal usability summarize the behavior in terms of availability and usability.

As suggested by Carlucci et al. (2015) visual comfort metrics can be distinguished according to the reference time and position. According to this useful classification, which can apply also to other comfort sensations, there may be short-term (instant) or long-term metrics, depending on their ability to describe the instant behavior or to synthesize the performance over an entire reference period. Moreover, local indexes are calculated with respect to a specific position in the analyzed space, while zonal indexes summarize the behavior over the whole environment.

In summary, the set of representation metrics proposed is able to represent the single and the global comfort conditions, on a long-term and/or on a zonal or local basis.

### 3.2.2 General description

As already specified, the metrics proposed in this work can represent comfort conditions related with different physical elements. For this reason in this paragraph the metrics will be described without reference to a specific comfort perception.

#### a. Local (Time) Availability metrics

The Local (Time) Availability metrics have been built starting from the definition of Daylight Autonomy, which represents the fraction of time in the reference period (year) when enough daylight is available in a given point. Generalizing the concept, it is possible to introduce a family of metrics expressing the fraction of time when comfort conditions are available at a given position in the considered space, from which the name Local Time Availability (LTA) derives. As in the case of DA, these metrics are local and long term. These indexes vary with position providing a value for each point inside a space and are presented through maps, which allow us to evaluate how the index changes over the whole space. These indices can support designers in the detailed definition of how the architectonic shape can influence the occupants' comfort perception of the environment according to a specific position. They can also be

interpreted as a way to predict the possibility that an occupant will interact with the space with the aim of modifying the environmental conditions.

**b. Zonal (Time) Availability metrics**

It can sometimes also be useful to describe the environment analyzed with a single value, for example to communicate with non-specialists or to use the information as input for other analysis techniques (e.g., optimization, sensitivity analysis, uncertainty analysis etc.). Starting from these considerations, the Zonal Time Availability metrics were introduced and they were determined according to the definition of spatial Daylight Autonomy (IES, 2012). sDA represents the fraction of space, in terms of floor area, with at least a given value of DA. Similarly the ZTA metrics represent the percentage of the analyzed area which met a minimum local availability of comfort for a specified fraction of the operating hours per year. These metrics are zonal and long-term.

**c. Instant (Space) Usability metrics**

The possibility to build a comfort metric using not a fixed condition but a climatic file allows us to analyze how it changes, moment by moment, according to the relationships between the external and internal environment. Starting from this consideration, the Instant Space Usability metrics were constructed expressing the fraction of space (the floor area is assumed as a reference) that is usable or in comfort conditions in a given moment. These metrics are zonal, because they are intended to underline the zonal quality; and are long-term, because they produce an annual evaluation of comfort within a space. In order to represent the metrics' variability during each time-step of the operating hours analyzed, the carpet plot graphs were chosen. Through this type of graph, it is possible to illustrate the interaction between two or more independent variables and one or more dependent variables in a two-dimensional plot.

**d. Long term usability metrics**

As for the Availability metrics, and with the same aims, also in this case a single value metric was introduced. It expresses and underlines the zonal quality of the environment analyzed and can be introduced as the fraction of time with at least a given fraction of space simultaneously in comfort conditions; i.e. with a minimum value of space usability.



### 3.2.3 Modelling metrics

As previously underlined, in recent years extreme energy performance has been pursued by architects and engineers through different approaches: enhanced insulation and air tightness levels of the opaque envelope, improved glazing and framing systems for window components, increased use of renewable sources and energy materials. In particular among the different renewable sources, solar radiation appears to be the most easily exploitable one. This fact, together with the current architectural tendency of using even more large transparent surfaces in response to occupants' increasing requests for daylighting and external view, has significantly increased the ratio between gains and losses, and put to the test the envelope's capability of ensuring an adequate level of thermal and visual comfort. This is the reason why in this work the analysis of the internal environmental conditions in a confined environment has concentrated on visual and thermal comfort.

In particular, the visual comfort has been described through two metrics' families: the amount of light, which expresses a quantitative evaluation of the visual environment; the glare occurrence, which instead provide a qualitative assessment.

Considering that both thermal and visual comfort conditions are closely related to the quantity and quality of solar radiation entering the confined environment and that the solar radiation is a physical phenomenon characterized by a strong directionality, all the metrics proposed in this study have been calculated referring to an analysis grid, whose density and distance from the floor change according to the specific metric analyzed.

#### a. Amount of light

All the regulations about lighting in confined spaces underline the importance of ensuring an adequate amount of light, natural or artificial, which allows the occupants to perform their tasks in comfort conditions and safety. For this reason a light level which is too high or too low, related with the specific task which has to be performed, should be avoided. The physical quantity usually adopted to quantify the amount of light that reaches a given point P of a given surface or work plane is illuminance:

$$E = \frac{d\varphi}{dA} \quad (8)$$

Where:

- $\varphi$  is the luminous flux incident on an infinitesimal surface in the neighborhood of the given point P
- A is the area of the infinitesimal surface which contains the point.

In this study the daylight illuminance reaching an internal point's grid has been used as the input for the calculation of the indices related to the Amount of light. The illuminance values have been calculated through the Daysim and Radiance software packages (F. C. Reinhart, 2010). Radiance is a validated, physically based backward raytracer that can simulate indoor illuminance and luminance distributions due to daylight for complex building geometries and a wide range of material surface properties for one sky condition at a time. Daysim is a daylighting analysis software that uses the Radiance algorithms to efficiently calculate annual indoor illuminance/luminances profiles based on a weather climate file. While Radiance simulates luminances and illuminances under selected sky conditions, Daysim uses its simulation algorithms to calculate illuminance distributions under all appearing sky conditions in a year. To do this, maintaining the calculation time within a reasonable range, the Radiance algorithms are coupled with a daylight coefficient approach.

The daylight coefficient approach used by Daysim refers to the calculation method proposed in Tregenza and Waters (1983). This method allows us to calculate indoor daylight illuminance levels considering different sky conditions. The celestial hemisphere is divided into sky patches and each one of them contributes to the total illuminance related to each internal points. Daylight coefficient  $DC_\alpha(x)$  describes the illuminance  $E_\alpha(x)$  at point x in the building that is caused by sky segment  $S_\alpha$  which is glowing with normalized luminance  $L_\alpha$ .

$$DC_\alpha(x) = \frac{E_\alpha(x)}{L_\alpha \Delta S_\alpha} \quad (9)$$

Where  $\Delta S_\alpha$  is the angular size of the singular sky segment.

Once the daylight coefficients for all segments of the sky have been calculated for a reference point, the illuminance or luminance at the reference point can be

calculated for any possible sky condition by combining the daylight coefficients with the luminous distribution of the sky. The luminances of individual sky patches for a given sky condition can be calculated by using the Perez sky model. The daylight coefficient approach used in Daysim has been tested in C. F. Reinhart and Walkenhorst (2001) for the calculation of interior illuminances in full scale offices with complex shading devices.

For each point of the grid Daysim calculates a set of daylight coefficients which, essentially, depend on the building geometry, material characteristics and the number of disjoint segments. This means that considering  $\alpha=1\dots N$  the number of segments:

$$E(x) = \sum_{\alpha=1}^N DC_{\alpha}(x)L_{\alpha}\Delta S_{\alpha} \quad (10)$$

In particular Daysim distinguishes between contributions from the diffused daylight, ground reflections and direct sunlight: the celestial hemisphere is divided into 145 disjoint sky segments according to Tregenza and Waters (1983), three additional ground daylight coefficients have been introduced for negative solar altitudes and the contributions from direct sunlight are modeled by some representative sun positions which are a subset of all possible sun positions throughout the year. The total number of direct daylight coefficients is site dependent and varies from 61 to 65 for latitudes below 70°. Near the poles the number decreases down to 48.

Through a specific Matlab code the annual illuminance profiles obtained for each grid point are then used to calculate the metrics related with the amount of light.

- i. Local (Time) Availability metric: Daylight Autonomy (DA). This quantifies the local availability of a sufficient daylighting level in the considered reference period. In other words, DA calculates the percentage of occupied hours per year, when a minimum illuminance level can be maintained by daylight alone. According to the classification proposed in Carlucci et al. (2015), DA can be defined as a local and long-term metric.

$$DA = \frac{\sum_i (wf_i \cdot t_i)}{\sum_i t_i} \in [0,1] \quad (11)$$

$$wf_i = \begin{cases} 1 & \text{if } E_{\text{daylight}} \geq E_{\text{limit}} \\ 0 & \text{if } E_{\text{daylight}} < E_{\text{limit}} \end{cases}$$

Where  $t_i$  is each occupied hour in a year,  $wf_i$  is a weighting factor depending on values of  $E_{\text{daylight}}$  and  $E_{\text{limit}}$ .  $E_{\text{limit}}$  value changes depending on the specific task to be executed.

- ii. Zonal (Time) Availability metric: spatial Daylight Autonomy (sDA). According to IES (2012), sDA is able to provide the annual sufficiency of ambient daylight levels in indoor environments and can be described by means of the percent of analysis area that meets a minimum daylight illuminance level for a specified fraction of the operating hours per year. In other words, it can be described as the area fraction in which the DA overcomes or reaches the  $E_{\text{limit}}$  for at least a predetermined percentage of working hours.

$$sDA_{x/y\%} = \frac{\sum_i (wf_i \cdot DA)}{\sum_i p_i} \quad (12)$$

$$wf_i = \begin{cases} 1 & \text{if } DA \geq DA_{\text{limit}} \\ 0 & \text{if } DA < DA_{\text{limit}} \end{cases}$$

In this case,  $x$  represents the reference illuminance level,  $y$  the time fraction,  $p_i$  are the points belonging to the calculation grid.  $DA_{\text{limit}}$  value changes depending on the specific task which has to be executed. sDA is a zonal and long-term metric.

- iii. Instant (Space) Usability metric: Daylight Usability (DU). It quantifies the usability of the space, in terms of the fraction of space with a sufficient daylighting level in a given moment.

$$DU = \left( \sum_{n=1}^N wf_n \cdot DA_{\text{limit}} \right) \cdot \%space_N \quad (13)$$

$$wf_n = \begin{cases} 1 & \text{if } DA \geq DA_{\text{limit}} \\ 0 & \text{if } DA < DA_{\text{limit}} \end{cases}$$

Where %space<sub>N</sub> represents the confined environment's space percentage belonging to each point of the calculation grid and N the total number of points which constitute the grid. DU is a short-term and zonal metric.

- iv. Long-term Usability metric: time Daylight Usability (tDU). This quantifies the percentage of time with a minimum DU in the room. tDU is defined as the percent of working hours that meets a minimum daylight illuminance level for a specified surface. In other words it can be described as the time fraction in which the DA overcomes or reaches the  $E_{limit}$  for at least a predetermined percentage of the total surface.

$$sDU_{x/y\%} = \frac{\sum(wf_i \cdot DU_{limit})}{\sum_i t_i} \quad (14)$$

$$wf_i = \begin{cases} 1 & \text{if } DU \geq DU_{limit} \\ 0 & \text{if } DU < DU_{limit} \end{cases}$$

In this case, x represents the reference illuminance level, y the surface percentage, t<sub>i</sub> the reference period used for the analysis.

#### b. Visual comfort

Glare is a measure of the physical discomfort of an occupant caused by excessive light or contrast in a specific field of view. As suggested in EN 12464:2011 (CEN, 2011a), glare should be limited to avoid errors, fatigue and accidents. The regulation distinguishes between disability glare or discomfort glare, underlining that in interior work places disability glare is not usually a major problem if discomfort glare limits are met. Glare can be described as a function of: the luminance of the glare source, the background luminance, the size of the glare source and its location in the field of view. Most of the indices used to detect glare issues combine these elements, but they have been derived from experiments with artificial glare sources, not under real daylight conditions.

Considering that one of the aims of this work is to build a consistent set of representation metrics able to really depict the effect of the solar radiation on the internal comfort conditions, the metrics related with the glare sensation have been built using the Daylight Glare Probability index (DGP) as input (Wienold & Christoffersen, 2005; Wienold & Christoffersen, 2006). This index is highly correlated with the user's response to glare perception, as it includes the

vertical eye illuminance, the brightness of the scene and not just the contrast between source and background luminance, and the observer's dissatisfaction (Carlucci et al., 2015). For all these reasons, DGP is especially suitable to evaluate the possibility that glare conditions related with natural light arise.

$$DGP = 5.87 \cdot 10^{-5} E_v + 9.18 \cdot 10^{-2} \log \left( 1 + \sum_i \frac{L_{s,i}^2 \omega_{s,i}}{E_v^{1.87} P_i^2} \right) + 0.16 \quad (15)$$

Where:  $E_v$  is the vertical illuminance;  $L_{s,i}$  is the luminance of the glare source;  $\omega_{s,i}$  is the solid angle of source;  $P_i$  is the position index, which expresses the change in discomfort glare experienced relative to the angular displacement (azimuth and elevation) of the source from the observer's line of sight.

Moreover, the DGP index is characterized by a precise limit value able to describe the percentage of observers who feel a certain luminous environment is uncomfortable. According to the classification proposed in Carlucci et al. (2015), DGP can be described as a local and short-term metric. Even if it is recognized as the most appropriate in a large group of possibilities to analyze absolute glare issues (Suk, Schiler, & Kensek, 2013), its use is not so common yet, because of the high computational time that consumes the calculation procedure.

In order to obtain the DGP annual profiles the evalglare tool (Wienold, Reetz, Kuhn, & Christoffersen, 2004) has been used. Evalglare calculates the DGP starting from a luminance image based on total vertical eye illuminance and contrast. The process is repeated for each hour in the year by using an annual Daysim prediction to calculate vertical eye illuminance and to predict contrast from direct sunlight. For the DGP calculation, in addition to the grid definition, it is necessary to define the view position for the observers.

Also in this case, through a specific Matlab code, the annual DGP profiles obtained for each grid point are then used to calculate the metrics related with the glare comfort.

- i. Local (Time) Availability metric: Visual Comfort Availability (VCA). This expresses the local availability of a sufficient visual comfort in the considered period. Using the DGP as a metric to describe the glare issue means a

comfort value lower than 0.35 (Wienold & Christoffersen, 2006). It is a local and long-term metric.

$$VCA_{DGP} = \frac{\sum_i (wf_i \cdot t_i)}{\sum_i t_i} \in [0,1] \quad (16)$$

$$wf_i = \begin{cases} 0 & \text{if } DGP > DGP_{limit} \\ 1 & \text{if } DGP \leq DGP_{limit} \end{cases}$$

Where  $t_i$  is each occupied hour in a year,  $wf_i$  is a weighting factor depending on values of DGP and  $DGP_{limit}$ .

- ii. Zonal (Time) Availability metric: spatial Visual Comfort Availability (sVCA). It indicates the fraction of space with a minimum VCA. This means that VCA is the fraction of positions in the room that is under visual comfort for at least a certain amount of time during the reference period.

$$sVCA_{0.35/y\%} = \frac{\sum (wf_i \cdot VCA)}{\sum p_i} \quad (17)$$

$$wf_i = \begin{cases} 0 & \text{if } VCA \geq VCA_{limit} \\ 1 & \text{if } VCA < VCA_{limit} \end{cases}$$

In this case, 0.35 represents the DGP value which expresses the limit glare not disabling,  $y$  the time fraction,  $p_i$  are the points belonging to the calculation grid.

- iii. Instant (Space) Usability metric: Visual Comfort Usability (VCU). It expresses the instant usability, in terms of the fraction of space with an adequate visual comfort in a given moment. Again, visual comfort means a DGP value lower than 0.35.

$$VCU = \left( \sum_{n=1}^N wf_n \cdot DGP \right) \cdot \%space_N \quad (18)$$

$$wf_i = \begin{cases} 1 & \text{if } DGP < DGP_{limit} \\ 0 & \text{if } DGP \geq DGP_{limit} \end{cases}$$

Where %space<sub>N</sub> represents the confined environment's space percentage belonging to each point of the calculation grid and N the total number of points which constitute the grid. VCU is a short-term and zonal metric.

- iv. Long-term Usability metric: time Visual Comfort Usability (tVCU). It indicates the fraction of time with a minimum VCU. tVCU is the fraction of time in the reference period with at least a certain amount of space contemporarily in visual comfort.

$$tVCU_{0.35/y\%} = \frac{\sum (w f_i \cdot VCU_{limit})}{\sum_i t_i} \quad (19)$$

$$w f_i = \begin{cases} 1 & \text{if } VCU \geq VCU_{limit} \\ 0 & \text{if } VCU < VCU_{limit} \end{cases}$$

In this case, 0.35 represents the reference DGP level, y the surface percentage  $t_i$  the reference period used for the analysis.  $DGP_{limit}$  is the value which expresses the limit glare not disabling.

#### c. Thermal comfort

Besides the air or the operative temperature, PMV and PPD are the reference quantities when thermal comfort is considered. Their use is suggested by the technical standards such as EN 15251:2007 (CEN, 2007b) when the indoor conditions are controlled by a mechanical heating and cooling system. Although their calculation is based on the air and mean radiant temperatures, which are local properties, their reduced variability can lead to using those metrics as zonal ones. Long-term performance can be evaluated as suggested by the mentioned standard in terms of discomfort time, which typically considers the sum of discomfort time (the time the percentage of dissatisfied is larger than or equal to 10 %) weighted by the PPD). In this study, for consistency with the other metrics, the percentage of satisfied people has been used (complement to the 100 % of the unsatisfied), with the aim of underlining the capacity of the space analyzed to guarantee suitable thermal comfort conditions.

As underlined in part II of paragraph 3.1.1, different studies underline the possibility, and the necessity, to include the effect of the entering solar radiation on the occupants' comfort in the calculation of PMV and PPD. In this study the analytical method proposed by La Gennusa et al. (2007) has been applied. This



enhances the sensitivity to the position, since radiation conditions change over the room. The analytical method cited allows for the easy evaluation of the thermal radiant field induced by the presence of the solar radiation. Starting from the consideration of all the radiative exchanges between the confined environment and human body, a different formulation of the MRT has been elaborated taking into account the direct and diffused component of the solar radiation.

$$T_r = \sqrt[4]{\sum_{i=1}^N F_{S \rightarrow i} T_i^4 + \frac{C_{dn}}{\varepsilon_s \sigma} \left( \alpha_{irr,d} \sum_{j=1}^M F_{S \rightarrow j} I_{d,j} + C_s \alpha_{irr,b} f_p I_b \right)} \quad (20)$$

$$PPD = 100 - 95 \cdot e^{-0.03353PMV^4 - 0.2179PMV^2} \quad (21)$$

As demonstrated in Figure 33 and Figure 34, which represent the PMV calculated using the standard and corrected MRT referring to a person seated in a south oriented open office and located 2 m from the transparent surface (WWR 75 %), the possibility to consider the solar radiation effects in the PMV calculation demonstrates how much short wave radiation can influence the comfort perception.

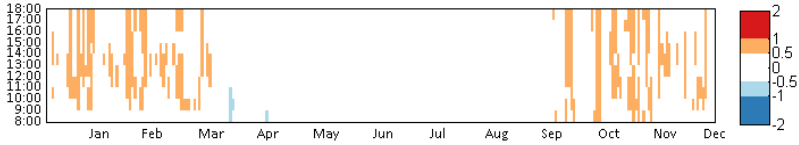


Figure 33 – Standard PMV

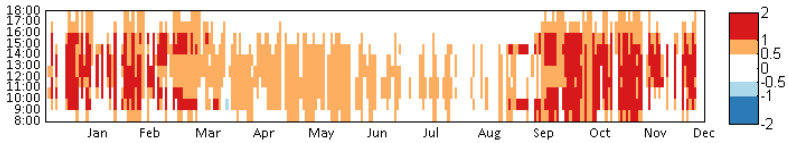


Figure 34 – Corrected PMV

- i. Local (Time) Availability metric: Thermal Comfort Availability (TCA). This expresses the local availability of a sufficient thermal comfort in the considered period. According to the technical standard EN 15251:2007 (CEN, 2007b) thermal comfort means a PPD value lower than 10 %.

$$TCA_{PPD} = \frac{\sum_i (w_{fi} \cdot t_i)}{\sum_i t_i} \in [0,1] \quad (22)$$

$$w_{fi} = \begin{cases} 0 & \text{if } PPD \geq PPD_{limit} \\ 1 & \text{if } PPD < PPD_{limit} \end{cases}$$

Where  $t_i$  is each occupied hour in a year,  $w_{fi}$  is a weighting factor depending on values of PPD and  $PPD_{limit}$ .

- ii. Zonal (Time) Availability metric: spatial Thermal Comfort Availability (sTCA). It expresses the fraction of space with a minimum TCA. In this work the minimum TCA is 90 %.

$$sTCA_{x/y\%} = \frac{\sum (w_{fi} \cdot TCA)}{\sum p_i} \quad (23)$$

$$w_{fi} = \begin{cases} 0 & \text{if } TCA > TCA_{limit} \\ 1 & \text{if } TCA \leq TCA_{limit} \end{cases}$$

In this case, x represents the PPD threshold, y the time fraction,  $p_i$  are the points belonging to the calculation grid.

- iii. Instant (Space) Usability metric: Thermal Comfort Usability (TCU). This expresses the instant usability, in terms of the fraction of space with an adequate thermal comfort in a given moment. Again, thermal comfort means a PPD value lower than 10 %.

$$TCU = \left( \sum_{n=1}^N w_{fn} \cdot PPD \right) \cdot \%space_N \quad (24)$$

$$w_{fi} = \begin{cases} 0 & \text{if } PPD < PPD_{limit} \\ 1 & \text{if } PPD \geq PPD_{limit} \end{cases}$$

Where  $\%space_N$  represents the confined environment's space percentage belonging to each point of the calculation grid and N the total number of points which constitute the grid. TCU is a short-term and zonal metric.

- iv. Long-term Usability metric: time Thermal Comfort Usability (tTCU). It expresses the fraction of time with a minimum TCU for at least a certain amount of occupied hours.

$$tTCU_{x/y\%} = \frac{\sum(wf_i \cdot TCU)}{\sum_i t_i} \quad (25)$$

$$wf_i = \begin{cases} 0 & \text{if } TCU < TCU_{limit} \\ 1 & \text{if } TCU \geq TCU_{limit} \end{cases}$$

In this case, x represents the PPD threshold, y the space percentage,  $t_i$  the reference period used for the analysis.

d. Global comfort

As far as the construction of the metrics related to a global comfort condition is concerned, only qualitative comfort metrics have been considered, neglecting quantitative availability of daylight.

- i. Local (Time) Availability metric: Global Comfort Availability (GCA). Based on the VCA and TCA, GCA is defined as the fraction of the considered period in which both visual and thermal comfort is available in the considered position.

$$GCA = \frac{\sum_i(wf_i \cdot t_i)}{\sum_i t_i} \in [0,1] \quad (26)$$

$$wf_i = \begin{cases} 0 & \text{if } PPD \geq PPD_{limit} \\ 1 & \text{if } PPD \leq PPD_{limit} \end{cases} \quad \begin{matrix} DGP \geq DGP_{limit} \\ DGP < DGP_{limit} \end{matrix}$$

Where  $t_i$  is each occupied hour in a year,  $wf_i$  is a weighting factor depending on values of PPD and  $PPD_{limit}$ , and DGP and  $DGP_{limit}$ .

- ii. Zonal (Time) Availability metric: spatial Global Comfort Availability (sGCA). This represents the fraction of space with a minimum GCA. It expresses a global spatial evaluation, and it represents the floor percentage in which both the comfort conditions are fulfilled simultaneously for at least a predetermined percentage of occupation time. It means that, considering the calculation grid, each single point can be considered in a global comfort condition only if both the comfort conditions are respected in the same instant.

$$sGCA_{x/y\%} = \frac{\sum(wf_i \cdot GCA)}{\sum_i p_i} \quad (27)$$

$$wf_i = \begin{cases} 0 & \text{if } GCA \geq GCA_{limit} \\ 1 & \text{if } GCA < GCA_{limit} \end{cases}$$

- iii. Instant (Space) Usability metric: Global Comfort Usability (GCU). Based on the VCU and TCU, GCU is defined as the fraction of the considered space in which both visual and thermal comfort is maintained in the considered moment. Also for this metric, considering the calculation grid, each single point can be considered in a global comfort condition only if both the comfort conditions are respected in the same instant.

$$GCU = \left( \sum_{n=1}^N w_{f_n} \cdot (VCU_n + TCU_n) \right) \cdot \%space_N \quad (28)$$

$$w_{f_i} = \begin{cases} 0 & \text{if } VCU < VCU_{limit} \quad TCU < TCU_{limit} \\ 1 & \text{if } VCU \geq VCU_{limit} \quad TCU \geq TCU_{limit} \end{cases}$$

Where  $\%space_N$  represents the confined environment's space percentage belonging to each points of the calculation grid and  $N$  the total number of points which constitute the grid. GCU is a short-term and zonal metric.

- iv. Long-term Usability metric: time Global Comfort Usability (tGCU). It is the fraction of time with a minimum GCU. This expresses the percent of analysis area in which both the comfort conditions are guaranteed simultaneously for at least a fixed spatial threshold during the reference period

$$tGCU_{x/y\%} = \frac{\sum(w_{f_i} \cdot GCU)}{\sum_i t_i} \quad (29)$$

$$w_{f_i} = \begin{cases} 0 & \text{if } GCU < GCU_{limit} \\ 1 & \text{if } GCU \geq GCU_{limit} \end{cases}$$

In this case,  $x$  represents the PPD and DGP threshold,  $y$  the space percentage,  $t_i$  the reference period used for the analysis.

#### e. Analysis grid definition

The assessment of the comfort conditions inside a confined space must take into consideration the presence of the occupants inside the confined space itself. Moreover, if the analysis is related to non-residential buildings, like offices, schools or hospitals, it is essential to consider that probably the occupants do not have the possibility to change their position in order to reach better comfort conditions. This aspect becomes more important when the comfort conditions

analyzed concern the solar radiation, physical phenomena characterized by a high directionality. For this reason, even if during the first steps of the designing phase it could be difficult to imagine the space as it could be organized, it is necessary to find a criterion to set a calculation grid.

The grid density and position is closely related to the physical phenomena analyzed and to their qualitative or quantitative nature. For this reason in this study different methods for the definition of the analysis grids have been proposed, according to the physical phenomena represented by the specific comfort metric.

Regarding the analysis grid related with the evaluation of the illuminance distribution, EN 12464:2011 (CEN, 2011a) can be used as a reference. The standard suggests that the grid cells should approximate a square, the ratio of length to width of a grid cell shall be kept between 0.5 and 2 and the grid should be preferably centered on a space. The maximum grid size shall be:

$$p \cdot 0.2 \cdot 5^{\log_{10}(d)} = x \quad (30)$$

Where:

- $p \leq 10$  m;
- $d$  is the longer dimension of the calculation area (m), however if the ratio of the longer to the shorter side is 2 or more then  $d$  becomes the shorter dimension of the area;
- $p$  is the maximum grid cell size (m).

The number of points in the relevant dimension is given by the nearest whole number of  $d/p$ .

A peripheral band 0.5 m deep, beside the walls, should be excluded from the analysis. Considering that the evaluation of the illuminance values are related with the specific task executed by the occupants, the calculation grid should be located at the height corresponding to the work-plane.

Instead, considering the metrics related with glare and thermal comfort, the analysis grid's density should be calculated according to the crowding index, in order to determine the number of people simultaneously present in the analyzed environment. The standard UNI 10339:1995 (UNI, 1995), in the Annex A, suggests different values for the crowding index  $n_s$  according to the building's intended use. For example, for an open-space office a crowding index equal to 0.12 person  $m^{-2}$  can be used. Also in this case a peripheral band 0.5 m deep,

beside the walls, should be excluded from the analysis, in order to take into account the presence of furniture or doors, and the grid should be preferably centered on a space. Once the occupants' number is known, it is possible to design the analysis grid whose points will indicate the position of the people inside the analyzed environment. The grid elevation changes with the comfort condition analyzed. If the possibility of glare occurrence has to be evaluated, the analysis grid should be located at the occupant's eyelevel, in order to correctly evaluate the level of illuminance perceived by the observer. If the analysis grid evaluated the thermal comfort, its elevation has to be established according to EN ISO 7726:2001 (CEN, 2001) Annex B and C.

## 4. Metrics Application in Simulated Environment

### 4.1 Simulation procedure

In order to represent the behavior of a building in sufficient detail to assess visual and thermal comfort aspects, the use of dynamic simulation codes is necessary. When evaluating the overall building performance, considering both the energy and the thermal and visual comfort aspects, a single simulation code would not be enough. Some of the references previously analyzed adopted this approach, deploying more than one simulation code at a time. In Vanhoutteghem et al. (2015) Energy Plus was complemented by DAYSIM for the daylighting analysis, while in Mainini et al. (2015) Energy Plus was coupled with Radiance, able to better depict the light distribution inside the indoor spaces. As underlined in Ramos and Ghisi (2010), the analysis by means of EnergyPlus can lead to an overestimation of daylighting and a subsequent underestimation of the artificial lighting needs.

In order to overcome this situation, in this paper besides EnergyPlus for the energy simulation, the lighting analysis of each configuration was conducted by means of DIVA, which uses Radiance and DAYSIM calculation algorithms. The daylight illuminance on the work-plane calculated by DIVA was processed through a MATLAB code in order to establish the control profiles for shading devices and artificial lights, based on the illuminance thresholds. Then the

daylighting performance of each configuration was obtained through the effective illuminance profiles determined by the shades position. Coupling the DGP profiles, calculated by DIVA for each shade positions, and the roller shades schedules, the effective DGP profiles were calculated and used as inputs for determining the visual comfort indices. The shading devices control profiles, in this case joined with the artificial lights schedule, were also used as inputs for the EnergyPlus simulation to calculate the MRT perceived by the subjects, according to EN ISO 7726:2001 (CEN, 2001), and the direct and diffused solar radiation passing through the transparent surfaces. These last outputs were post processed through MATLAB to calculate the influence of solar radiation on occupants' thermal comfort sensation according to La Gennusa et al. (2005) and La Gennusa et al. (2007). At the end, the visual and thermal comfort metrics were analyzed and represented together in order to evaluate the global comfort performance for the different configurations analyzed. The flowchart in Figure 35 depicts the whole simulation procedure.

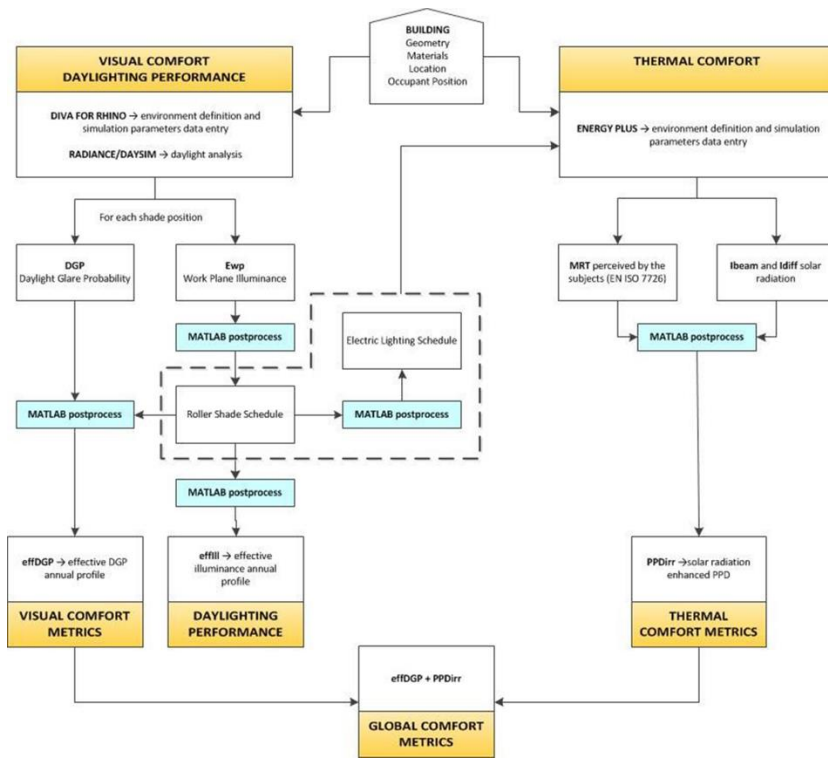


Figure 35 – Methodology flowchart and calculation approach

## 4.2 Reference building and parametrical analysis





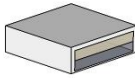
In order to verify the capability of the metrics proposed to describe and discriminate the performance of different building configurations, an open-space office module was defined as a test building. The module is characterized by a floor area equal to 100 m<sup>2</sup> and 3 m internal height and it is located in Rome, Italy (Lat. N 42° 54' 39''; HDD18: 1420 K d - CDD18: 827 K d). All the opaque envelope elements are composed by an internal clay block layer and an external insulation layer, 0.1 m thick. In this way the envelope thermal transmittance, 0.28 W m<sup>-2</sup> K<sup>-1</sup> complies with the requisites of the national legislation for the considered climatic conditions. The entire envelope is exposed to the outdoor environment, except for the floor which was assumed as adiabatic.



The office is occupied from Monday to Friday from 8:00 a.m. to 6:00 p.m., with an occupation density of 0.12 people m<sup>-2</sup>. The occupants' metabolic heat flux is equal to 70 W m<sup>-2</sup> (75 W sensible portion, 55 W latent). The clothing unit thermal resistance is 1 clo during the heating season (conventionally 1<sup>st</sup> October–31<sup>st</sup> March), and 0.5 clo during the cooling season (1<sup>st</sup> April–30<sup>th</sup> September). The electrical equipment internal loads are equal to 13.7 W m<sup>-2</sup>, while the light power density is 12 W m<sup>-2</sup>.

In order to understand if the proposed metrics are able to discriminate between small differences, some variations were progressively introduced to the reference building, in a sequential approach. To this aim, the less impacting parameter was selected first, defining a corresponding configuration, as reported in Table 15.

Table 15 – Building configurations and configuration parameters values

Configuration		Shading Devices	Window to Wall Ratio	Glazing	Window Position
Base		W/O	S1	DH	S
Shading		SH	S1	DH	S
Large WWR		SH	S2	DH	S
Low SHGC Glazing		SH	S2	DL	S
East- oriented Windows		SH	S2	DL	E

The symbols in Table 15 represent different properties for the configuration parameters indicated in Table 16.

Table 16 – Building configuration parameters and corresponding values

Parameters	Possible values and symbols
Glazing	DH: Double Glazing high SHGC; $U_{gl} = 1.14 \text{ W m}^{-2} \text{ K}^{-1}$ ; SHGC = 0.60; $\tau_{vis} = 0.81$ DL: Double Glazing low SHGC; $U_{gl} = 1.08 \text{ W m}^{-2} \text{ K}^{-1}$ ; SHGC = 0.35; $\tau_{vis} = 0.58$
WWR	S1: 45 %; S2: 75 %
Shading devices	W/O: Without shades SH: High solar transmittance roller shades (external side): $q_s=0.58$ ; $\tau_s=0.16$ ; $q_v=0.51$ ; $\tau_v=0.15$
Window position	S: South E: East

### 4.3 Control strategies and comfort evaluation grid

To ensure suitable indoor comfort conditions, both visual and thermal, the dynamic components of the building, namely the shading systems, when present, the artificial lighting and the heating/cooling system, need to react to the external and internal solicitations.

The artificial luminous flux was varied to complement daylighting, in order to maintain 500 lux on the work-plane, according to the indications of the technical standards EN 12464:2011 (CEN, 2011a). The illuminance value is controlled in three different positions, on the axis perpendicular to the window façade, 0.8 m above the floor, in order to ensure higher uniformity and energy savings.

The shades' position, totally closed or open, is defined according to the daylighting measured in a point on the same axis, 2 m apart from the windows. The reference set-points are respectively the range 500–2000 lux (respectively to open or close the shades).

The evaluation of the illuminance is done on a grid located at 0.8 m from the floor level and composed of 81 equally distributed points, according to EN 12464:2011 (CEN, 2011a). A peripheral band 0.5 m deep, beside the walls, was excluded from the analysis.

For the assessment of glare, the grid spacing was established in order to uniformly cover the indoor space under evaluation. Nine equidistant points were then considered, 3 m apart from each other, again leaving an empty peripheral band of 0.5 m. The occupants' view direction selected is parallel to the window plane, Eastward for South oriented windows and Northward for East windows. Moreover, considering that the DGP accounts for the level of illuminance perceived by the observer, i.e. the vertical illuminance ( $E_v$ ), the calculation grid was located 1.1 m above the floor, approximate height for a sitting person.

Regarding the HVAC system, the inlet air temperature during working hours is controlled to maintain the Operative Temperature (OT) within the comfort range 20 °C–24 °C in the heating season and 23 °C–26 °C in the cooling one, as suggested for the II class comfort level according to EN 15251:2007 (CEN, 2007b). The relation between the air temperature,  $T_a$ , the mean radiant temperature,  $T_{mr}$  and the operative temperature,  $T_o$ , is in agreement with the technical standard EN ISO 13790:2008 (CEN, 2008)

$$T_a = 1.52 \cdot T_{mr} + 2.52 \cdot T_o \quad (31)$$

During the non-occupation period, the system is operated only if the operative temperature is lower than 15 °C, and a maximum value, which depends on the hour of the day. This is 38 °C from 18:00 to 24:00 and it then gradually reduces to 28 °C at 8:00.

The thermal comfort conditions are evaluated on the same 9 points as in the glare evaluation, but 0.6 m above the floor level.

## 4.4 Results

The results of the analysis are the values of the different metrics, namely local time availability (LTA), zonal time availability (ZTA), instant space usability (ISU) and long term usability (LtU) for daylighting (Figure 36), visual comfort

(Figure 37), thermal comfort (Figure 38) and global comfort (Figure 39), comparing the performance of each of the five considered building configurations. As for the LTA metrics, which are local and long term, a value is provided for each of the positions in the calculation grid summarizing the yearly behavior. Therefore, it is possible to represent these values on a schematic plan of the considered room, mapping the comfort conditions and assessing their distribution in space. Besides numerical values, a color shades scale is useful to underline the critical positions, as in the first column of each of the Figure 36 to Figure 39. DA in the first row of Figure 36 has been considered just in 9 of the 81 positions calculated, to make the visualization more consistent with the one of the remaining comfort conditions in Figure 37 to Figure 39.

As to the ISU metrics, which are instant and zonal, an overall value is available for the entire room per each time step in the occupation period. The most suitable representation is a temporal plot, as in the second column of the Figure 36 to Figure 39. For each hour of the working day (on the vertical axis) in each working day of the year (on the horizontal axis), the color shade is related to the value of the indicator. It is then possible to identify the most critical periods in the year or hours in the day.

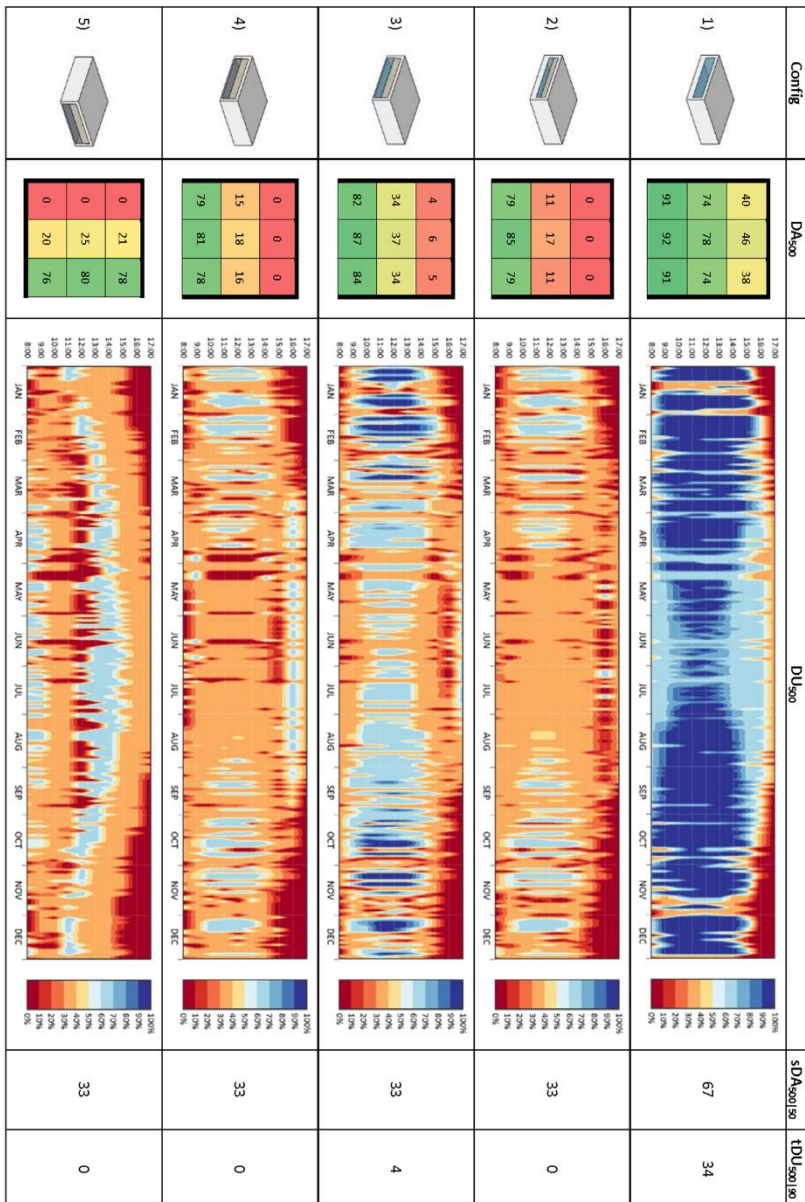


Figure 36 – Daylight performance: comparison between daylight autonomy, daylight usability, spatial daylight autonomy (sDA) and time daylight usability (tDU) for the five building configurations analyzed

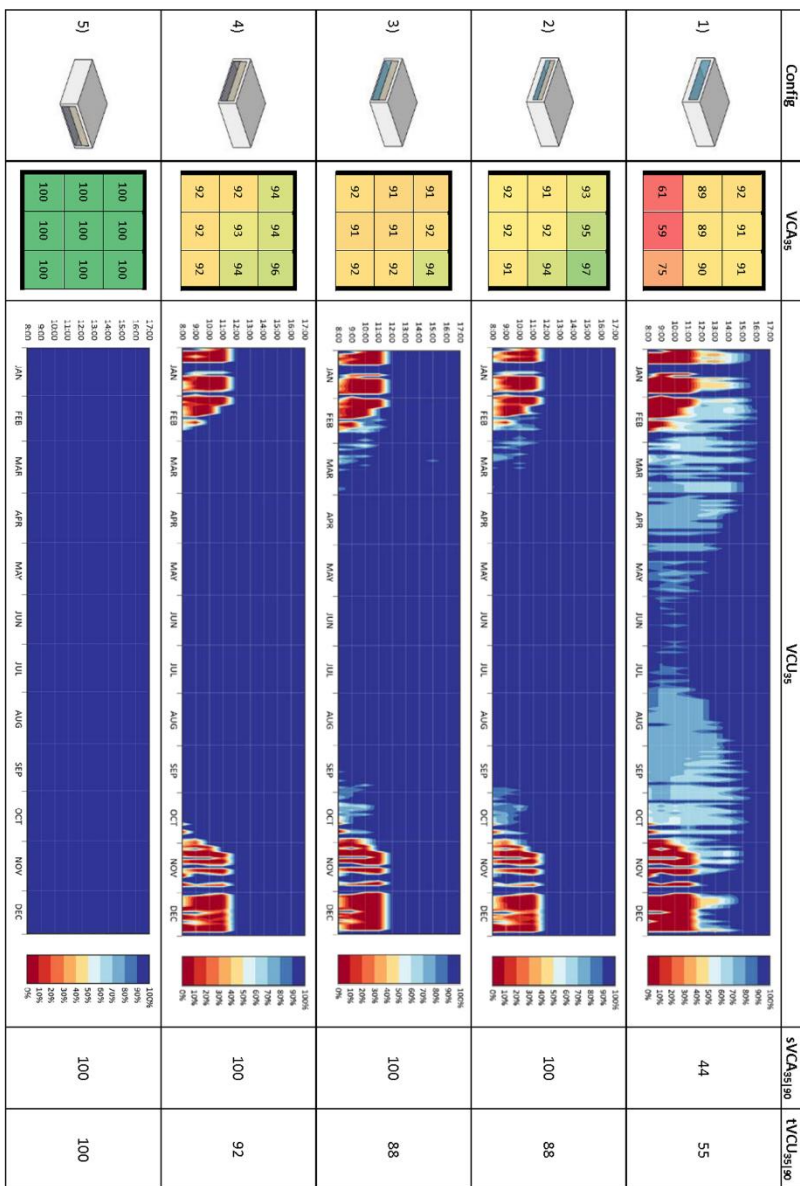


Figure 37 – Visual Comfort: comparison between visual comfort availability, visual comfort usability, spatial visual comfort availability (sVCA) and time visual comfort usability (tVCU) for the five building configurations analyzed

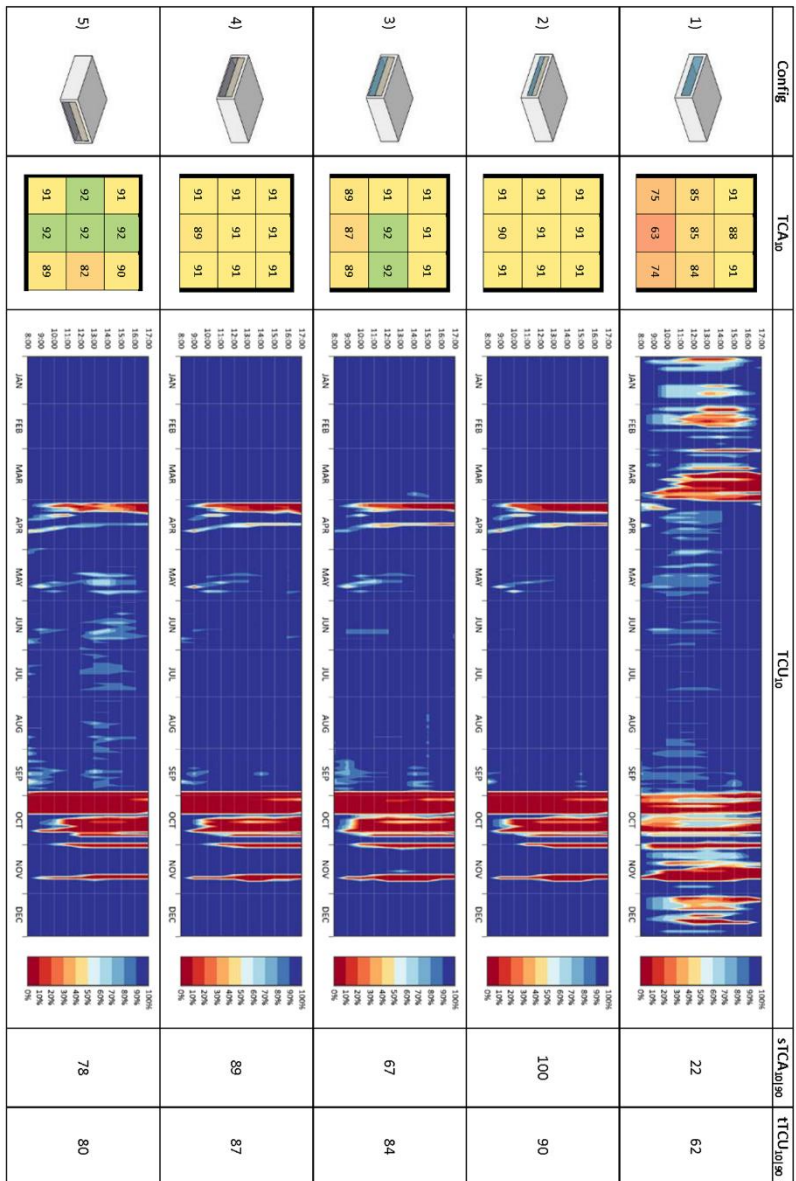


Figure 38 – Thermal Comfort: comparison between thermal comfort availability, thermal comfort usability, spatial thermal comfort availability (sTCA) and time thermal comfort usability (tTCU) for the five building configurations analyzed

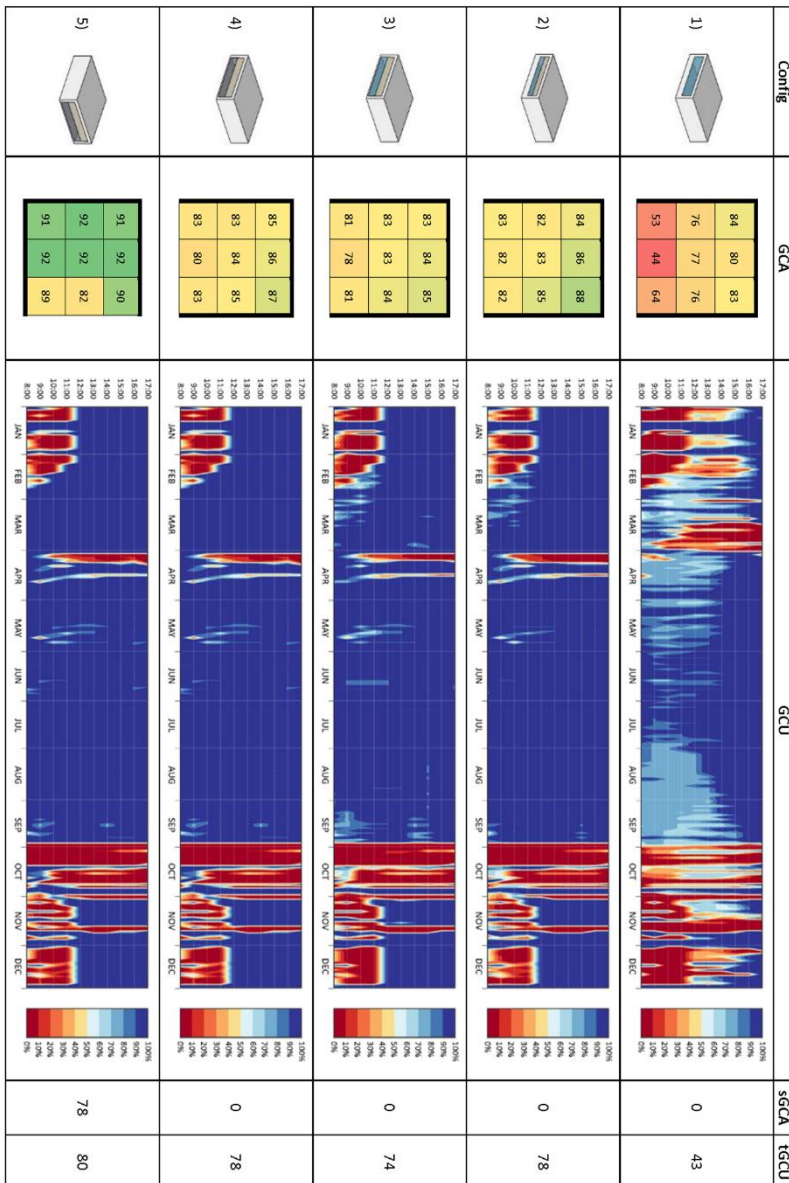


Figure 39 – Global Comfort performance: comparison between global comfort availability, global comfort usability, spatial global comfort availability (sGCA) and time global comfort usability (tGCU) for the five building configurations analyzed



## 4.5 Comments

### 4.5.1 Daylighting performance

The absence of shading devices in Configuration 1 leads to the largest accessibility to daylight. The room's depth and the position of the windows just on one single side are expected to result in a non-ideal spatial distribution of daylight, especially in the middle of the day, if daylight is available, and when the sun is higher on the horizon, as in summer. This is confirmed by the considered metrics and representations. In particular:

DA significantly decreases while moving away from the window. It can be seen that there is not a large difference for points at the same distance from the window, meaning that the time under sufficient daylighting even if differently distributed in time, has almost the same overall occurrence at each position.

DU contributes to the analysis, confirming the expectations and showing the uniformity of appropriate daylighting across the room, which is higher in the central part of the day, and in winter. Cloudy days and the first and last hours in the working day are the most critical.

sDA is relatively large, also because of the low reference threshold (50 %), synthesizing what was already seen for DA, i.e. an adequate to high level of daylighting for the points closer to the window.

tDU is relatively low, summarizing the performance in terms of DU, and showing a totally different aspect from the sDA. In this case, there is quite a short period in the year in which 90 % of the positions have simultaneously adequate daylight levels.

In Configuration 2, roller shades, controlled on the working plane illuminance level of the central point closest to the window, cut a significant part of daylight. They are closed for 76 % of the working period starting from the first hours of the working day. It is expected this is reducing the daylight availability in the points further from the window, increasing the inhomogeneity of the room conditions especially when the sun is higher. The metrics confirm the above situation:

DA is reduced especially for the points further from the window.

DU is reduced especially in summer when shades tend to stay closed for longer. The fraction of the room simultaneously under appropriate level of daylighting is then smaller.

sDA is significantly affected, meaning that also the points in the middle of the room never tend to receive appropriate daylight for less than 50 % of time.

tDU is now very low, showing that 90 % of the surface is never simultaneously usable in terms of daylighting.

In Configuration 3, the larger windows are expected to allow for larger daylight availability for all the points of the calculation grid, even if the roller shades' closing time increases to 79 %. The largest transparent surface should also ensure a better daylight distribution, being able to maximize the radiation contribution even when the sun is low. The above conditions are well represented by the metrics, which highlight:

DA values larger than the one for Configuration 2, especially for the two first rows closer to the window.

DU slightly increased during the entire year, especially during the central working hours, thanks to the largest uniformity of suitable conditions.

sDA constant, which does not allow the appreciation of any difference with Configuration 2.

tDU, still very low (4 %), it is anyhow different from the null value of Configuration 2, underlying some improvement.

In Configuration 4, the glazing systems with lower SHGC allow us to reduce the period shades are closed to a few hours in the central part of the day, 68 % of the occupied time in total. This probably does not compensate for the reduction in daylighting availability, because of the significant reduction in the glazing system visible transmission, which is almost halved. The proposed metrics confirm the analysis, showing that:

DA is generally reduced to values quite close to those of Configuration 2. DU is generally lower along the year, quite similar to Configuration 2, with some exception in the late afternoon in summer, when shades can stay open.

sDA value is again the same of the two previous configurations.

tDU is again reduced to 0, as in Configuration 2, confirming what underlined by the DU. The high reference target of 90 % could be the main reason for the poor discrimination between the two configurations.

Moving the orientation of the windows from South in Configuration 4 to East in Configuration 5, the shadings are closed just in the morning, when the sun is lower, 38 % of the occupied period. This is expected to compensate for the orientation and to provide a somehow higher availability and usability at least in the first hours of the afternoon. The metrics allow us to confirm that:

DA values show a slight increase for the points belonging to the second row, the mid one.

DU shows a different daylight distribution during the day, with a fair usability in the first hours after midday, especially in the summer period.

sDA is not able to explain any difference with the three previous configurations.

tDU is also the same of Configuration 2 and 4, probably because of the high reference target.

#### 4.5.2 Visual comfort

The largest accessibility to daylight, which characterizes the first configuration without shades, makes the occupants more easily subjected to glare problems, in particular for the points closest to the window. This condition is likely to be even more critical and diffused during the early morning and in winter, because of both the occupants' sight direction, East, and the sun's altitude. Actually, the metrics' representations underline that:

VCA increases moving away from the windows. The representation is able to highlight the most critical position, the central point of the row closest to the window.

VCU is able to underline the criticalities during the first hours of the day, especially during the winter season related to the occupants' orientation. The first row's poor conditions prevent the achievement of a uniform environment during almost all the year except that in summer.

sVCA helps highlight that even some of the points belonging to the mid row are slightly affected by the glare, which does not allow visual comfort for more than 90 % of the occupation time.

tVCU underlines the inappropriateness of the configuration analyzed in ensuring the simultaneously usability of the surface in terms of glare.

The roller shade presence in Configurations 2 and 3, cutting the incoming solar radiation, reduces the visual discomfort hours ensuring a more homogeneous distribution of the comfort conditions throughout the space. The larger size of widows is almost compensated by the longer closure time of shades. As for the metrics:

VCA increases, especially for the points belonging to the first row, showing an apparently satisfactory situation, at least in terms of time frequency of visual comfort at each point.

VCU integrate that information showing that visual comfort is not achieved simultaneously in the room. Moreover, the metric is able to prove some limitations of the considered roller shades, unable to prevent glare when the sun is low respect to the line of the horizon.

sVCA confirms that all the points are able to ensure the right internal visual comfort conditions for more than 90 % of the occupation time.

tVCU underlines the larger usability of the surface, 88 % of which is simultaneously under the right comfort conditions for at least 90 % of time.

The glazing system used in Configuration 4, characterized by a lower visual transmittance, should help to improve the visual comfort conditions, increasing the quantity of surface usable in the same instant. This is what appears also from the metrics representation:

VCA slightly increases especially for the points in the rows further from the window.

VCU underlines how the low visual transmittance glazing system is able to remove the glare discomfort conditions during the first hours of the day in February and September increasing the quantity of usable space.

sVCA maintains a constant value, showing again some limitations in capturing the differences between configurations.

tVCU slightly increases, consistently with the improvement of the overall performance.

In Configuration 5, even if with East oriented windows, the shading features and control strategies are definitely able to guarantee, for each point and for every instant, comfortable visual conditions. Even if this may seem in contrast with the critical conditions generally associated with East oriented windows, this is consistent with the Northward view of the occupants, which would make glare issues just in the hours before the occupation period.

#### 4.5.3 Thermal comfort

A transparent surface without any sun protection exposes the occupants to possible overheating problems. This is what actually happens in Configuration 1, where a window facing south, even if with a low window-to-wall ratio, makes the environment uncomfortable, especially considering the positions closest to the glazing system. This behavior is effectively described by the metrics proposed. In particular:

TCA shows the situation is particularly critical for the points belonging to the first row, especially for the central one, which is in a thermal comfort condition for only 63 % of the working time. Moving away from the transparent surface, the situation improves, as is expected.

TCU allows us to evaluate how the comfort thermal sensation is spread in the space, demonstrating that in the summer period, when the sun is higher on the horizon and is not able to penetrate deep in the room, the space usability is at a maximum.

sTCA confirms the poor quality of Configuration 1, which is able to ensure the right thermal comfort only in 22 % of the space.

tTCU highlights a critical situation, showing that the total surface is simultaneously under the comfort conditions for only 62 % of the time.

Considering the high roller shades shuttering time, equal to 76 % of the occupation time in Configuration 2, an improvement of the thermal comfort conditions is expected.

TCA improves showing a more homogeneous distribution of the thermal comfort conditions along the time for all the analysis points considered.

TCU allows us to understand how the transitional seasons are the most critical period in the year, during which all the space appears not usable, in relation to the combination of setpoint ranges and clothing level, so independently of solar radiation.

sTCA confirms what is shown by the TCA metrics, underlining that the configuration is able to maintain thermal comfort in 100 % of the space for 90 % of the working time.

The presence of the critical areas in spring and autumn is confirmed by the tTCU metric, but the value of the time of contemporary comfort has increased from 62 % to 90 %.

An increased WWR leads to longer shuttering times, but at the same time allows a larger amount of solar radiation to enter the confined environment, especially considering that both the roller shades and the glazing are characterized by high levels of solar transmission.

TCA underlines this aspect highlighting the reduction of the hours in thermal comfort conditions for the points closest to the window, at the same time, the increase for the points in the second row.

TCU also confirms for this configuration that the transitional seasons are the most critical, while the larger transparent surface, allowing more solar radiation to enter, reduces the usable surface by a small amount also during the central part of the year.

sTCA synthesizes what is suggested by TCA, showing a consistent reduction compared to the previous configuration.

The percentage of time with the space in simultaneous comfort conditions appears less influenced, showing a tiny contraction if compared with the previous case.

Moving from Configuration 3 to 4 the SHGC of the glazing system decreases, which reduces the roller shades shuttering time (from 79 % to 68 %). This way:

TCA highlights the importance of the solar filtering action of the glazings, especially for the occupants' positions located close to the transparent surface.

TCU remains essentially the same moving from one configuration to the other, again because of the combination of clothing and setpoint range.

sTCA confirms what was already underlined by the TCA metrics, assigning a higher value to the configuration characterized by a lower SHGC.

tTCU slightly improves compared to the previous case.

Changing the orientation from South to East further decreases the period during which the shades stay closed (38 %) and this is expected to lead to a slight worsening of thermal comfort. In the meanwhile, thermal comfort should be less affected by entering solar radiation. Therefore:

TCA is characterized by lower values in the positions closest to the window, while in the remaining points it slightly increases.

The space percentage simultaneously under thermal comfort appears slightly less than in the previous configurations, especially during the summer period.

Both the aspects previously described are confirmed by the synthetic metrics.

#### 4.5.4 Global comfort

The Global Comfort metrics allow us to analyze the contemporaneity of the thermal and visual comfort conditions looked for and evaluate the environmental quality with a global approach. No relative weight has been assumed for the two aspects. As expected, the first configuration is characterized by the worst performance in terms of both time constancy and spatial uniformity of comfort conditions. Moreover, looking at the GCU metric, it is possible to notice how the less comfortable area related to the two different sensations tends to overlap. The use of the roller shading system seems to affect each specific comfort sensation in different moments of the day and the year, but it guarantees at the same time a more homogeneous environment. Increasing the WWR or

changing the glazing typology does not cause significant variations for any of the metrics analyzed. Only modifying the windows' orientation from South to East is it possible to increase the spatial availability of the comfort sensation.

## 4.6 Conclusions

The set of representation metrics introduced is able to consider either time constancy or spatial uniformity of a suitable comfort level, in terms of comfort availability and comfort usability. These metrics allow us to analyze the building performance distinguishing between daylighting, visual and thermal comfort. Moreover, the consistent definition of the metrics related to daylighting amount, visual comfort and thermal comfort has made it possible to compare and combine the different comfort aspects in order to evaluate the global comfort. Even if in this work global comfort has been defined in conditions of both visual and thermal comfort, the defined metrics would allow us to weight them according to the needs or assumptions for any specific applications.

The purpose was to provide the designer with a method to understand and compare the availability of the proper comfort conditions not only in time, for a specific position, but also over the space.

To test the metrics' potential, they have been applied to a set of configurations of open-space office, contrasting their capability to highlight how and by how much different design configurations perform with respect to comfort. To this aim, an integrated simulation approach has been necessary, coupling simulation and programming codes for maximizing their specific potentiality.

The analysis of the simulation results leads to the following conclusions:

When the comparison between different design configurations is necessary in order to find the ones able to ensure the best performance in terms of comfort conditions, space (availability) and time (usability) indexes are both necessary. Spatial and temporal representations of the comfort sensation contribute to the overall evaluation of the quality of a built environment supporting the designer in the optimization of the different aspects.

The synthetic zonal or long-term metrics derived from the above local or instant indices can be useful to communicate with non-specialists and can help the designer to maximize the efficacy of the technical solution chosen, by means of



multi-objective optimization which can include the above metrics together with other performance indicators (annual energy, total costs, etc.).

Conversely, zonal or long term indexes may benefit from the space and time representation of the corresponding instant or local metrics, to understand the reasons of a specific behavior.

Finally, the application of the proposed metrics and their representation has clearly shown the capability of discriminating the effects on the building performance of different design characteristics.

## 5. Practical Aspects: How to Efficiently Model Roller Shading Systems

### 5.1 Introduction

In the period between 1990 and 2012, the energy consumption for thermal use in the tertiary sector rose by 70 % and for electric use by 120 %. During the same period, in the residential sector the thermal use maintained a constant trend, while the electric one was characterized by a 30 % increase. The main part of these electric consumptions are related to the need for cooling (Zinzi, Agnoli, and Fasano, 2014). In order to reduce cooling consumption, the European Directives on the Energy Performance of Building (EPBD 2002/91/EC, 2002) (EPBD 2010/31/EC, 2010), focused on the importance of avoiding an increase in indoor overheating through the use of passive systems, i.e. solar protection and shading systems. Different studies showed that the shading systems, if efficiently operated, can reduce the energy consumption due to cooling needs and, at the same time, improve the internal environmental quality, related to both thermal and visual comfort. As underlined in Kiritat et al. (2016), shading devices can be used to prevent the penetration of direct sunlight and solar radiation into the building in a cooling period and to permit the wanted solar gains in a heating period. Through shading devices it is also possible to manage the daylight distribution in order to make it as homogenous as possible, which is a characteristic desired both in heating and cooling periods. Considering that thermal and visual requests, regardless of whether we are dealing with comfort or energy aspects, can lead to completely different conclusions, the analysis of

the solar shading devices effects on the global building performance has to be performed from the early design stages.

As underlined in the *2013 ASHRAE Handbook–Fundamentals* (ASHRAE, 2013a), fenestrations with shading devices have a degree of thermal and optical complexity far greater than that of unshaded fenestrations. For this reason they are referred to as complex fenestration systems (CFS). Currently different types of shading devices exist: overhangs, external roller shades, venetian blinds and internal shading. Between them, roller shades, regardless of their specific position, represent one of the most commonly shading devices used in buildings, in particular in the tertiary sector. Not only can they be easily installed and maintained, but also they often represent the only design choice when existing buildings are considered. Kirmat et al. (2016) analyzing the studies about simulation modelling on shading devices on buildings from 1996 to 2015, demonstrated that roller shades constitute the third type of shading devices most commonly studied in the literature. In order to maximize the possible positive effects that the roller shades can have with regard to energy and comfort aspects, it is necessary to define an efficient way of simulating how they act on solar and visible transmission. Ye, Xu, Mao, and Ji (2015), in order to demonstrate that internal shading devices can be as effective in cooling reduction as external ones, analyzed the effect of internal roller shades made of highly reflective materials through experimental tests and simulation validations. The final results show that if proper materials are used, the internal shading devices' performance in terms of energy reductions are comparable with the external ones, sometimes even better. Moreover by putting the shades internally, it is possible to reduce the overall cost of the shading system and to provide flexibility to the design of building facades. Through a grey relational analysis they underlined the significant factors influencing the internal shading device performance (thickness, infrared hemispherical emissivity, visible reflectivity, and solar reflectivity). The simulation analysis was carried out by means of Energy Plus, using the WindowMaterial:Shade object to represent the shade's behavior. In Hoffmann et al. (2016), twelve different coplanar shades with different geometry, material properties, and cut-off angles were investigated for two California climates. The simulation analysis was performed combining three research-grade software programs (Radiance, EnergyPlus, and

Window 7) to calculate heat transfer, daylight, and glare resulting from optically-complex fenestration systems (CFS) more accurately. The researchers analyzed different exterior shading devices: slat shading systems, louvers, meshes, and external stainless steel roller shades. Fabric roller shades were used also as an internal layer in order to prevent glare issues. In order to obtain the CFS's optical properties, the external shades' geometries were modeled with Sketch-up, and the Radiance module *genbsdf* was used to generate the bidirectional scattering function (BSDF). The solar energy absorbed in the layers of the fenestration system and the amount of solar radiation incident on the interior surfaces was calculated using Radiance, and then it was provided as external files to EnergyPlus. Regarding the internal roller shades, these were simulated using the WindowMaterial:Shade:EquivalentLayer EnergyPlus object. Chan, Tzempelikos, and Konstantzos (2015) proposed a methodology to identify the range of shading optical properties (openness factor and visible transmittance) that can reduce daylight glare issues. Useful guidelines for selecting properties of shading fabrics were provided, considering the annual visual discomfort frequency that can be associated to a specific fabric. In order to simulate the roller shading system effect on visual comfort conditions, a hybrid ray-tracing and radiosity daylighting model, validated using full-scale experiments, was used, applying the Kotey model (Kotey, Wright, and Collins, 2009) in order to correct shades' solar-optical properties. Yao (2014b), considering that ideal shading control strategies may lead to a significant deviation in energy performance evaluation, carried out field measurements to determine the main environmental factors influencing manual shade adjustment. Using the Markov transition matrix, the author built a stochastic model able to reflect the occupants' dynamic and real behavior characterizing shading state transition. Then, adopting a BCVTB (Building Controls Virtual Test Bed, a software environment for co-simulation) a co-simulation with EnergyPlus was carried out, in order to compare the energy reduction achievable using a manual or an idealized automated control methods. Also in this study the roller shading systems, located both internally and externally, were simulated using the WindowMaterial:Shade object. The same author, in Yao (2014a), carried out field measurements and simulation analysis on a retrofitted residential building in China. The aim of the study was to understand how roller shading systems can

influence energy needs (cooling and heating) and thermal and visual comfort conditions. The same EnergyPlus object was used to simulate the shading device. Athanasios Tzempelikos and Shen (2013) analyzed four different dynamic controls for roller shading systems in order to quantify their influence on cooling, heating and lighting annual demand and annual source, using the assumption that shades have a uniform diffused shade transmittance. Even if the authors underlined the existence of a small direct component of transmitted light, the simulation predicts illuminance values within an acceptable error; in the back of the room (where there are no traces of direct sunlight present) the results are almost identical. The same authors (Shen & Tzempelikos, 2013) conducted a sensitivity analysis to identify the most influencing factors on daylighting and energy performance of perimeter offices with automated interior roller shading systems. An advanced integrated thermal and lighting simulation model was used, which treats the roller shades as Lambertian diffusers. Appelfeld, McNeil, and Svendsen (2012) evaluated the performance of an integrated micro structural perforated shading screen (MSPSS) with respect to a clear glazing, woven roller shades and venetian blinds. All the CFSs were simulated through Radiance to generate a bi-directional scattering distribution function (BSDF). A method for analyzing the façade design of private perimeter offices considering both daylighting and thermal performance was proposed by Shen and Tzempelikos (2012). In this study the roller shade is treated as a Lambertian surface having an initial luminous exitance equal to the total transmitted illuminance. In Kapsis, Tzempelikos, Athienitis, and Zmeureanu (2010) the daylighting performance of bottom-up roller shades, according to different control strategy, was analyzed, developing a daylighting simulation model validated with full-scale experiments. The daylight transmitted through the shade was assumed to be perfectly diffused. As underlined by the authors, this led to an underestimation of the work plane illuminance up to 15% during clear days. In Bessoudo et al. (2010) the effects of venetian blinds and roller shades, coupled with different glazing systems, were evaluated, with the aim of optimizing comfort and energy savings. The roller shades were assumed to be perfect diffusers with constant transmittance over all wavelengths. The hourly evolution of the Mean Radiant Temperature (MRT), corrected for the effect of the solar radiation falling on the person, was analyzed for two representative

days. Tzempelikos et al. (2010) validated through in situ measurements and used the same approach to evaluate different glazing and shading properties. Even if the literature analysis has been restricted to the last five years, it is possible to notice the lack of agreement in the scientific community about what could be the best way to simulate the real behavior of a roller shading system, both from a thermal and visual point of view. It underlines the necessity of defining a common and standardized method for simulating roller shades' behavior.

Concerning the modeling of the shading devices, the most limiting hypotheses deal with the assumption of equal reflectance and emissivity on both sides and of perfect diffuser behavior, with transmittance and reflectance independent of the solar radiation incidence angle. Actually, roller shading systems are characterized by a beam-beam transmittance, by virtue of their material openness factor, and by a beam-diffuse transmittance. Both these quantities change according to the incidence angle, as the solar radiation passing through the material decreases with the increase of its angle. Neglecting the daily variability of these properties can lead to underestimating their impact on the occupants' comfort conditions, decreasing the positive influence that these devices can have at the same time.

## 5.2 Simulating roller shades material: State of the art

As specified in Kotey et al. (2009), a roller blind is made up of strands of yarn that may be woven loosely, leaving open areas, or woven tightly, with no open areas. Its specific composition operates in such a way that the direct solar radiation that hits the roller shade's surface is split in two components: a portion directly transmitted through the openings, and a scattered portion, which, regardless the fact that it can be transmitted or reflected, is considered purely diffuse. Nevertheless, the major part of the technical standards or simulation codes dealing with the calculation of complex fenestration system made with roller shades do not take into account this evidence.

In the *ASHRAE Handbook* (ASHRAE, 2013a) a simplified approach is proposed to calculate the solar shading system effects on thermal exchange introducing the indoor solar attenuation coefficient (IAC). This represents the fraction of heat flow, direct and diffused, that enters the room, considering what have been excluded by the shading. In other words, it represents the ratio between the

solar heat gain coefficient (SHGC) of the glazing system considering the shade's presence and the SHGC not considering it. IAC values have been determined using the standard ASHWAT models (Wright J.L., 2008), and can be used in order to obtain the shaded SHGC. As far as the roller shades are concerned, the Standard assumes that they are equivalent to drapery of 0% fullness (a flat fabric), and then the IAC value can be considered constant as it is independent of incident angle of irradiation. Even if roller shades are described as simply diffusing materials, the Standard underlines that generally shades are able to both transmit and diffuse solar radiation, and that for this reason more complex models would have been needed.

Currently in Europe there are two standards providing a method to estimate the total solar energy transmittance of a solar protection device combined with glazing: EN 13363-1:2007 (CEN, 2007a) and EN 13363-2:2005 (CEN, 2005a). Both of the standards assume the hypothesis that the CFS is hit only by the solar radiation coming from the sun, without considering the sky vault's component, and that all the radiation passing through the solar shading systems is totally diffuse (Zinzi et al., 2014). The methods can be applied to all types of solar protection devices parallel to the glazing (louver, venetian or roller blinds), and they can be located externally, internally or between the glass panes. EN 13363-1:2007 (CEN, 2007a) specifies a simplified method to estimate the total solar energy transmittance of a solar protection device combined with glazing. The method is considered valid as long as the total solar energy transmittance of the glazing is between 0.15 and 0.85 and the solar transmittance and solar reflectance of the solar protection devices are between 0 and 0.5, 0.1 and 0.8, respectively. The simplified method is based on the normal incidence of radiation and does not take into account either the angular dependence of transmittance and the reflectance or the differences of spectral distribution. The total solar energy, light and solar direct transmittance calculation changes according to the shade's position. Synthetically, it is possible to say that the total solar energy transmittance depends on what is transmitted directly through the CFS and what is transmitted according to the absorbance and transmission properties of the shading device. In EN 13363-2:2005 (CEN, 2005a) a detailed method, based on the spectral transmission data of solar protection devices and the glazing, has

been specified to determine the total solar energy transmittance and other relevant solar-optical data of the combination. The method is based on a normal incidence of radiation and does not take into account an angular dependence of transmittance or reflectance of the materials. Diffuse irradiation or radiation diffused by solar protection devices is treated as if it was direct.

Concerning the simulation codes, EnergyPlus makes available three different modelling approaches to simulate roller shades material. The WindowMaterial:Shade model assumes that the transmission, absorption and reflection of material such as drapery or translucent roller shades are not dependent of incidence angle. In other words, they are considered to be perfect diffusers (all transmitted and reflected radiation is hemispherically-diffuse). Moreover, reflectance and emissivity properties are assumed to be the same on both sides of the shade. In contrast, with the WindowMaterial:Shade:EquivalentLayer model it is possible to consider that, by virtue of their material openness, roller shades can also have a beam-beam transmittance. It is assumed to be the same for both sides of the shade and equal to the openness area fraction (OF). Beam-diffuse transmittance and reflectance, and emissivity properties can be different for the front and back of the shade. The off-normal solar property calculation of shades (roller blind) is based on a set of correlations developed from measurement of samples of commercially produced roller blind material with openness fraction less than 0.14 (Kotey et al., 2009). The term off-normal specifies that the model is able to calculate the solar properties values at angles different from the normal one. The model is not intended for materials with unusually high values of openness and should be limited to a maximum openness fraction of 0.20. At the moment the visible spectrum solar properties are not implemented in the calculation. Finally, the WindowMaterial:ComplexShade can be used for modeling shades whose properties are represented by a BSDF file, which contains the optical properties of the Complex Fenestration layers. Generally, the optical properties are given as a two-dimensional matrix describing the basis- and four two-dimensional matrices of system bidirectional optical properties. All these objects are commonly exported directly from the WINDOW program. As underlined in Chan et al. (2015), also Radiance provides different options for simulating roller shades, each one characterized by a different level of

complexity. The simplest model is called trans. s reported in Larson and Shakespeare (2003), it is able to trace direct source rays through a semi-specular surface in order to determine the diffuse and specular transmitted components. Using the trans material, it is not possible to vary the light passing through the material according to the incidence angle, so the specular component is considered fixed. Through the trans model it is possible to define the amount of forward scattering versus ideal diffuse scattering (Apian-Bennewitz, 2013). Therefore, according to the value associated to a specific parameter, starting to an ideally perfect diffuser material up to a forward scattering without diffuse component material can be represented.

In C. F. Reinhart and Andersen (2006), it has been pointed out that Radiance offers also other models which can be used to adjust the direct part of the transmitted component according to the incidence angle: the transdata or transfunction model. The authors validated these models for a translucent glass with diffuse characteristics. In order to simulate non-redirecting and forward scattering materials,) Apian-Bennewitz (2013) affirms that the transdata or transfunction represents the more precise model when BSDF data are not available. Even if BSDF data should be available, as underlined in Chan et al. (2015), the geometrical radiosity method used in WINDOW does not show good agreement between simulated and measured data, while the genBSDF Radiance function performs well for micro-perforated shading system, but it has not been validated yet for open-weave shading fabrics.

### 5.3 Methodological approach

Moving from the considerations reported in 5.1 and 5.2, appears clear the necessity of evaluating the different approaches for the characterization of the roller shade materials behavior embedded in the common simulation codes with the aim of understanding which is able to provide more realistic results. In order to reach this goal, a set of measured data, recorded at the Bowen laboratories of the Purdue University (Indiana, USA), called LAB1 and LAB2, has been used for verifying and validating the different roller shade models. The data were recorded over five days, from 2<sup>nd</sup> to 8<sup>th</sup> June 2015. During this period, the roller shades located in the LAB1 were maintained constantly closed, and constantly open in the LAB2. Both the heating, cooling and lighting systems were kept



switched off. In this way, the only internal gain able to act on the internal air temperature value was the one coming from the acquisition system, a laptop and a data-logger in each room. The external air temperature and the global solar radiation on a horizontal plane, with a one minute measurement time-step, were used for creating a specific climatic file thanks to the Weather Converter EnergyPlus Auxiliary Program. The Weather Converter Program allows creating an epw file regardless from the duration of the measured data used as input. In order to check if the input data were interpreted correctly by the software, a first simulation was performed asking as output the provided input data:

- Environment:Site Diffuse Solar Radiation Rate per Area [ $\text{Wm}^{-2}$ ] (TimeStep)
- Environment:Site Direct Solar Radiation Rate per Area [ $\text{W m}^{-2}$ ](TimeStep)
- Environment:Site Solar Altitude Angle [deg](TimeStep).

Actually, EnergyPlus only uses the solar radiation data for Direct Normal and Diffuse Horizontal radiation in its calculations so, in order to perform the check it is necessary to calculate the global horizontal radiation as:

$$Global_{horradiation} = Direct_{horradiation} + Diffuse_{horradiation} \quad (32)$$

where

$$Direct_{normalradiation} = \frac{Direct_{horizontalradiation}}{\sin(Solar_{height})} \quad (33)$$

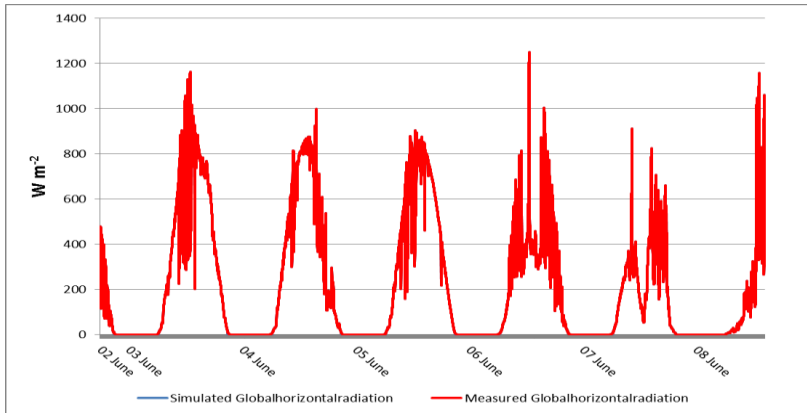


Figure 40 – Simulated VS Measured Global Horizontal Radiation

Also the total vertical solar radiation on the Southern wall calculated thanks to the simulation was compared with the measured data. The two curves show a good agreement considering a ground reflectivity equals 0.35 during the monitored period.

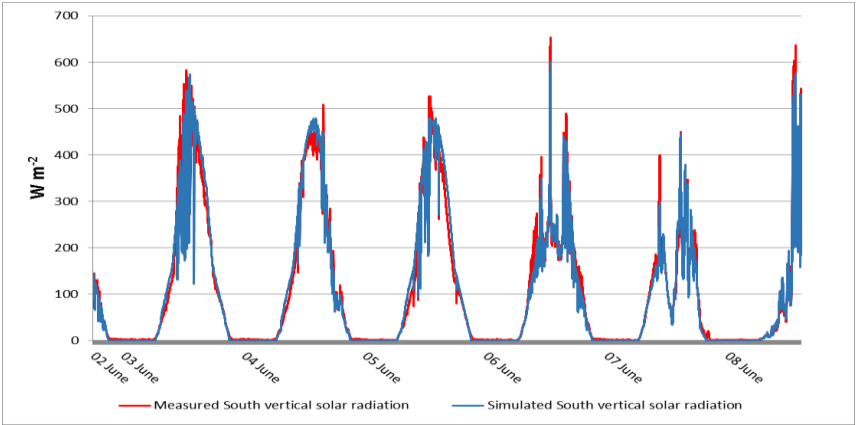


Figure 41 – Measured VS Simulated South Vertical Solar Radiation

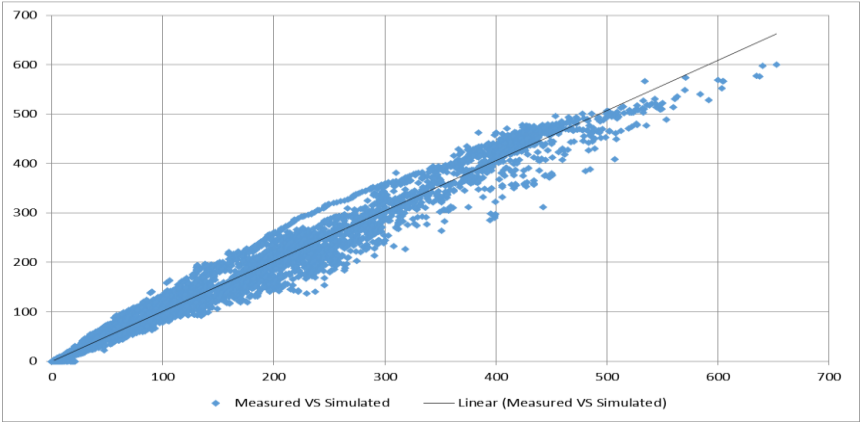


Figure 42 – Measured VS Simulated South Vertical Solar Radiation scatter plot

Starting from a simplest model, which assumes the roller shades as perfect dif-fusers, more complex characterizations were used with the aim of comparing

the results and to understand the extent to which a sophisticated model can influence the designing decisions. The models performance were compared with the measured data in terms of internal air temperature, solar radiation and illuminance, both collected on the work-plane, and vertical illuminance. Considering that one of the analysis aims is the assessment of the shade's influence on internal conditions, in a first stage the simulation results and the measured data were compared through the internal air temperature, in order to evaluate the model reliability. Even if the building's model allowed us to contain the deviation between measured and simulated values within the measurements' uncertainty, it was not able to represent the internal air temperature trend as efficiently as needed, especially during the day. This would prevent us from evaluating the shade's influence on the internal air temperature starting from a neutral condition.

The importance of using building simulation tools in order to evaluate and forecast the "building system" overall behavior, considering energy and comfort aspects has already been underlined. Obviously, the building model used for the analysis has to be able to simulate correctly the physical processes which characterize it. When the first assumptions are not able to provide a sufficiently reliable model, through the model calibration it is possible to reduce the deviation between the real building behavior and the simulated one. In order to better predict the building's physical behavior, a calibration process was carried out by means of jEplus+EA, using as objective function the difference between model predictions and monitored data. The internal air temperature measured in the LAB\_2 was used as argument for the objective function.

## 5.4 Simulations assumptions: First approach

### 5.4.1 Case study and reference test case: geometrical characteristics

The two test cells used as the monitoring site are located inside the Bowen Laboratories area in West-Lafayette (Indiana, USA). The dimensions of the two rooms are 5 m wide  $\times$  5.2 m deep  $\times$  3.4 m high, with a glass facade facing south. According to the environmental conditions kept during the measurements, the LAB\_1 (on the right side of Figure 43) was simulated with the shades always closed, while the LAB\_2 (on the left side of Figure 43) was modelled with a bare

window. In the tests surroundings, there are no other buildings that can intercept the solar radiation.



Figure 43 – Southern façade Bowen Lab. Source: CE Architectural Engineering – Overview Presented to the Civil Engineering Advisory Council April 13, 2012

#### 5.4.2 Characteristics of components: Opaque envelope

The thermal properties of the building components were selected according to on-site surveys and technical documentation. In particular, the insulation layer was simulated as a no-mass material. All the opaque elements confine with the external environment.

Table 17 – Thermal properties of the building components

Construction element	Layer	Material	Thermal resistance	Thickness	Thermal conductivity	Density	Specific heat
Floor	1	Concrete		0.1524	0.53	1280	840
	2	Insulation	3.32				
Exterior wall	1	Gypsum board		0.0159	0.16	800	1090
	2	Insulation	3.32				
	3	Sheating		0.0127	0.055	290	1300
Interior wall	1	Gypsum board		0.0159	0.16	800	1090
	2	Insulation	3.32				
Roof	1	Acoustic tile		0.0191	0.06	368	590
	2	Insulation	3.32				
	3	Air space	0.18				
	4	Concrete		0.1524	0.53	1280	840

### 5.4.3 Characteristics of components: Transparent envelope

The windows are located on the south façade with a WWR equal to 60 %, set 0.6 m from the floor. The glazing system used is a high performance glazing unit produced by PPG Performance Glazings and called Solarban 70XL(2) Clear. It is a transparent, coated, solar control, low-emmissivity (lowe) architectural glass with superior solar control characteristics (Table 18 – Glazing system properties).

Table 18 – Glazing system properties

Glazing	$U_{gl} = 1.130 \text{ W m}^{-2} \text{ K}^{-1}$ ; $SHGC = 0.28$ ; $\tau_{vis} = 0.65$
Window size	width = 4.8 m; height = 2.1 m; area = 10.08 m <sup>2</sup> (WWR 60 %)
Window distribution	South (S)

#### 5.4.4 Heating, cooling and lighting systems

As specified above, during the measurement period both the heating, cooling and lighting systems were switched off. For this reason, the two rooms were simulated as a free floating environment and the lighting system was considered as constantly switched off. Only during the first day, June 2<sup>nd</sup>, was an ideal HVAC system used, in order to reduce the simulation warm-up period.

#### 5.4.5 Internal gains

Both the rooms have a laptop switched on for 24 hours inside with a design level equal to 36 W (ASHRAE, 2013a).

#### 5.4.6 Results

As underlined in 5.3, the first simulation approach provided a simulated trend for the internal air temperature able respecting the limits established as functions of measure uncertainty (Joint Committee for Guides in Metrology (JCGM/WG), 2008). Nevertheless, as highlighted in Figure 44, the simulated trend is not able to match the measured one especially regarding the maximum values. The differences between the peaks are more evident during the last days, characterized by an overcast sky with less effective solar gains.

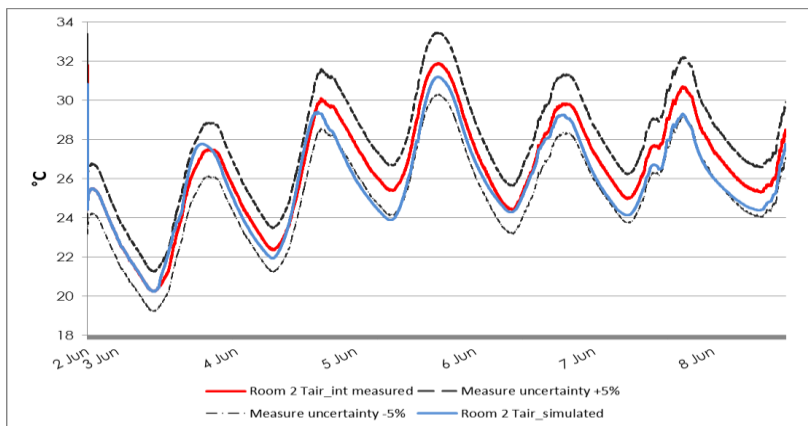


Figure 44 – Internal air temperature measured and simulated Room\_2

## 5.5 Building model calibration through an optimization-based approach

Optimization can be defined as the procedure or procedures used to make a system or design as effective or functional as possible, especially the mathematical techniques involved. Generally, optimization objectives for building design and operation aim to minimize energy demand and/or operational cost, to maximize indoor environmental qualities such as daylight, air quality and thermal comfort or even to optimize all these aspects together. In this work, an optimization-based approach has been used with the intention of reducing the deviation between the real building behavior and the simulated one. In other words, in order to find the parameter values those match, as close as possible, the “measurement” data.

The calibration process was carried out by means of jEplus+EA that is a full-fledged optimization GUI for EnergyPlus which offers out-of-the-box support for jEPlus projects, with user-defined objective functions. It is a highly efficient multi-objective optimization method based on a customized NSGA-II (Deb and Srinivas's Nondominated Sorting Genetic Algorithm). Even if NSGA II is one of the widely multiple-objective Genetic Algorithms (MOGAs) used nowadays, the total number of possible algorithms is practically infinite.

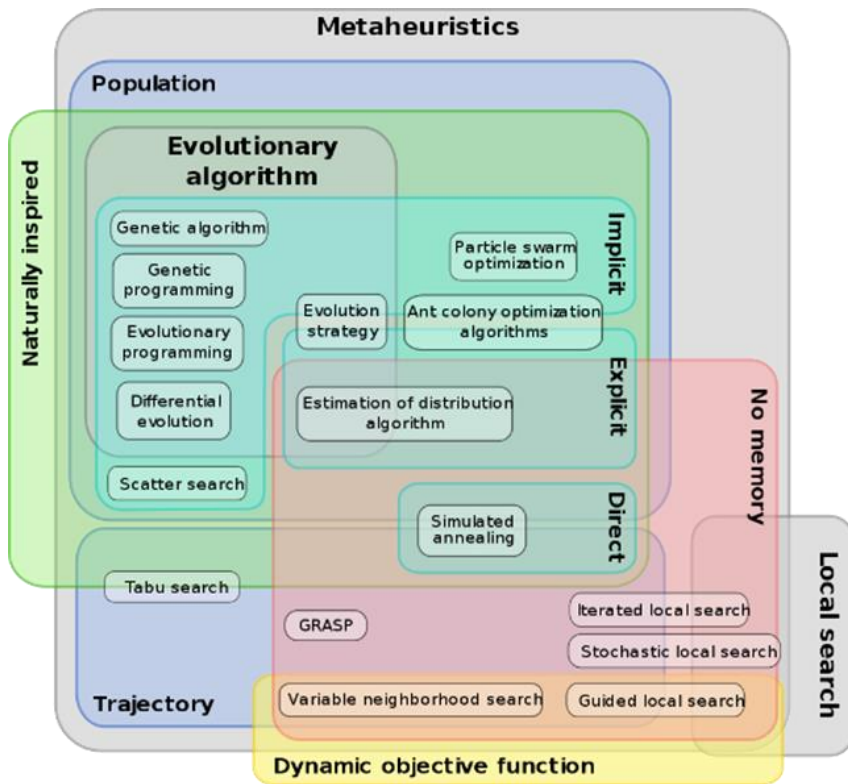


Figure 45 – Heuristic algorithm diagram. Source: Johann “nojhan” Dréo, Caner Candan ([https://commons.wikimedia.org/wiki/File:Metaheuristics\\_classification.svg](https://commons.wikimedia.org/wiki/File:Metaheuristics_classification.svg)), “Metaheuristics classification”, <https://creativecommons.org/licenses/by-sa/3.0/legalcode>

Between this, Evolutionary Algorithms are the most popular choice because of their “robustness”, i.e. a correctly implemented EA tends to solve the problem, no matter what kind of problem it is.

The “goodness of fit” between the calibrated energy model and the utility data was evaluated comparing the result between two different model validation measures: the normalized mean bias error (NMBE) and the coefficient of variation of the root mean square error (CV(RMSE)). These statistical methods are suggested by ASHRAE Guideline 14 which recommends, if dealing with monthly data, a NMBE of +/- 5 % and a CV(RMSE) of +/- 15 % and a NMBE of +/- 10 % and a CV(RMSE) of +/- 30 % with hourly data. The NMBE measures



the variation between predicted and observed values, while the CV(RMSE) the scatter of the data.

$$NMBE = \frac{\sum_{i=1}^n (y_{simulated,i} - y_{measured,i})}{\bar{y}_{measured} \cdot (n - p)} \quad (34)$$

$$CV(RMSE) = \frac{1}{\bar{y}_{meas}} \cdot \sqrt{\frac{\sum_{i=1}^n (y_{sim,i} - y_{meas,i})^2}{(n - p - 1)}} \quad (35)$$

Where:

- $y$  = simulated or measured parameter,
- $\bar{y}$  = mean of measured parameter,
- $n$  = number of data point,
- $sp$  = number of predictor variables.

The optimization procedure which characterizes jEplus+EA does not aim to provide the user with the best solution; instead it helps identify better solutions, improving rather than optimizing the procedure's results. The model calibration was carried out comparing the internal air temperature measured and simulated in the room 2 (bare window) modifying four parameters:

thermal conductivity of the innermost layers which characterize the ceiling, floor and walls' stratigraphy; specific heat of the innermost layers which characterize the ceiling, floor and walls' stratigraphy; flow rate; design level of the electric equipment.

As specified in Prada, Cappelletti Baggio (2013), when the insulation layer is located on the external stratigraphy's part, the internal air temperature is mainly influenced by the innermost layer, characterized by a higher mass. Except for the equipment design level, for all the parameters a variation range of approximately 20 % was considered with respect to the first tentative value.

Table 19 – Input parameters

Input parameters	Acronym	Material	Initial value	Range value	Unit measure
Specific heat	P1	Concrete	840	[672;...;1000]	$\text{J kg}^{-1} \text{K}^{-1}$
	P2	Acoustic Tile	590	[472;...;708]	
	P3	Gypsum	1090	[872;...;300]	
Flow rate	P4		0.1	[0.05;...;0.2]	ACH
Thermal conductivity	P5	Concrete	0.53	[0.42;...;0.64]	$\text{W m}^{-1} \text{K}^{-1}$
	P6	Acoustic Tile	0.06	[0.048;...;0.072]	
	P7	Gypsum	0.16	[0.13;...;0.19]	
Design level electric equipment	P8		36	[40;50;60]	W

Considering the brevity of the monitored period, three days were used for the model calibration and two for its validation. In Figure 46 the horizontal solar radiation trend was plotted. It is possible to underline how during June 3<sup>rd</sup>, 4<sup>th</sup> and 5<sup>th</sup> the sky was mainly clear, while during the last two days an overcast sky prevailed. In order to calibrate the model evaluating climatic condition variability as large as possible, regardless how long the monitored period lasts, the days marked with the red rectangle in the figure were used for the calibration. Therefore, the validation process was performed using June 4<sup>th</sup> and 7<sup>th</sup>. Moreover during the first day, June 2<sup>nd</sup>, the internal air temperature was used as a simulation input, imposing an ideal HVAC unit able to supply air stream using the measured internal air temperature as set-point and decreasing consequently the warm-up period.

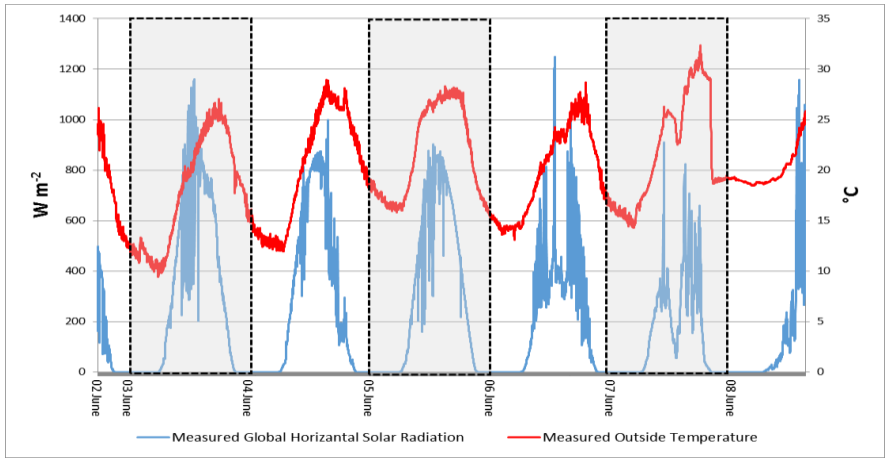


Figure 46 – Measured horizontal solar radiation and external air temperature

The NSGA II optimization algorithm analyzed 677 combinations identifying 19 best solutions (Figure 47, Figure 48).

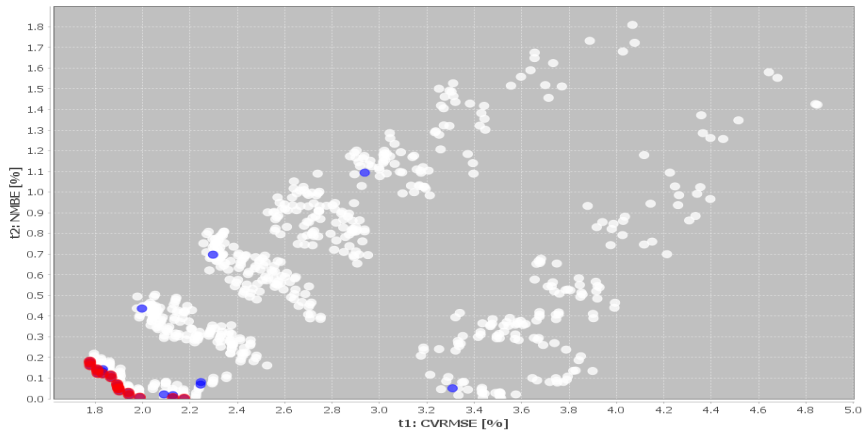


Figure 47 – Scatter plot with the 677 combination analyzed

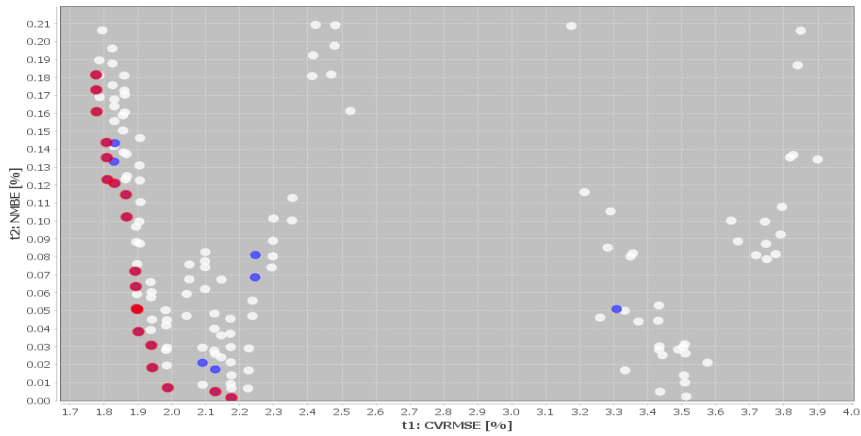


Figure 48 – Zoom on the 19 best solutions

Table 20 provides a general overview of the values assumed by the parameters chosen for performing the calibration procedure.

Table 20 – Parameter values distribution

Acronym	P1	P2	P3	P4	P5	P6	P7	P8	t1 = CV(RMSE) [%]	t2 = NMBE [%]
CASE_0	672	590	872	0.05	0.53	0.048	0.16	60	2.174871212	0.001679751
CASE_1	672	708	1090	0.05	0.64	0.06	0.19	60	1.7769686	0.181436223
CASE_2	672	590	1090	0.05	0.53	0.048	0.13	60	1.866682505	0.102299313
CASE_3	672	472	1090	0.05	0.42	0.048	0.13	60	1.987583958	0.007214566
CASE_4	672	708	1090	0.05	0.64	0.06	0.13	60	1.778351029	0.160935376
CASE_5	672	708	1090	0.05	0.42	0.048	0.13	60	1.901368737	0.038444302
CASE_6	672	590	1090	0.05	0.42	0.048	0.16	60	1.939172524	0.030790656
CASE_7	672	590	1090	0.05	0.53	0.048	0.16	60	1.864659999	0.114663897

CASE_8	672	708	872	0.05	0.53	0.048	0.13	60	2.127512313	0.005015341
CASE_9	672	590	1090	0.05	0.64	0.048	0.19	60	1.807528476	0.143754848
CASE_10	672	590	1090	0.05	0.42	0.048	0.13	60	1.942268224	0.018394624
CASE_11	672	708	1090	0.05	0.42	0.06	0.19	60	1.892086155	0.0720804
CASE_12	672	590	1090	0.05	0.64	0.048	0.13	60	1.810146419	0.123067249
CASE_13	672	708	1090	0.05	0.64	0.06	0.16	60	1.777360281	0.173093385
CASE_14	672	708	1090	0.05	0.42	0.06	0.16	60	1.893532432	0.063540527
CASE_15	672	708	1090	0.05	0.42	0.048	0.16	60	1.898582976	0.050777277
CASE_16	672	708	1090	0.05	0.42	0.06	0.13	60	1.896056784	0.05119934
CASE_17	672	590	1090	0.05	0.64	0.048	0.16	60	1.808433694	0.135334126
CASE_18	672	708	1090	0.05	0.53	0.048	0.13	60	1.831069774	0.121049814

As already underlined, the main aim of the performed calibration procedure was to define the combination of the 4 parameters chosen able to provide an internal air temperature trend as close as possible to the measured values and especially during the hours characterized by the sun presence. Analyzing the values assumed by the two indices, all the best solutions show a trend clearly similar to the measurements, even if those characterized by the lowest NMBE values deviate mainly from the measured maximum value. Figure 49 represents the air temperature trend plotting the measured values (red line), the CASE\_0 curve (light green line), characterized by the lowest NMBE value, and the curve obtained in the first simulation. The grey shaded areas indicate the days chosen for the calibration procedure.

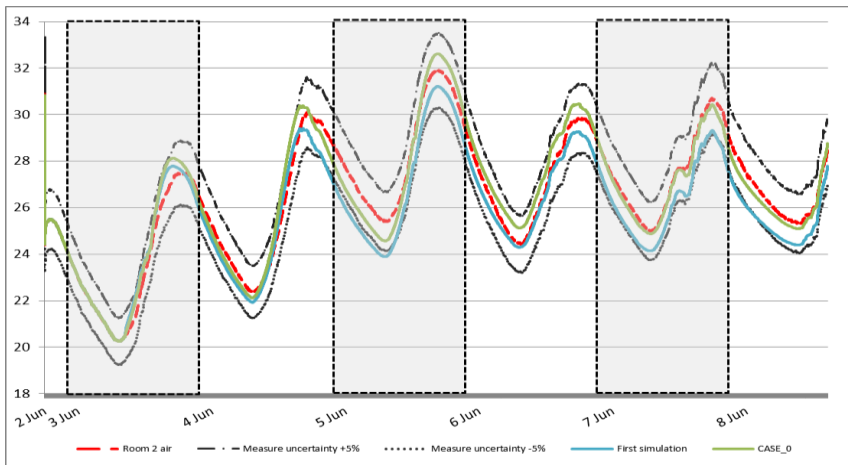


Figure 49 – Measured and simulated internal air temperature comparison

Therefore, according to the purpose of this calibration process, the best solution turns out to be the CASE\_18, characterized by the following indices' values: 1.831069774 for the CV(RMSE) and 0.121049814 for the NMBE (Figure 50).

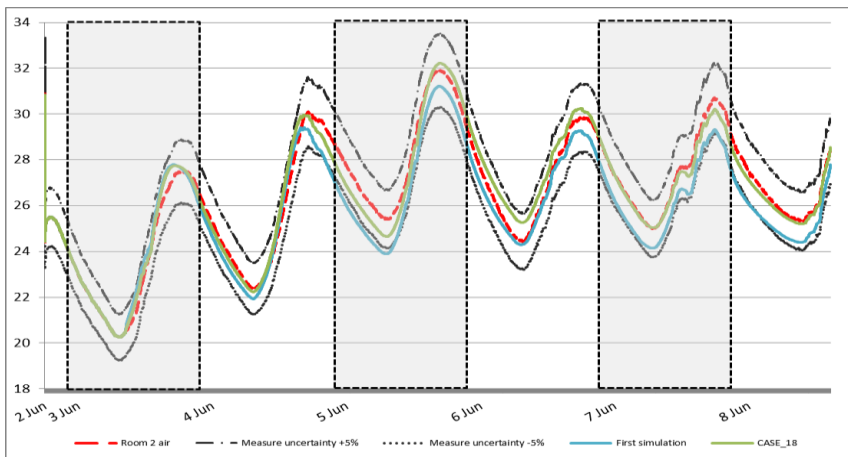


Figure 50 – Measured and simulated internal air temperature comparison

## 5.6 Roller shade models validation through on situ measurements

### 5.6.1 Characteristics of components: Roller shades

The solar and visible roller shade characteristics can be seen in Table 21 and Table 22. They have been calculated by an integrated sphere.

Table 21 – Solar roller shade characteristic (SS-EC02-4 dark color silver screen)

	Normal	15	30	45	60	Side
Beam-Total Transmission	5	5.1	5.1	4.3	2.9	
Beam-Beam Transmission	4.2	3.8	3.1	1.7	0.6	
Beam-Diffuse Transmission	0.8	1.3	2	2.6	2.3	
Beam-Total Reflectance	74.5	74	74.9	74.8	75.9	external side
	28.3					internal side

Table 22 – Visible roller shade characteristic (SS-EC02-4 dark color silver screen)

	Normal	15	30	45	60	Side
Beam-Total Transmission	5	4.9	5	4.1	2.7	
Beam-Beam Transmission	4.2	3.9	3	1.7	0.6	
Beam-Diffuse Transmission	0.8	1	2	2.4	2.1	
Beam-Total Reflectance	72.3	71.7	72.2	72.4	74.2	external side
	28.3					internal side

As stated in Kotey et al. (2009), roller blinds have negligible specular component; hence, the beam-beam (specular) reflectance, is zero. The beam-total reflectance is therefore equal to the beam-diffuse reflectance.

Considering that the diffuse-diffuse transmission can be calculated as follows:

$$\tau_{dd} = 2 \int_0^{\pi/2} \tau_{bt}(\theta) \cos(\theta) \sin(\theta) d\theta \quad (36)$$

According to the measured value it is possible to obtain the diffuse-diffuse transmission value which corresponds to the area underlying the curve in (Figure 51):  $\tau_{dd} = 3.94$ .

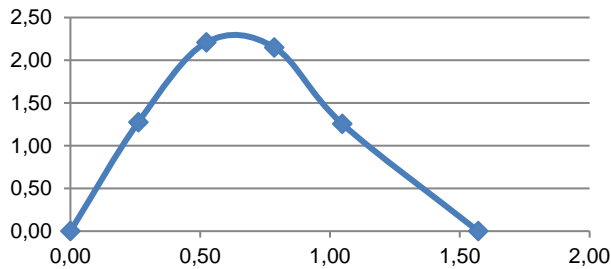


Figure 51 – Incidence angle (rad)

### 5.6.2 Analysis points

The analysis points used to compare the simulation results with the measured quantities were located according to the sensors' position inside the rooms. Considering the orientation, for each room the point (0,0,0) of the reference system in the intersection between the eastern and southern wall was located. In Table 23 all the analysis points with the specific physical quantity measured have been listed.

Table 23 – Sensors coordinate and aim

Sensor name	x	y	z	Physical quantity
Front Right 1	1.7	1.5	0.8	Work-plane illuminance
Front Right 2	1.9	1.5	0.8	Work-plane illuminance
Back Right	3.5	3.7	0.8	Work-plane illuminance
Middle Left	3.5	2.5	0.8	Work-plane illuminance
Vertical Illuminance	2.7	2.5	1.2	Vertical Illuminance
Solar Radiation 1	1.7	3.7	0.8	Work-plane solar radiation
Transmitted Sol Rad 2	Solar Radiation transmitted through window on a vertical plane			
Transmitted Ill	Ill transmitted through window on a vertical plane			

LAB 1



	Sensor name	x	y	z	Physical quantity
LAB_2	Back Left	1.9	3.2	0.8	Work-plane illuminance
	Back Right	1.7	3.2	0.8	Work-plane illuminance
	Front Right 1	1.9	1.6	0.8	Work-plane illuminance
	Front Right 2	1.7	1.6	0.8	Work-plane illuminance
	Front Left 1	3.5	1.6	0.8	Work-plane illuminance
	Front Left 2	3.5	1.6	0.8	Work-plane illuminance
	Vertical Illuminance	2.7	2.5	1.2	Vertical Illuminance
	Solar Radiation 1	1.7	1.6	0.8	Work-plane solar radiation
	Transmitted Sol Rad 2	Sol Rad transmitted through window on a vertical plane			
	Transmitted Ill	Ill transmitted through window on a vertical plane			

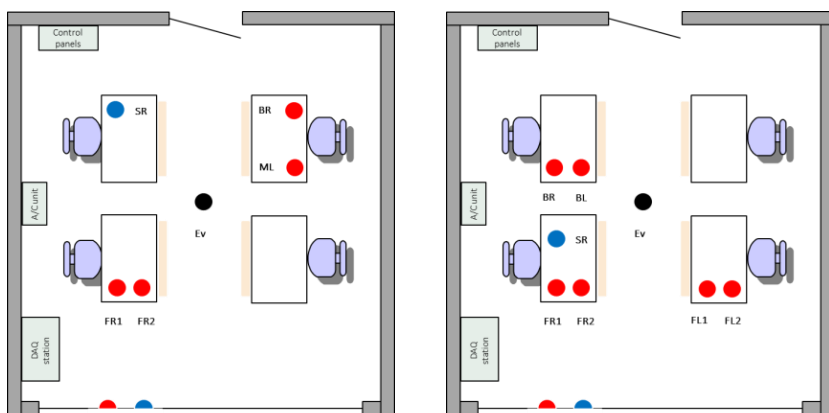


Figure 52 – Sensors' location in LAB1 (right) and LAB2 (left): transmitted or work-plane illuminance = red dots; vertical illuminance = black dots; transmitted or work-plane solar radiation = blue dots

### 5.6.3 Roller shade model descriptions

#### Model A: Shade

In this step the EnergyPlus WindowMaterial:Shade model was used to simulate the roller shade material. According to the solar and visible solar shade characteristics listed in 5.6.1, the following values have been used for the shade's characterization:

Table 24 – Model characteristics

Quantity	Value
Solar Transmittance	0.05
Solar Reflectance	0.745
Visible Transmittance	0.05
Visible Reflectance	0.723

#### Model B: Shade:EquivalentLayer model

In this step the EnergyPlus WindowMaterial:Shade:EquivalentLayer model was used to simulate the roller shade material. According to the solar and visible solar shade characteristics listed in 5.6.1, the following values have been used for the shade's characterization:

Table 25 – Model characteristics

Quantity	Value
Shade Beam-Beam Solar Transmittance	0.042
Front Side Shade Beam-Diffuse Solar Transmittance	0.008
Back Side Shade Beam-Diffuse Solar Transmittance	0.008
Front Side Shade Beam-Diffuse Solar Reflectance	0.723
Back Side Shade Beam-Diffuse Solar Reflectance	0.283

Model C and Model D: Trans model (ideally perfect diffuser versus forward scattering plus diffuse scattering)

According to Larson and Shakespeare (2003), a trans material can be defined through the following surface properties:

Diffuse reflectance (RGB): the color will affect both diffusely reflected light (if there is any surface roughness) and transmitted light. Knowing the red, green and blue components (Cr,Cg, Cb) it is possible to calculate the photopic average of the RGB (Rd);

- Reflected specularly: this is the fraction of light that is reflected off the first surface in a mirror-like way (Rs);
- Surface roughness (RMS): facet slope (Sr);
- Diffuse transmissivity: fraction of light that passes all the way through the surface diffusely (Td);
- Transmitted specularly: fraction of light transmitted as a beam; that is the fraction of light not diffusely scattered (Ts).
- Considering the roller shade properties listed in 5.6.1 the surface properties which define the trans material have values:  $T_s = 0.042$ ,  $T_d = 0.008$ ,  $R_s = R_r = 0$  and  $C_r = C_g = C_b = 0.283$ , considering both the beam-beam and the beam-diffuse component; while in case the shade material is considered as a ideally perfect diffuser:  $T_s=0$  and  $T_d=0.05$ .

In the Radiance programming code the trans model is described through seven parameters which can be calculated by means of a set of equations which mix the surface parameters described above. As specified in (Apian-Bennewitz, 2013) through the floating parameter A7 it is possible to specify the amount of forward scattering versus ideal diffuse scattering. In this analysis two different trans model were used. The first (case A) was built as an ideally perfect diffuser, in order to make the comparison with the EnergyPlus simulations in which the WindowMaterial:Shade model was used possible. The second (case B), however, was modeled taking into account the beam-beam and beam-diffuse transmittance at normal incidence, as it was done using the WindowMaterial:Shade:EquivalentLayer. In Table 26 the equations for calculating the floating parameters and the values used for each of them in the simulations have been listed.

Table 26 – Trans model Case A and Case B

Equation	Case A	Case B
$A7 = Ts / ((Td + Ts))$	0	0.84
$A6 = (Td + Ts) / (Rd + Td + Ts)$	0.15	0.15
$A5 = Sr$	0	0
$A4 = Rs$	0	0
$A3 = Cb / (1 - Rs) * (1 - A6)$	0.33	0.33
$A2 = Cg / (1 - Rs) * (1 - A6)$	0.33	0.33
$A1 = Cr / (1 - Rs) * (1 - A6)$	0.33	0.33

A. Jacobs (Jacobs, 2014) proposes a useful sketch which describes how the energy is split up as light when it passes through a trans material (Figure 53).

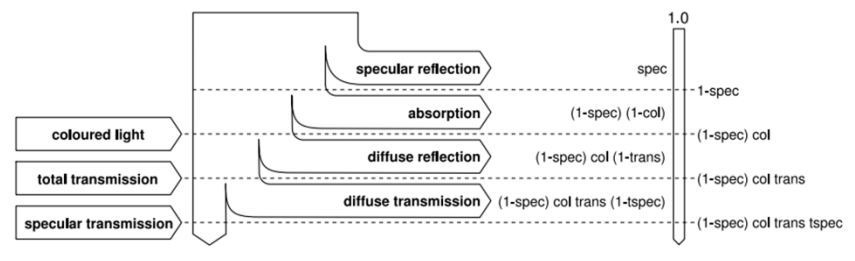


Figure 53 – Light split-up through trans model (source (Jacobs, 2014))

According to this figure, a set of equations was proposed which allows us to calculate the diffuse reflectance and transmittance and the specular transmittance of a material described with the trans model:

- Diffuse reflectance =  $(1 - \text{spec}) \times \text{color} \times (1 - \text{trans})$
- Diffuse transmittance =  $(1 - 0) \times \text{color} \times \text{trans} \times (1 - \text{tspec})$
- Specular transmittance =  $(1 - \text{spec}) \times \text{color} \times \text{trans} \times \text{tspec}$

Where color is the floating number A1, spec the floating number A5, trans the floating number A6 and tspec the floating number A7.

According to these equations and the floating parameters used in the trans model for the Case B, it is possible to obtain the following values:

Table 27 – Case B properties

	Calculated	Measured
Diffuse reflectance	0.2805	0.28
Diffuse transmittance	0.00792	0.008
Specular transmittance	0.04158	0.042

#### Model E: Transdata

The transdata model allows us to modify the visible transmittance according to the radiation incidence angle. In this way it is possible to take into account that the transmitted radiation through the material decreases as the incidence angle rises. This correction can be applied only to a beam light source, which means that the diffused light sources are still represented as constant. In order to better understand what the implications of this assumption are, it is necessary to remember that Radiance uses a raytracing model to simulate the light distribution inside a confined environment. This means that given a generic point inside the environment, all the light that strikes on it has projected into the environment until it reaches a possible source. Roller shades represent a beam light source as well as diffused. Regarding the diffuse-diffuse component, the assumption does not represent a limit, as there is no connection between the incidence angle and the diffuse-diffuse component. At the same time, not considering how the incidence angle modifies the beam-diffuse component can determine a less accurate model. The transdata is defined through the same parameters used for the trans model, except for the surface roughness which is not considered:

- $A6 = Ts / (Td + Ts)$
- $A5 = (Td + Ts) / (Rd + Td + Ts)$
- $A4 = Rs$
- $A3 = Cb / ((1 - Rs) * (1 - A6))$
- $A2 = Cg / ((1 - Rs) * (1 - A6))$
- $A1 = Cr / ((1 - Rs) * (1 - A6))$

Through the transfunction model, the A6 floating parameters can be modified according to a specific function which contains the values, calculated for the different incidence angles, of the ratio  $T_s/(T_s+T_d)$ , which represents the direct hemispherical visual transmittance. Practically, in this work the A6 parameter was fixed equal to 1 and, thanks to the above mentioned function, it will change its value according to the incidence angle, representing how the beam-beam component changes along the day. In order to modulate also the beam-diffuse component another floating parameter would be needed, through which modify the ratio  $T_d/(T_d+T_s)$ . According to (C. F. Reinhart and Andersen, 2006), the function used in order to calculate the angle “rang” between the direction of the incident light  $(dx,dy,dz)$  and the surface normal  $(N_x,N_y,N_z)$  is called “rang.cal”. “rang” represents the coordinate index for the data file .dat which contains corrective values for “rang” values between 0 and 90 degrees. In other words, according to the incidence angle which characterizes the solar radiation in a certain time-step, the “rang” function will use a corrective value contained inside the .dat file in order to obtain the real direct-direct component value. The corrective value has been calculated has the ration between the beam-total transmittance and the beam-beam transmittance at each incidence angle.

As specified in EN 14501:2005 (CEN, 2005b), when the opening is directly lit by the sun:

- the incident radiation is mainly directional;
- the transmitted radiation is partially directional ( $\tau_{v, \text{dir-dir}}$ ), partially diffuse ( $\tau_{v, \text{dir-dif}}$ );
- the total transmitted light flow is the sum of these two components.

$$\tau_{v, \text{dir-h}} = \tau_{v, \text{dir-dir}} + \tau_{v, \text{dif-dif}} \quad (37)$$

These characteristics depend on the incidence angle  $\theta$ . The value  $\tau_{v, \text{dir-h}}$  is representative of the global reduction of natural light by the solar protection device when the light is coming from one specific direction. If an average value is required,  $\tau_{v, \text{dif-h}}$  is representative. The diffused part  $\tau_{v, \text{dir-dif}}$  of transmitted radiation results in the luminance of the solar protection device, which appears as a light source.

C. F. Reinhart and Andersen (2006), obtained the diffuse-diffuse component through the following equation:

$$T_{diffuse-diffuse} = \int_{\theta=0}^{\frac{\pi}{2}} T(\theta) \sin(2\theta) d\theta \quad (38)$$

In other words, they calculated the diffuse-diffuse component integrating the direct hemispherical visual transmittance, which is defined in EN 14501:2005 (CEN, 2005b) as that radiation portion collected in the half space behind the sample plane.

In the transdata model used in this study, the A5 parameter represents the radiation which is transmitted through the material in a diffused way, which is the direct-diffuse component. Considering that the direct-diffuse component should vary according to the incidence angle, an average value obtained considering the values assumed between 30° and 60° will be used. Under 30° the direct-diffuse component can be considered as irrelevant, as long as referring to openness factors below 10 %. At the same time, using values over 60° could cause an overestimation of the direct-diffuse component to daylighting.

## 5.7 Results and discussion

The dynamic simulation software used in this study is not able to provide an output for each one of the physical quantities measured inside the two laboratories. Sometimes the availability of a specific output that can be used for the comparison procedure depends on the model used for representing the shade's behavior or on software's limitation.

Table 28 allows doing a quick comparison between measured quantities and available output.

Table 28 – Measured quantities VS simulation output comparison

Validation aspects	Shade model	Model	Software
Internal air temperature and transmitted solar radiation*	WindowMaterial: Shade	A	Energy Plus
	WindowMaterial: Shade: EquivalentLayer	B	Energy Plus
Work-plane illuminance	WindowMaterial: Shade	A	Energy Plus

Validation aspects	Shade model	Model	Software
Vertical eye illuminance	Trans	C1 C2	DIVA
	Transdata	D1 D2	DIVA
	Trans	C1 C2	DIVA
	Transdata	D1 D2	DIVA

\* Quantities measured just after the glazing before the shade.

Considering that Energy Plus does not allow us to calculate illuminance values on a vertical plane as DIVA does, the Daylight Glare Probability index (DGP) has been calculated and compared with the total hours during which the Discomfort Glare Index (DGI) overcomes a specific value. An intended use as office has been supposed and the maximum allowable DGI value has been set equal 22, according to EN 15251:2007 (CEN, 2007b).

Three main aspects of the modelling performance were assessed, namely temperatures regarding thermal simulation, work-plane and vertical eye illuminance for lighting simulation.

a. Internal air temperature

As regards thermal simulation, it is quite clear that:

- Calibration improves the performance of the model (Figure 54).
- When adding shades (Figure 55) the performance keeps quite good, even if the Model B seems to overestimate the temperature profile.
- As for the entering radiation behind the glazing surface without shades (Figure 56), both models A and B seems to provide a good response, considering that their performance is just analyzing the glazings.

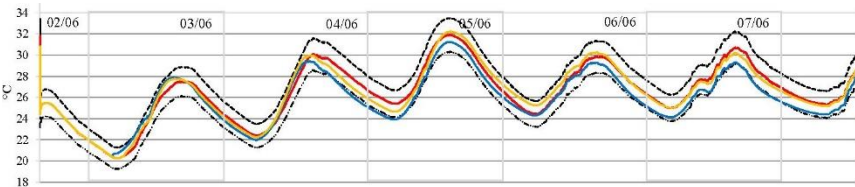
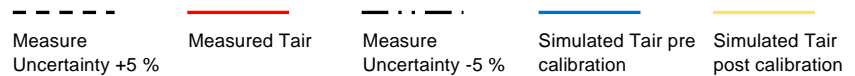


Figure 54 – LAB2 measured and simulated, pre and post calibration, internal air temperature





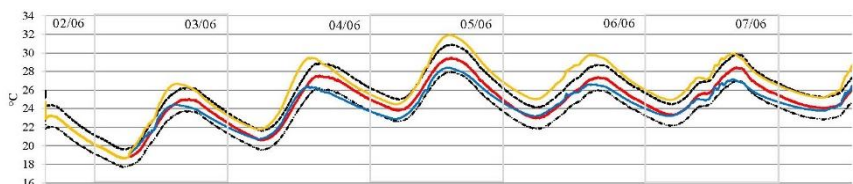


Figure 55 – LAB2 measured and simulated, pre and post calibration, internal air temperature

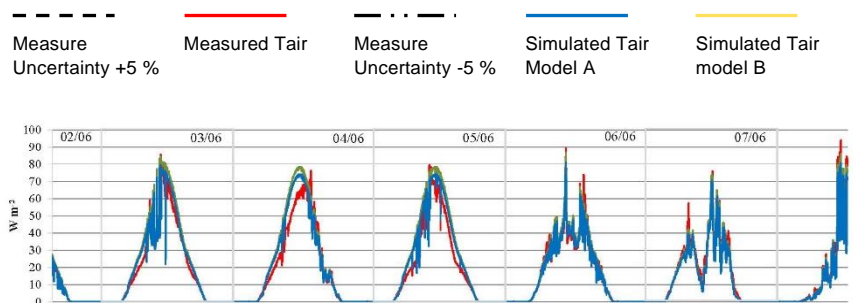


Figure 56 – LAB2 simulated and measured transmitted solar radiation Model A and Model b

#### b. Work-plane illuminance

Both the software programs are able to calculate the illuminance values on a horizontal plane. Regarding DIVA, it can be made simple by defining an evaluation grid through its distance from a reference surface and the spacing between the analysis points. On the contrary, Energy Plus does not provide the illuminance values as a standard output, but hypothesizing an artificial lighting control system, it is possible to fix two control points and then obtain the values sought. Only the results obtained for the FR1 sensor located 1.5 meters from the window have been reported in the following, since similar trends can be identified also for the other points. The charts underline some aspects:

1. A poor agreement between simulated and measured work-plane illuminance values using Model A (Figure 57), Model C1 (Figure 58) or Model D1 (Figure 59) ( $Q_{b-t}=0$ ) when the direct-direct component prevails. In clear sky conditions, this fact can determine:
  - 1.1 an overestimation of the available natural light

- 1.2 an incorrect evaluation of glare occurrence
- 1.3 a possible underestimation of artificial light consumptions if a lighting system dimmed according to the natural light availability is considered.
2. A good agreement between simulated and measured work-plane illuminance values using Model C2 (Figure 60) and Model D2 (Figure 61) ( $q_b \neq 0$ ) when the direct-direct component prevails.
3. A good agreement between simulated and measured work-plane illuminance values when the direct-diffuse component prevails.
4. A good agreement between simulated and measured vertical eye illuminance using Model D2 (Figure 62, Figure 63, Figure 64, Figure 65).
5. Also for the other positions in the room, the same trends can be underlined. As expected, increasing the distance between the sensor and the window, as happens considering the ML and the BR sensors located respectively 2.5 and 3.7 meters from the daylight source, the discrepancy between the measured and simulated trend decreases. In fact, these points, especially the BR sensor, are located far enough not to be affected by the direct-direct component of the visible radiation, which is less efficiently calculated by the shade models applied.

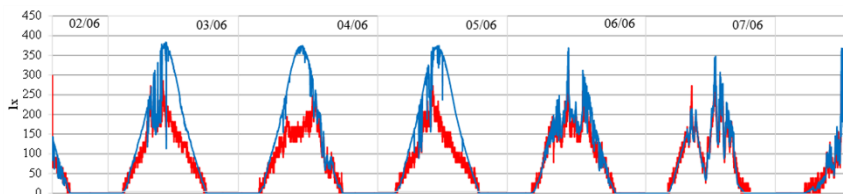


Figure 57 – LAB1 measured and simulated work-plane illuminance for sensor FR1 – Model A

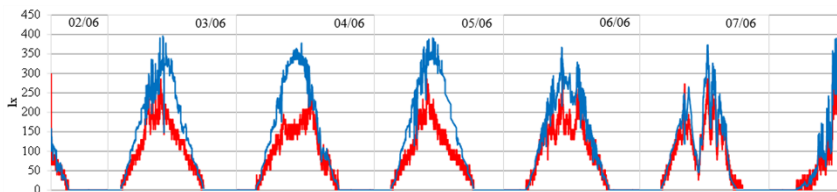


Figure 58 – LAB1 measured and simulated work-plane illuminance for sensor FR1 – Model C1

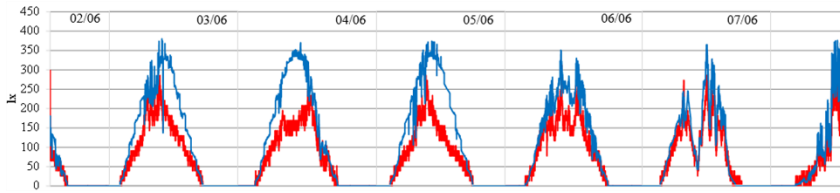


Figure 59 – LAB1 measured and simulated work-plane illuminance for sensor FR1 – Model D1

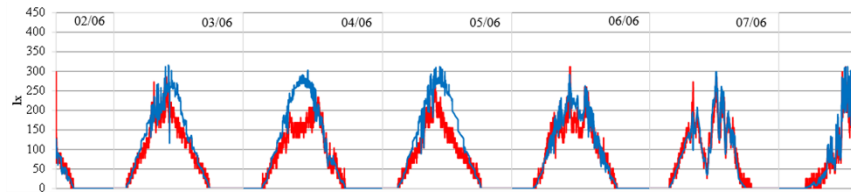


Figure 60 – LAB1 measured and simulated work-plane illuminance for sensor FR1 – Model C2

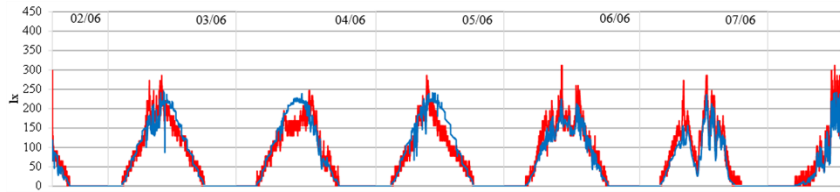


Figure 61 – LAB1 measured and simulated work-plane illuminance for sensor FR1 – Model D2

Measured work-plane illuminance

Simulated work-plane illuminance

Summarizing, it is possible to affirm that when a Lambertian diffuser material is used to simulate roller shades' influence on visible light, the illuminance in the confined space is always overestimated when the direct-direct component prevails. At the same time, if overcast sky conditions or points far enough from the window are considered, even a simplified model which does not distinguish between the direct-direct and the direct-diffuse component of the solar radiation can provide reliable results.

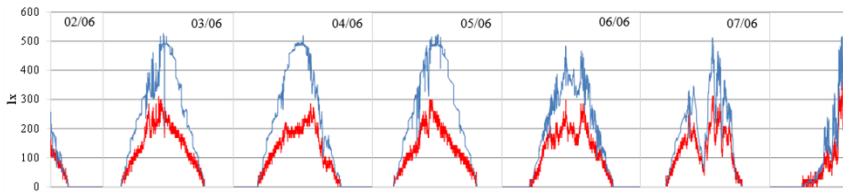


Figure 62 – LAB1 measured and simulated vertical eye illuminance for sensor Ev – Model C1

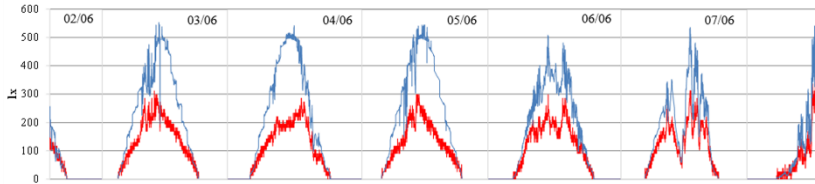


Figure 63 – LAB1 measured and simulated vertical eye illuminance for sensor Ev – Model D1

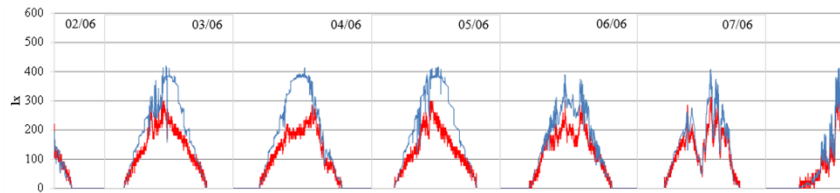


Figure 64 – LAB1 measured and simulated vertical eye illuminance for sensor Ev - Model C2

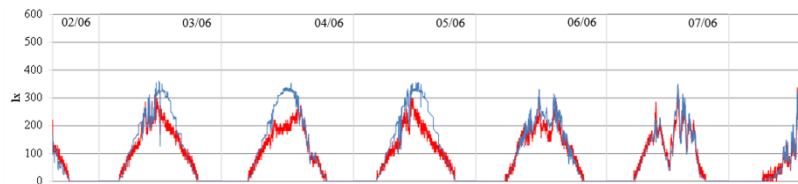


Figure 65 – LAB1 measured and simulated vertical eye illuminance for sensor Ev – Model D2

Measured vertical eye illuminance

Simulated vertical eye illuminance

## 5.8 Conclusions

Roller shades can have several positive effects on the building's global performance, reducing the energy consumption and improving the comfort conditions. However, in order to maximize their contribution it is necessary to consider realistically their effects right from the design phase. At the moment, there is no agreement as to which modelling approach is considered the best.

In this chapter, different models for representing the roller shades behavior, embedded in two widely diffused simulation codes, have been compared with a set of measured data, recorded at the Bowen laboratories at Purdue University (Indiana, USA), coupling thermal (Energy Plus) and lighting simulation (Energy Plus or DIVA for Rhino). The thermal properties of the building materials and the internal gains have been calibrated for the thermal simulation, in order to evaluate better the models' capability of predicting the roller shades behavior and their contribution to the thermal balance. Then, starting from the simplest daylighting model (Model A), which assumes the roller shades as perfect diffusers, more complex characterizations have been considered and validated through the comparison with the measured data.

The results coming from the thermal simulation demonstrates that adding the shades' model the simulation performance keeps quite good, even if the Model B seems to overestimate the temperature profile, underestimating consequently the shades' ability to control solar gains with respect to Model A. This inaccuracy could be particularly critical when the aim of the analysis consists in assessing the internal thermal comfort conditions and/or calculating the heating or cooling consumptions.

On the contrary, Chan et al. (2015) demonstrated that, thanks to the calculation approach suggested in Kotey et al. (2009) and used in the Model B just for thermal simulation, it is possible to model accurately the visual performance of a roller shading system. Further analysis is then necessary in order to understand the model's overall potential.

The analysis related to the optical behavior of the roller shades, has emphasized, once again, the strong correlation between the solar radiation incidence angle and the amount of visible light able to pass through the fabric material. From this point of view, the trans or transdata model (C and D) showed a good

agreement between simulated and measured trends, but only if the specular reflected component is assumed to be different from zero. This aspect appears even clearer considering the vertical eye illuminance trends. In this case, the Model D2 shows the best behavior, while all the other models tend to overestimate the daylight contribution. Assuming the hypothesis that the specular reflection component is different from zero apparently diverges from what has been established through the measurement campaign described in Kotey et al. (2009), and suggests that more measured data coming from different roller shades and from different periods of time, both in terms of duration and season of the year, are needed.

Once the strengths and weaknesses of the different lighting models are identified and they are validated against experimental data, a further step in the work is to evaluate their influence in assessing comfort and energy aspects, with the aim of understanding to what extent a more sophisticated model can improve the design decisions.

## 6. Overall Conclusions and Future Developments

The present research deals with the need for modelling and measuring building integrated performances in order to design and build high efficiency buildings. As underlined in the Introduction, a building design approach which is oriented only to “energy reduction” without considering occupants’ comfort requirements can fail the objective of actual high energy efficiency. Indeed, occupants are used to interacting with the building and if they feel discomfort their actions can create higher energy consumption. For this reason, indoor comfort needs to have the same level of importance as energy efficiency targets in the design stage. In order to achieve this goal, when the internal environmental quality (IEQ) is analyzed, thermal, visual and acoustic comfort conditions and air quality should be taken into account. Considering the recent extensive use of transparent façades in building design, because of both energy and architectonic reasons, larger and larger importance has been given to the solar radiation entering the internal environment, as well as the impacts both on energy balance and on indoor visual and thermal comfort perception.

The objective of this work has been to define a methodological approach able to analyze thermal and visual comfort conditions together with the energy consumptions for heating, cooling and lighting. Actually, only considering all these elements since the early design stage, it is possible to define a design solution capable of increasing environmental quality and minimizing energy demand. Given the inlet solar radiation as a physical parameter to investigate, the first problem was to define how to describe, realistically, its effects on thermal and visual occupants' perception and energy consumption. Considering that the solar radiation enters the building through the fenestration systems, Complex Fenestrations System (CFS) global performance has been compared by means of dynamic simulation through a parametric approach. The results from this step confirmed:

- The necessity to analyze energy consumption and comfort conditions at the same time, in order to prevent the possibility that a poor environmental quality determines an increase in the energy consumption due to the occupants' actions during the service building life.
- The importance of assessing the direct and diffused solar radiation effects on occupants' well-being during the evaluation of thermal and visual comfort. It has been demonstrated that a thermal comfort index which does not account for solar radiation can underestimate critical situations that can determine overheating discomfort conditions. At the same time, neglecting the contribution of the direct-direct component of the visible radiation when assessing visual comfort can represent as comfortable, from a visual point of view, even design configurations that in reality are not so.
- The lack of a standardized and consistent set of metrics able to express the time constancy or space uniformity of comfort and to evaluate different comfort aspects simultaneously with the energy behavior.

Considering the latter point, in the second step a set of representation metrics has been proposed, which can help the designers to analyze and synthesize the global performance of different design characteristics, considering different comfort aspects together and at the same time. Two families of metrics have been proposed based on the concepts of time comfort availability and space comfort usability. When the comfort performance was represented with respect

to a position or to an instant, the metrics represent the fraction of time and space in comfort conditions, respectively. However, when a representation with respect to the overall building surface or reference period is necessary, spatial availability and time or temporal usability summarize the behavior in terms of availability and usability. Moreover, the set of representation metrics proposed is able to represent also the global comfort conditions, on a long-term and/or on a zonal or local basis, giving the possibility to visualize the state of being of different comfort conditions at the same time. These metrics were tested on a simulated environment in order to prove their capability of representing and qualifying the performance of the envelope components when comparing building configurations characterized by high solar and daylighting gains and different window and shading configurations. The analysis of the simulation results led to the following conclusions:

- When the comparison between different design configurations is necessary in order to find the ones able to ensure the best performance in terms of comfort conditions, space (availability) and time (usability) indexes are both necessary. Spatial and temporal representations of the comfort sensation contribute to the overall evaluation of the quality of a built environment supporting the designer in the optimization of the different aspects.
- The synthetic zonal or long-term metrics derived from the above local or instant indices can be useful to communicate with non-specialists and can help the designer to maximize the efficacy of the technical solution chosen, by means of multi-objective optimization which can include the above metrics together with other performance indicators (annual energy, total costs, etc.).
- Conversely, zonal or long term indexes may benefit from the space and time representation of the corresponding instant or local metrics, to understand the reasons of a specific behavior.
- Finally, the application of the proposed metrics and their representation has clearly shown the capability of discriminating the effects on the building performance of different design characteristics.

After defining a suitable approach for analyzing comfort conditions and energy consumptions and defining a set of representation metrics able to represent global performance of different design characteristics considering together, and



at the same time, different comfort aspects, a practical aspect has been considered. Are we representing the complex fenestration system (CFS) performance realistically? Solar transmission, considering both the visible and thermal part, through glazing systems does not represent a problem. On the contrary, the large numbers of studies which deal with the assessment of solar shading systems representation models demonstrate the lack of a standardized approach. In the last chapter of this study, different approaches for the characterization of the roller shade materials' behavior embedded in common simulation codes were evaluated, with the aim of understanding which is able to provide more realistic results. In order to reach this goal, a set of measured data, recorded at the Bowen laboratories of Purdue University (Indiana, USA) were used to validate four different roller shade models. The models were compared in terms of internal air temperature and work-plane illuminance, using two simulation codes: EnergyPlus and DIVA, which uses the calculation algorithms embedded in Radiance and Daysim. It was found:

- A poor agreement between simulated and measured work-plane illuminance values using Model A (Figure 57), Model C1 (Figure 58) or Model D1 (Figure 59) ( $Q_{b-b}=0$ ) when the direct-direct component prevails. In clear sky conditions, this fact can determine:
  - an overestimation of the available natural light
  - an incorrect evaluation of glare occurrence
  - a possible underestimation of artificial light consumptions if a lighting system dimmed according to the natural light availability is considered.
- A good agreement between simulated and measured work-plane illuminance values using Model C2 (Figure 60) and Model D2 (Figure 61) ( $Q_{b-b}\neq 0$ ) when the direct-direct component prevails.
- A good agreement between simulated and measured work-plane illuminance values when the direct-diffuse component prevails.
- A good agreement between simulated and measured vertical eye illuminance using Model D2 (Figure 62, Figure 63, Figure 64, Figure 65).
- Also for the other positions in the room, the same trends can be underlined. As expected, increasing the distance between the sensor and the window, as happens considering the ML and the BR sensors located respectively 2.5

and 3.7 meters from the daylight source, the discrepancy between the measured and simulated trend decreases. In fact, these points, especially the BR sensor, are located far enough not to be affected by the direct-direct component of the visible radiation, which is less efficiently calculated by the shade models applied.

Summarizing, it appears clear that there is a necessity to define a model for the simulation of roller shade material really able to describe its behavior, especially concerning the visible aspects.

Further developments in this research work will concern:

- the validation of the metrics proposed through long-term on site measurements, in order to verify the metrics ability of representing comfort conditions across different climatic conditions;
- the definition of a model to represent efficiently the roller shades' behavior in terms of thermal and visual comfort and, consequently, in terms of energy consumption.



## References

- American Society of Heating Refrigerating and Air Conditioning Engineers. (1981). *Thermal Environmental Conditions for Human Occupancy* (ANSI/ASHRAE Standard 55-1981). Atlanta, GA: ASHRAE.
- American Society of Heating Refrigerating and Air Conditioning Engineers. (2013a). *2013 ASHRAE Handbook–Fundamentals* (Inch-pound ed.). Atlanta, GA: ASHRAE.
- American Society of Heating Refrigerating and Air Conditioning Engineers. (2013b). *Thermal Environmental Conditions for Human Occupancy* (ANSI/ASHRAE Standard 55-2013). Atlanta, GA: ASHRAE.
- Apian-Bennewitz, P. (2013). Review of simulating four classes of window materials for daylighting with non-standard BSDF using the simulation program Radiance. Retrieved from <http://arxiv.org/abs/1307.4214>
- Appelfeld, D., McNeil, A., & Svendsen, S. (2012). An hourly based performance comparison of an integrated micro-structural perforated shading screen with standard shading systems. *Energy and Buildings*, 50, 166–176. <http://dx.doi.org/10.1016/j.enbuild.2012.03.038>
- Arens, E., Berglund, E., & Gonzalez, R. (1986). Thermal comfort under an extended range of environmental conditions. *ASHRAE Transactions*, 92(1), 18–26.
- Arens, E., Hoyt, T., Zhou, X., Huang, L., Zhang, H., & Schiavon, S. (2015). Modeling the comfort effects of short-wave solar radiation indoors. *Building and Environment*, 88, 3–9. <http://dx.doi.org/10.1016/j.buildenv.2014.09.004>
- Attia, S., & Carlucci, S. (2015). Impact of Different Thermal Comfort Models on Zero Energy Residential Buildings in Hot Climate. *Energy and Buildings*, 102, 117–128. <http://dx.doi.org/10.1016/j.enbuild.2015.05.017>
- Atzeri, A. M., Cappelletti, F., Gasparella, A., & Tzempelikos, A. (2013). Office energy needs and indoor comfort with different types of external roller shades in a southern Europe climate. In E. Wurtz (Ed.), *Buildings Simulation: 13th International Conference of the International Building Performance Simulation Association*, 25–28 August 2013 Chambéry, France, (pp. 2626–2633). Toronto: IBPSA.
- Bessoudo, M., Tzempelikos, A., Athienitis, A. K., & Zmeureanu, R. (2010). Indoor thermal environmental conditions near glazed facades with shading

- devices – Part I: Experiments and building thermal model. *Building and Environment*, 45(11), 2506–2516. <http://dx.doi.org/10.1016/j.buildenv.2010.05.013>
- Buratti, C., Moretti, E., Belloni, E., & Cotana, F. (2012). Unsteady simulation of energy performance and thermal comfort in non-residential buildings. *Building and Environment*, 59, 482–491. <http://dx.doi.org/10.1016/j.buildenv.2012.09.015>
- Cappelletti, F., Prada, A., Romagnoni, P., & Gasparella, A. (2014). Passive performance of glazed components in heating and cooling of an open-space office under controlled indoor thermal comfort. *Building and Environment*, 72, 131–144. <http://dx.doi.org/10.1016/j.buildenv.2013.10.022>
- Carlucci, S., Causone, F., De Rosa, F., & Pagliano, L. (2015). A review of indices for assessing visual comfort with a view to their use in optimization processes to support building integrated design. *Renewable and Sustainable Energy Reviews*, 47, 1016–1033. <http://dx.doi.org/10.1016/j.rser.2015.03.062>
- Carlucci, S., & Pagliano, L. (2012). A review of indices for the long-term evaluation of the general thermal comfort conditions in buildings. *Energy and Buildings*, 53, 194–205. <http://dx.doi.org/10.1016/j.enbuild.2012.06.015>
- Chaiyapinunt, S., Phueakphongsuriya, B., Mongkornsaksit, K., & Khomporn, N. (2005). Performance rating of glass windows and glass windows with films in aspect of thermal comfort and heat transmission. *Energy and Buildings*, 37(7), 725–738. <http://dx.doi.org/10.1016/j.enbuild.2004.10.008>
- Chan, M., & Mak, C. (2008). Thermal Comfort Levels in a Room with Solar Radiation. *Indoor and Built Environment*, 17(6). doi: 10.1177/1420326X08097388
- Chan, Y.-C., Tzempelikos, A., & Konstantzos, I. (2015). A systematic method for selecting roller shade properties for glare protection. *Energy and Buildings*, 92, 81–94. <http://dx.doi.org/10.1016/j.enbuild.2015.01.057>
- Chauvel, P., Collins, J. B., Dogniaux, R., & Longmore, J. (1982). Glare from windows: current views of the problem. *Lighting Research and Technology*, 14, 31–46.
- da Silva, P. C., Leal, V., & Andersen, M. (2012). Influence of shading control patterns on the energy assessment of office spaces. *Energy and Buildings*, 50, 35–48. <http://dx.doi.org/10.1016/j.enbuild.2012.03.019>

- David, M., Donn, M., Garde, F., & Lenoir, A. (2011). Assessment of the thermal and visual efficiency of solar shades. *Building and Environment*, 46(7), 1489–1496. <http://dx.doi.org/10.1016/j.buildenv.2011.01.022>
- Directive 2002/91/EC of the European Parliament and of the Council of 16 December 2002 on the energy performance of buildings. (2002). *Official Journal of the European Union*, L 1/65, 65–71. Retrieved from <http://eur-lex.europa.eu/legal-content/EN/TXT/PDF/?uri=CELEX:32002L0091&qid=1491386525148&from=en>
- Directive 2010/31/EU of the European Parliament and of the Council of 19 May 2010 on the energy performance of buildings. (2010). *Official Journal of the European Union*, L 135, 13–35. Retrieved from <http://eur-lex.europa.eu/legal-content/EN/TXT/PDF/?uri=OJ:L:2010:153:FULL&from=EN>
- Djongyang, N., Tchindac, R., Njomoa, D. (2010). Thermal comfort: A review paper. *Renewable and Sustainable Energy Reviews*, 14, 2626–2640. <https://doi.org/10.1016/j.rser.2010.07.040>
- Eskin, N., & Türkmen, H. (2008). Analysis of annual heating and cooling energy requirements for office buildings in different climates in Turkey. *Energy and Buildings*, 40(5), 763–773. <http://dx.doi.org/10.1016/j.enbuild.2007.05.008>
- Ente italiano di normazione. (1995). *Impianti aeraulici a fini di benessere. Generalità, classificazione e requisiti. Regole per la richiesta d'offerta, l'offerta, l'ordine e la fornitura* (UNI 10339:1995). Milan: UNI.
- European Committee for Standardization. (2001). *Ergonomics of the thermal environment - Instruments for measuring physical quantities* (EN ISO 7726:2001). Brussels: CEN.
- European Committee for Standardization. (2005a). *Solar protection devices combined with glazing – Calculation of total solar energy transmittance and light transmittance – Part 2: Detailed calculation method* (EN 13363-2:2005/AC 2006). Brussels: CEN.
- European Committee for Standardization. (2005b). *Blinds and shutters – Thermal and visual comfort – Performance characteristics and classification* (EN 4501:2005). Brussels: CEN.

- European Committee for Standardization. (2005c). *Ergonomics of the thermal environment - Analytical determination and interpretation of thermal comfort using calculation of the PMV and PPD indices and local thermal comfort criteria* (ISO 7730:2005). Brussels: CEN.
- European Committee for Standardization. (2007a). *Solar protection devices combined with glazing – Calculation of solar and light transmittance – Part 1: Simplified method* (EN 13363-1:2003 + A1:2007). Brussels: CEN.
- European Committee for Standardization. (2007b). *Indoor environmental input parameters for design and assessment of energy performance of buildings- addressing indoor air quality, thermal environment, lighting and acoustics* (EN 15251:2007). Brussels: CEN.
- European Committee for Standardization. (2008). *Energy performance of buildings – Calculation of energy use for space heating and cooling* (EN ISO 13790:2008). Brussels: CEN.
- European Committee for Standardization. (2011a). *Light and lighting Lighting of work places Part 1: Indoor work places* (EN 12464-1). Brussels: CEN.
- European Committee for Standardization. (2011b). *Light and lighting – Basic terms and criteria for specifying lighting requirements* (EN 12665:2011). Brussels: CEN.
- Fanger, P. O. (1972). *Thermal Comfort: analysis and applications in environmental engineering*. New York: McGraw-Hill.
- Fasi, M. A., & Budaiwi, I. M. (2015). Energy performance of windows in office buildings considering daylight integration and visual comfort in hot climates. *Energy and Buildings*, 108, 307–316. <http://dx.doi.org/10.1016/j.enbuild.2015.09.024>
- Gagge, A. P., Fobelets, A. P., & Berglund, L. G. (1985). A standard predictive index of human response to the thermal environment. *ASHRAE Transactions*, 92(2B), 709–731.
- Galasiu, A. D., Atif, M. R., & MacDonald, R. A. (2004). Impact of window blinds on daylight-linked dimming and automatic on/off lighting controls. *Solar Energy*, 76(5), 523–544. <http://dx.doi.org/10.1016/j.solener.2003.12.007>
- Halawa, E., van Hoof, J., & Soebarto, V. (2014). The impacts of the thermal radiation field on thermal comfort, energy consumption and control — A

- critical overview. *Renewable and Sustainable Energy Reviews*, 37, 907–918. <http://dx.doi.org/10.1016/j.rser.2014.05.040>
- Helioscreen. (2017). Helioscreen – Weaving performance into Fabrics. Retrieved February 24, 2017, from <http://www.helioscreen.com/en/home#&panel1-1>
- Hensen, J. L. M. (1991). *On the thermal interaction of building structure and heating and ventilating system*. (Doctoral dissertation, Technische Universiteit Eindhoven). Retrieved from [http://www.esru.strath.ac.uk/Documents/PhD/hensen\\_thesis.pdf](http://www.esru.strath.ac.uk/Documents/PhD/hensen_thesis.pdf)
- Hodder, S. G., & Parsons, K. (2006). The effects of solar radiation on thermal comfort. *International Journal of Biometeorology*, 51(3), 233–250. doi: 10.1007/s00484-006-0050-y
- Hoes, P., Hensen, J. L. M., Loomans, M. G. L. C., de Vries, B., & Bourgeois, D. (2009). User behavior in whole building simulation. *Energy and Buildings*, 41(3), 295–302. <http://dx.doi.org/10.1016/j.enbuild.2008.09.008>
- Hoffmann, S., Lee, E. S., McNeil, A., Fernandes, L., Vidanovic, D., & Thanachareonkit, A. (2016). Balancing daylight, glare, and energy-efficiency goals: An evaluation of exterior coplanar shading systems using complex fenestration modeling tools. *Energy and Buildings*, 112, 279–298. <http://dx.doi.org/10.1016/j.enbuild.2015.12.009>
- Huizenga, C., Zhang, H., Mattelaer, P., Yu, T., Arens, E., & Lyons, P. (2006). *Window Performance for Human Thermal Comfort* (Final report to the NFRFC). Berkley, CA: Center for the Built Environment, University of California.
- Humphreys, M. A., & Nicol, J. F. (1998). Understanding the adaptive approach to thermal comfort. *ASHRAE Transactions Symposia*, 104(1b), 991–1004.
- Hwang, R.-L., & Shu, S.-Y. (2011). Building envelope regulations on thermal comfort in glass facade buildings and energy-saving potential for PMV-based comfort control. *Building and Environment*, 46(4), 824–834. <http://dx.doi.org/10.1016/j.buildenv.2010.10.009>
- Illuminating Engineering Society. (2012). LM-83-12 – Approved Method: IES Spatial Daylight Autonomy (sDA) and Annual Sunlight Exposure (ASE). New York, NY: IES.
- Inoue, T., Kawase, T., Ibamoto, T., Takakusa, S., & Matsuo, Y. (1988). The development of an optimal control system for window shading devices based on investigations in office buildings. *ASHRAE Transactions*, 94, 1034–1049.



- Jacobs, A. (2014). *RADIANCE Cookbook*. Retrieved from [http://www.jaloxa.eu/resources/radiance/documentation/docs/radiance\\_cookbook.pdf](http://www.jaloxa.eu/resources/radiance/documentation/docs/radiance_cookbook.pdf)
- Joint Committee for Guides in Metrology. (2008). *Evaluation of measurement data - Guide to the expression of uncertainty in measurement*. JCGM 100:2008. Sèvres: BIPM.
- Jonas, H. (1984). *The imperative of responsibility: in search of an ethics for the technological age*. Chicago, IL: University of Chicago Press.
- Kapsis, K., Tzempelikos, A., Athienitis, A. K., & Zmeureanu, R. G. (2010). Day-lighting performance evaluation of a bottom-up motorized roller shade. *Solar Energy*, 84(12), 2120–2131. <http://dx.doi.org/10.1016/j.solener.2010.09.004>
- Kim, G., Lim, H. S., Lim, T. S., Schaefer, L., & Kim, J. T. (2012). Comparative advantage of an exterior shading device in thermal performance for residential buildings. *Energy and Buildings*, 46, 105–111. <http://dx.doi.org/10.1016/j.enbuild.2011.10.040>
- Kirimtat, A., Koyunbaba, B. K., Chatzikonstantinou, I., & Sariyildiz, S. (2016). Review of simulation modeling for shading devices in buildings. *Renewable and Sustainable Energy Reviews*, 53, <http://dx.doi.org/10.1016/j.rser.2015.08.020>
- Kolarik, J., Toftum, J., Olesen, B. W., & Jensen, K. L. (2011). Simulation of energy use, human thermal comfort and office work performance in buildings with moderately drifting operative temperatures. *Energy and Buildings*, 43(11), 2988–2997. <http://dx.doi.org/10.1016/j.enbuild.2011.07.008>
- Kotey, N. A., Wright, J. L., & Collins, M. R. (2009). Determining off-normal solar optical properties of roller blinds. *ASHRAE Transactions*, 115(1), 145–154.
- Kunkel, S., Kontonasiou, E., Arcipowska, A., Mariottini, F., & Atanasiu, B. (2015). *Indoor Air Quality, Thermal Comfort and Daylight – Analysis of Residential Building Regulations*. Retrieved from [http://bpie.eu/wp-content/uploads/2015/10/BPIE\\_\\_IndoorAirQuality2015.pdf](http://bpie.eu/wp-content/uploads/2015/10/BPIE__IndoorAirQuality2015.pdf)
- La Gennusa, M., Nucara, A., Pietrafesa, M., & Rizzo, G. (2007). A model for managing and evaluating solar radiation for indoor thermal comfort. *Solar Energy*, 81(5), 594–606. <http://dx.doi.org/10.1016/j.solener.2006.09.005>
- La Gennusa, M., Nucara, A., Rizzo, G., & Scaccianoce, G. (2005). The calculation of the mean radiant temperature of a subject exposed to the solar radiation – A generalised algorithm. *Building and Environment*, 40(3), 367–375. <http://dx.doi.org/10.1016/j.buildenv.2004.06.019>

- Larson, G. W., & Shakespeare, R. (2003). *Rendering with Radiance : the art and science of lighting visualization*. London: Morgan Kaufmann.
- Lawrence Berkeley National Laboratory. (n. d.). EnergyPlus Documentation v.8.4.0 – Input output reference. Retrieved from <http://bigladdersoftware.com/epx/docs/8-4/input-output-reference/title.html#energyplustm-documentation-v8.4.0>
- Liu, M., Wittchen, K. B., & Heiselberg, P. K. (2015). Control strategies for intelligent glazed façade and their influence on energy and comfort performance of office buildings in Denmark. *Applied Energy*, 145, 43–51. <http://dx.doi.org/10.1016/j.apenergy.2015.02.003>
- Mahdavi, A., & Dervishi, S. (2011). Exploring the energy performance of simulation-powered lighting and shading systems controls in buildings. In *Building Simulation 2011: Proceedings of the 12<sup>th</sup> Conference of the International Building Performance Simulation Association* (pp. 772–778). Sydney, Australia: IBPSA Australasia.
- Mainini, A. G., Bonato, D., Poli, T., & Speroni, A. (2015). Lean Strategies for Window Retrofit of Italian Office Buildings: Impact on Energy Use, Thermal and Visual Comfort. *Energy Procedia*, 70, 719–728. <https://doi.org/10.1016/j.egypro.2015.02.181>
- Marino, C., Nucara, A., & Pietrafesa, M. (2015). Mapping of the indoor comfort conditions considering the effect of solar radiation. *Solar Energy*, 113, 63–77. <http://dx.doi.org/10.1016/j.solener.2014.12.020>
- Newsham, G. R. (1994). Manual Control of Window Blinds and Electric Lighting: Implications for Comfort and Energy Consumption. *Indoor and Built Environment*, 3(3), 135–144.
- Nicol, J. F., & Wilson, M. (2010). An overview of the European Standard EN 15251. In *Proceedings of Conference: Adapting to Change: New Thinking on Comfort*. London: Network for Comfort and Energy Use in Buildings. Retrieved from <http://nceub.org.uk/dokuwiki/lib/exe/fetch.php?media=nceub:uploads:members:w2010:session1:16-01-02-nicol.pdf>
- Nielsen, M. V., Svendsen, S., & Jensen, L. B. (2011). Quantifying the potential of automated dynamic solar shading in office buildings through integrated simulations of energy and daylight. *Solar Energy*, 85(5), 757–768. <http://dx.doi.org/10.1016/j.solener.2011.01.010>

- Ochoa, C. E., Aries, M. B. C., van Loenen, E. J., & Hensen, J. L. M. (2012). Considerations on design optimization criteria for windows providing low energy consumption and high visual comfort. *Applied Energy*, 95, 238–245. <http://dx.doi.org/10.1016/j.apenergy.2012.02.042>
- Oh, M. H., Lee, K. H., & Yoon, J. H. (2012). Automated control strategies of inside slat-type blind considering visual comfort and building energy performance. *Energy and Buildings*, 55, 728–737. <http://dx.doi.org/10.1016/j.enbuild.2012.09.019>
- Poirazis, H., Blomsterberg, Å., & Wall, M. (2008). Energy simulations for glazed office buildings in Sweden. *Energy and Buildings*, 40(7), 1161–1170. <http://dx.doi.org/10.1016/j.enbuild.2007.10.011>
- Prada, A., Cappelletti, F., Baggio, P., & Gasparella, A. (2014). On the effect of material uncertainties in envelope heat transfer simulations. *Energy and Buildings*, 71, 53–60. <http://dx.doi.org/10.1016/j.enbuild.2013.11.083>
- Ramos, G., & Ghisi, E. (2010). Analysis of daylight calculated using the EnergyPlus programme. *Renewable and Sustainable Energy Reviews*, 14(7), 1948–1958. <http://dx.doi.org/10.1016/j.rser.2010.03.040>
- Reinhart, C. F., & Andersen, M. (2006). Development and validation of a Radiance model for a translucent panel. *Energy and Buildings*, 38(7), 890–904. <http://dx.doi.org/10.1016/j.enbuild.2006.03.006>
- Reinhart, C. F., & Walkenhorst, O. (2001). Validation of dynamic RADIANCE-based daylight simulations for a test office with external blinds. *Energy and Buildings*, 33(7), 683–697. [http://dx.doi.org/10.1016/S0378-7788\(01\)00058-5](http://dx.doi.org/10.1016/S0378-7788(01)00058-5)
- Reinhart, C. F., & Voss, K. (2003). Monitoring manual control of electric lighting and blinds. *Lighting Research and Technology*, 35(3), 243–260.
- Reinhart, C. F. (2010). *Tutorial on the Use of Daysim Simulations for Sustainable Design*. Cambridge, MA: Harvard University Graduate School of Design.
- Roetzel, A., Tsangrassoulis, A., & Dietrich, U. (2014). Impact of building design and occupancy on office comfort and energy performance in different climates. *Building and Environment*, 71, 165–175. <http://dx.doi.org/10.1016/j.buildenv.2013.10.001>
- Shen, H., & Tzempelikos, A. (2012). Daylighting and energy analysis of private offices with automated interior roller shades. *Solar Energy*, 86(2), 681–704. <http://dx.doi.org/10.1016/j.solener.2011.11.016>

- Shen, H., & Tzempelikos, A. (2013). Sensitivity analysis on daylighting and energy performance of perimeter offices with automated shading. *Building and Environment*, 59, 303–314. <http://dx.doi.org/10.1016/j.buildenv.2012.08.028>
- Singh, M. C., Garg, S. N., & Jha, R. (2008). Different glazing systems and their impact on human thermal comfort—Indian scenario. *Building and Environment*, 43(10), 1596–1602. <http://dx.doi.org/10.1016/j.buildenv.2007.10.004>
- Singh, R., Lazarus, I. J., & Kishore, V. V. N. (2015). Effect of internal woven roller shade and glazing on the energy and daylighting performances of an office building in the cold climate of Shillong. *Applied Energy*, 159, 317–333. <http://dx.doi.org/10.1016/j.apenergy.2015.09.009>
- Suk, J. Y., Schiler, M., & Kensek, K. (2013). Development of new daylight glare analysis methodology using absolute glare factor and relative glare factor. *Energy and Buildings*, 64, 113–122. <https://doi.org/10.1016/j.enbuild.2013.04.020>
- Sullivan, R. (1986). *Thermal Comfort Issues in the LRI Study*. Internal Memorandum/Report. Berkeley, CA: LBLN.
- Thellier, F., Monchoux, F., Bonnis-Sassi, M., & Lartigue, B. (2008). Modeling additional solar constraints on a human being inside a room. *Solar Energy*, 82(4), 290–301. <https://doi.org/10.1016/j.solener.2007.10.004>
- Tregenza, P. R., & Waters, I. M. (1983). Daylight coefficients. *Lighting Research and Technology*, 15(2), 65–71. <https://doi.org/10.1177/096032718301500201>
- Tsikaloudaki, K., Theodosiou, T., Laskos, K., & Bikas, D. (2012). Assessing cooling energy performance of windows for residential buildings in the Mediterranean zone. *Energy Conversion and Management*, 64, 335–343. <https://doi.org/10.1016/j.enconman.2012.04.020>
- Tzempelikos, A., & Athienitis, A. K. (2007). The impact of shading design and control on building cooling and lighting demand. *Solar Energy*, 81(3), 369–382. <https://doi.org/10.1016/j.solener.2006.06.015>
- Tzempelikos, A., Bessoudo, M., Athienitis, A. K., & Zmeureanu, R. (2010). Indoor thermal environmental conditions near glazed facades with shading devices – Part II: Thermal comfort simulation and impact of glazing and shading properties. *Building and Environment*, 45(11), 2517–2525. <https://doi.org/10.1016/j.buildenv.2010.05.014>

- Tzempelikos, A., & Shen, H. (2013). Comparative control strategies for roller shades with respect to daylighting and energy performance. *Building and Environment*, 67, 179–192. <https://doi.org/10.1016/j.buildenv.2013.05.016>
- Vanhoutteghem, L., Skarning, G. C. J., Hviid, C. A., & Svendsen, S. (2015). Impact of façade window design on energy, daylighting and thermal comfort in nearly zero-energy houses. *Energy and Buildings*, 102, 149–156. <https://doi.org/10.1016/j.enbuild.2015.05.018>
- Wang, Y., Kuckelkorn, J., Zhao, F.-Y., Liu, D., Kirschbaum, A., & Zhang, J.-L. (2015). Evaluation on classroom thermal comfort and energy performance of passive school building by optimizing HVAC control systems. *Building and Environment*, 89, 86–106. <https://doi.org/10.1016/j.buildenv.2015.02.023>
- Wienold, J., & Christoffersen, J. (2005). Towards a new daylight glare rating. In *Lighting for humans – 10<sup>th</sup> European Lighting Conference, Lux Europa 2005* (pp. 157–161). Berlin: LiTG.
- Wienold, J., & Christoffersen, J. (2006). Evaluation methods and development of a new glare prediction model for daylight environments with the use of CCD cameras. *Energy and Buildings*, 38(7), 743–757. doi: 10.1016/2006-03-017
- Wienold, J., Reetz, C., Kuhn, T. & Christoffersen, J. (2004). *Evalglare – A new RADIANCE-based tool to evaluate daylight glare in office spaces*. 3<sup>rd</sup> International Radiance Workshop, Fribourg.
- Wright J.L. (2008). Calculating Centre-Glass Performance Indices of Glazing Systems with Shading Devices. *ASHRAE Transactions*, 114(2), 199–209.
- Yao, J. (2014a). An investigation into the impact of movable solar shades on energy, indoor thermal and visual comfort improvements. *Building and Environment*, 71, 24–32. <http://dx.doi.org/10.1016/j.buildenv.2013.09.011>
- Yao, J. (2014b). Determining the energy performance of manually controlled solar shades: A stochastic model based co-simulation analysis. *Applied Energy*, 127, 64–80. <http://dx.doi.org/10.1016/j.apenergy.2014.04.046>
- Yao, J., & Zhu, N. (2012). Evaluation of indoor thermal environmental, energy and daylighting performance of thermotropic windows. *Building and Environment*, 49, 283–290. <http://dx.doi.org/10.1016/j.buildenv.2011.06.004>
- Ye, Y., Xu, P., Mao, J., & Ji, Y. (2015). Experimental study on the effectiveness of internal shading devices. *Energy and Buildings*, 111, 154–163. <http://dx.doi.org/10.1016/j.enbuild.2015.11.040>

- Zhu, J., Chew, D. A. S., Lv, S., & Wu, W. (2013). Optimization method for building envelope design to minimize carbon emissions of building operational energy consumption using orthogonal experimental design (OED). *Habitat International*, 37, 148–154. <http://dx.doi.org/10.1016/j.habitatint.2011.12.006>
- Zinzi, M., Agnoli, S., & Fasano, G. (2014). *Comparazione tra standard e strumenti di calcolo per le prestazioni solari e luminose di componenti vetrati con accoppiamento di schermature solari*. Retrieved from [http://www.enea.it/it/Ricerca\\_sviluppo/documenti/ricerca-di-sistema-elettrico/edifici-pa/2013/rds-par2013-143.pdf](http://www.enea.it/it/Ricerca_sviluppo/documenti/ricerca-di-sistema-elettrico/edifici-pa/2013/rds-par2013-143.pdf)



## The Author

Anna Maria Atzeri is a research fellow at the Free University of Bozen-Bolzano, Faculty of Science and Technology with a teaching contract in Design of illumination systems. She has been involved in the lab development for the new technology park in Bozen-Bolzano and in the setup of the Classroom Spaces Living Lab to test environmental conditions and performance of different envelope and HVAC systems in two classroom spaces at the Free University of Bolzano. Since 2017 she is engaged in the Intelligent Building Automation System (IBAS) project dealing with the development of active controlling systems for the reduction of the buildings' energy consumption, including heating, cooling and lighting, and the optimization of indoor comfort conditions.